ACOA 2014 Bathymetric Lidar Pilot Project Report:

Cape John, John Bay, and Little Harbour, Nova Scotia

Prepared by

Tim Webster, PhD
Kevin McGuigan, Nathan Crowell, Kate Collins, Candace MacDonald
Applied Geomatics Research Group
NSCC, Middleton
Tel. 902 825 5475
email: tim.webster@nscc.ca

Submitted to

Atlantic Canada Opportunities Agency

December 17, 2014

How to cite this work and report:

Webster, T., McGuigan, K., Crowell, N., Collins, K., MacDonald, C. 2014. ACOA 2014 Bathymetric Lidar Pilot Project Report: Cape John, John Bay, and Little Harbour, Nova Scotia. Technical report, Applied Geomatics Research Group, NSCC Middleton, NS.

Executive Summary

An airborne topographic-bathymetric lidar survey was undertaken at Little Harbour, Nova Scotia on September 25, 2014, and at Cape John and John Bay, Nova Scotia on September 26, 2014. The sensor used was a Chiroptera II integrated topographic bathymetric lidar sensor equipped with a 60 megapixel multispectral camera. Strong winds along the Northumberland Strait during the week of the planned survey reduced water clarity and delayed the surveys at Cape John and John Bay, but good data was collected in between wind events. The aircraft required ground-based high precision GPS data to be collected during the lidar survey in order to provide accurate positional data for the aircraft trajectory. At Little Harbour, a Leica GS14 base station was set up over a temporary monument in Melmerby Beach Provincial Park. The temporary monument was occupied the previous week and tied into an NS High Precision Network (HPN) monument. At Cape John and John Bay the provincial CANSEL active GPS network was accessed for the aircraft trajectory. Boat-based ground truth data collection occurred on September 25 at Little Harbour during the lidar survey in a 15 foot aluminum boat; ground truth data was collected in a 24 foot Bayliner on September 24 at John Bay and John Bay, and on several dates in late October for Cape John. Ground truth surveys included water clarity measurements using a Secchi disk and turbidity sensor, depth validation measurements using an echosounder and a lead ball on a rope, underwater photographs of the seabed using a GoPro camera, and GPS measurements for lidar validation. Scientists from Fisheries and Oceans Canada in Moncton also collected ground truth data in Little Harbour on September 25 and 26. The underwater photographs were used in post-processing to provide information on seabed type, such as sand, rock, or eelgrass. Lidar data were processed in Lidar Survey Studio and classed into ground, water surface, and seabed points and used to produce a Digital Elevation Model (DEM) for each study area. Maps of lidar intensity data were also produced; these show information on the bottom type and with further research will be used to generate classified bottom type maps, including classes for submerged vegetation such as eelgrass. The maximum depth achieved with the lidar sensor at Cape John and John Bay was 6 m, and at Little Harbour the sensor achieved complete coverage of the study area, with a maximum depth of 6.5 m. The aerial photos were orthorectified using the lidar DEMs and direct georeference information from the aircraft trajectory. The original aerial photos were captured and orthorectified at a resolution of ~5 cm. The orthophotos were then up sampled to 20 cm and merged into a mosaic.

Table of Contents

Table of Figures

List of Tables

1 Introduction

The requirement for accurate and detailed information along Nova Scotia's coastal zone is imperative in order to protect existing infrastructure and plan for future development, and to make sound decisions with regard to activities that support economic growth. Recently the Applied Geomatics Research Group (AGRG) at the Nova Scotia Community College (NSCC) acquired a topographic-bathymetric (topo-bathy) lidar sensor and high resolution aerial camera that is capable of surveying the land elevations and the submerged coastal topography. The ability of an airborne sensor to accurately survey the near shore bathymetry (submerged elevation) offers an opportunity to produce detailed information across the land-sea boundary in an area that has traditionally not been mapped because of the expense and limitations of traditional mapping technologies (air photos on land and boats and echo sounders on the water).

The lidar system utilizes lasers mounted in an aircraft to precisely measure the topography surrounding coastal waters and also sees through the water to measure what is below. The reflection of the laser from the seabed can be used to map submerged vegetation, for example eelgrass, which is often used by regulators, such as the Department of Fisheries and Oceans (DFO), as a measure of ecosystem health. These data can be used to capture the state of the seabed and aquatic vegetation and act as a quantitative baseline prior to any coastal developments. The lidar sensor is coupled with a high resolution aerial camera (Leica RCD30) which is capable of collecting traditional true colour images (red, green, and blue or RGB) and also a near-infrared (NIR) imagery which is highly sensitivity to the existence of vegetation, such as exposed seaweed in the coastal zone or the forest or agriculture crops. The ability of the lidar sensor to acquire detailed elevation data on land and continuously into the submarine environment provides information that can be used for coastal flood risk assessment, erosion and geohazard assessment, for the land areas. For the intertidal and subtidal areas, this level of information has never been surveyed and provides details to aid in siting suitable aquaculture locations. For example, these types of data are required for wave and hydrodynamic modelling for the assessment of currents and wave run-up and possible exposure of infrastructure to storms and site suitability analysis for aquaculture operations.

John Bay, Cape John and Little Harbour, Nova Scotia (Figure 1) were surveyed in the fall of 2014 with funding support from various agencies and departments (Table 1). These study areas were deemed to be good candidates for research on the technological capability of the topo-bathy lidar sensor for several reasons. The Cape John area is the site of previous research and topographic lidar collection, and the coastal processes there are well-studied. The John Bay area represents an estuary, where River John enters the ocean, and has different characteristics than that of the exposed ocean study area at Cape John. Little Harbour is a site for potential shellfish aquaculture operations, is sheltered and is shallow and contains eelgrass. The outer coast of Little Harbour is the site of Melmerby Beach Provincial Park located along a major sand dune. The Little Harbour and Cape John areas both contain exposed coasts, but with very different bottom types. These different environments offered an opportunity to test the limitations and benefits of the lidar sensor under different conditions, and will enable the production of multiple data products to support coastal management.

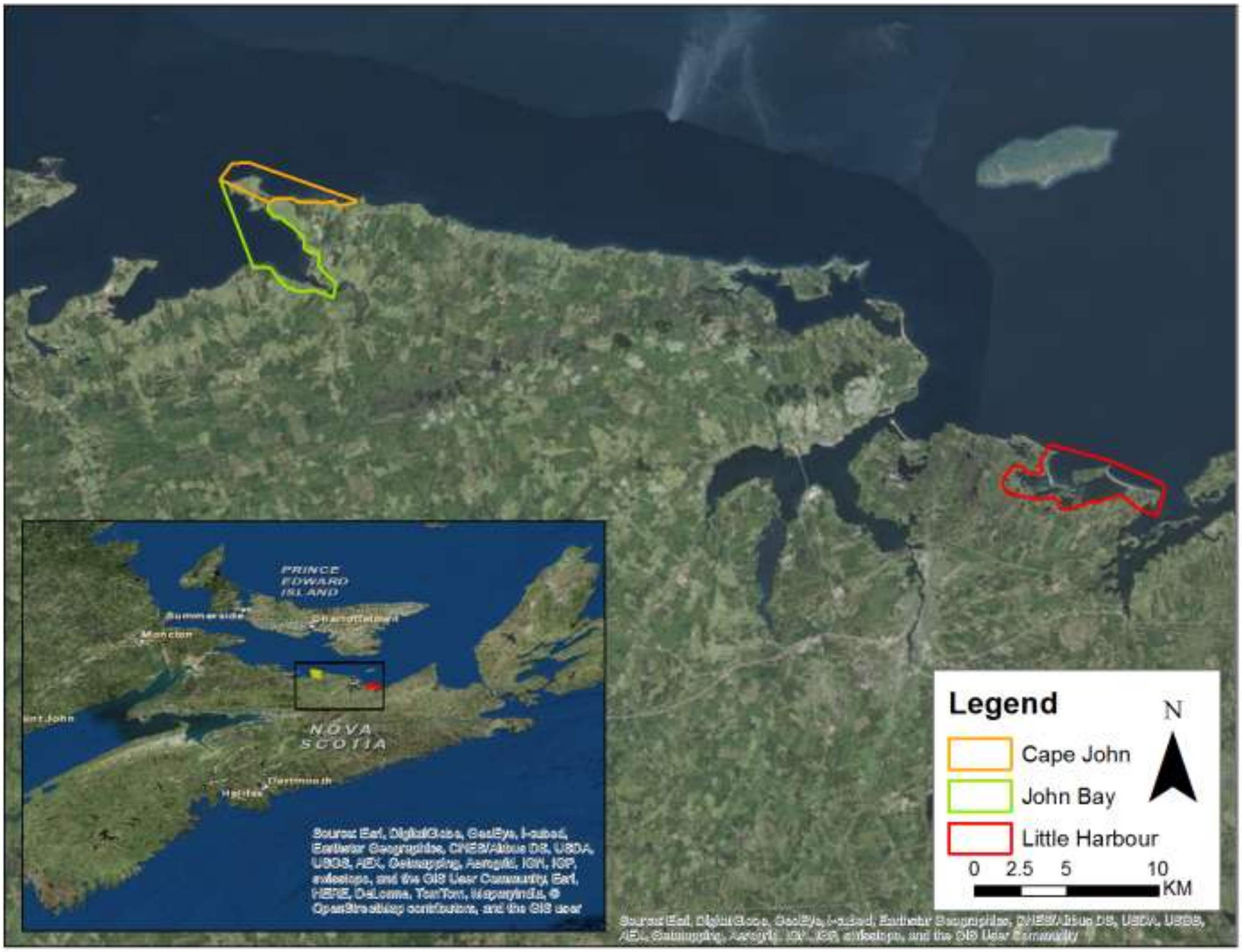

Figure 1: Study area showing survey polygons for John Bay, Cape John, and Little Harbour.

Funding Partner
ACOA
GeoNOVA
NS Natural Resources
NS Fisheries and Aquaculture
DFO- Gulf Fisheries Centre
NS Agriculture
NS Inland Fisheries Division

Table 1: Funding Partners for the September 2014 topo-bathy lidar survey of Cape John-John Bay and Little Harbour.

This report provides details on fieldwork and instrumentation in the Methods section, including details on the Chiroptera II lidar sensor used for the surveys (Section 2.1) and the survey details (Section 2.2), the meteorological conditions during the survey (Section 2.2), the ancillary data collected on the ground during the lidar flights (Section 2.4), and the data processing methods (Section 2.5). The results include lidar point cloud representations as well as maps of bathymetry, reflectance, and possible eelgrass coverage, and are found in Section 3.

1.1 Copyright and Data Ownership

The Applied Geomatics Research Group of the Nova Scotia Community College maintains full ownership of all data collected by equipment owned by NSCC and agrees to provide the end user who commissions the data collection a license to use the data for the purpose they were collected for upon written consent by AGRG-NSCC. The end user may make unlimited copies of the data for internal use; derive products from the data, release graphics and hardcopy with the copyright acknowledgement of "Data acquired and processed by the Applied Geomatics Research Group, NSCC". Data acquired using this technology and the intellectual property (IP) associated with processing these data are owned by AGRG/NSCC and data will not be shared without permission of AGRG/NSCC.

2 Methods

2.1 Sensor Specifications and Installation

The lidar used was a Chiroptera II (CH2) integrated topographic bathymetric lidar sensor equipped with a 60 megapixel multispectral camera. The system incorporates a 1064 nm near infrared laser for topographic (topo) laser for ground returns and a green 532 nm laser for hydrographic (hydro) returns (Figure 2). The lasers utilize a Palmer scanner, which forms an elliptical pattern with angles of incidence of 14^{o} forward and back and 20^{o} to the sides of the flight track. This enables more returns, lidar coverage from many different angles, on vertical faces, causes less shadow effects in the data, and is less sensitive to ocean wave interaction. The beam divergence of the topo laser is 0.5 mrad and from the hydro laser (green) is 3 mrad. The topo laser can scan with a pulse repetition frequency up to 400 kHz and the hydro laser can scan with a pulse repetition frequency up to 35 kHz. The hydro laser is limited by depth and water clarity, and has a depth penetration rating of approximately 1.5 x the Secchi depth (a measure of turbidity or water clarity). The Leica RCD30 camera collects co-aligned RGB+NIR motion compensated photographs which can be orthorectified and mosaicked into a single image in post-processing, or analyzed frame by frame for maximum information extraction. The RCD30 is a 60MPIX camera with a focal length lens of 53 mm and produces images 6732 by 9000 pixels in the across and along track direction, respectively. The across track field of view is 54^{o}.

AGRG-NSCC does not own an aircraft, only the sensor, and thus partnered with our Canada Foundation for Innovation project partner, Leading Edge Geomatics (LEG) to assist in the operations of the survey and arranging the aircraft. For the September 2014 field campaign, a twin engine aircraft that was certified to carry the Chiroptera II sensor suite and had a hole suitable to house the sensor head. The main base of operations for the September mission was Fredericton, NB. The aircraft arrived in Fredericton from Virginia (Dynamic Aviation) on Sunday, Sept. 21. The CH2 sensor also arrived on Sunday with AGRG researchers from Middleton, NS. Staff from Leica Geosystems, who produce the CH2, were delayed in their arrival to Fredericton until late Sunday night.

The sensors were installed in the aircraft on Monday, September 22 (Figure 3a). The aircraft had a hole cut in the bottom for the laser and cameras to image the ground and installation involved fitting the sensor head into the hole (Figure 3c) and the associated control rack on the floor and user display screens on another rack in the aircraft (Figure 3b). Along with the lasers and high resolution camera, the lidar system also includes a 5 megapixel quality assurance camera that the lidar operator is able to view during the flight, along with the waveform of the returning pulse and the flight plan (Figure 3b). Figure 3d shows the downward facing portion of the sensor head, including the red (topographic) and green (bathymetric) lasers, which shoot and return to the large red circles; the lenses on the left and right are the low and high resolution cameras, respectively. During installation the laser systems and camera were calibrated and aligned with the navigation system which consists of a survey grade GPS mounted on the roof of the aircraft and an inertial measurement unit (IMU) mounted above the laser system. Calibration flights were conducted over Fredericton at altitudes of 400 m and 1000 m on Tuesday, Sept. 23, following a wind and rain event on Sept. 22.

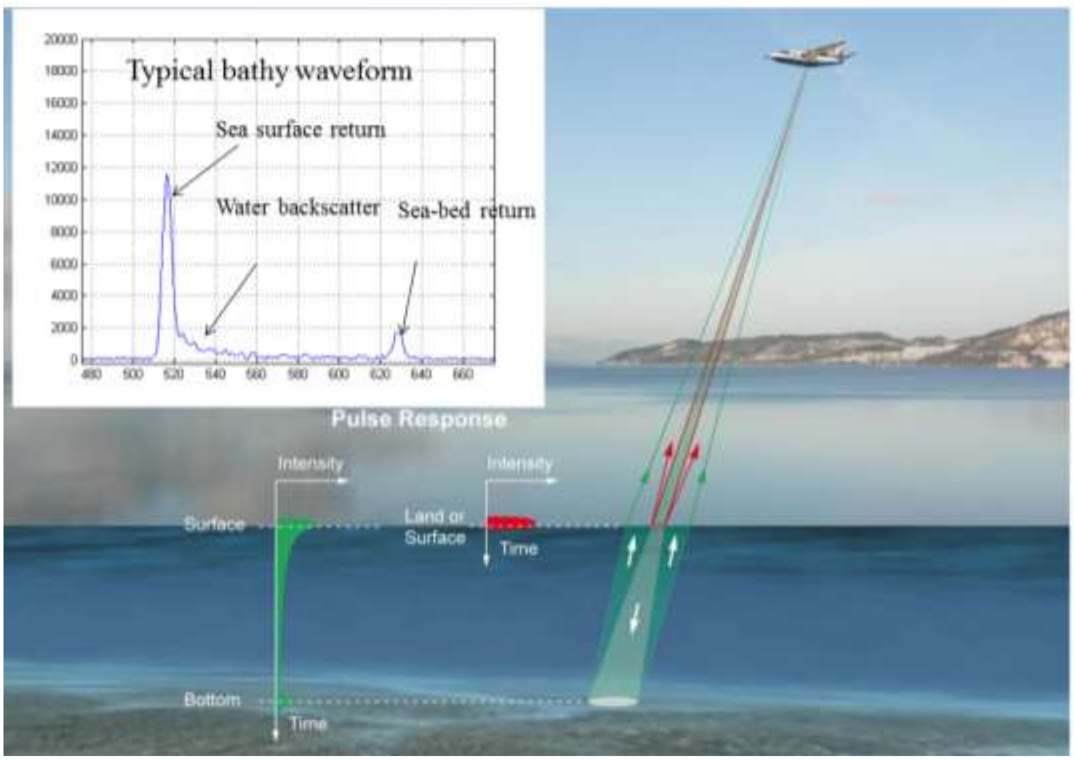

Figure 2 Principals of topo-bathymetric lidar. The system utilizes two lasers: a near infrared and a green laser to surface the land and marine topography.

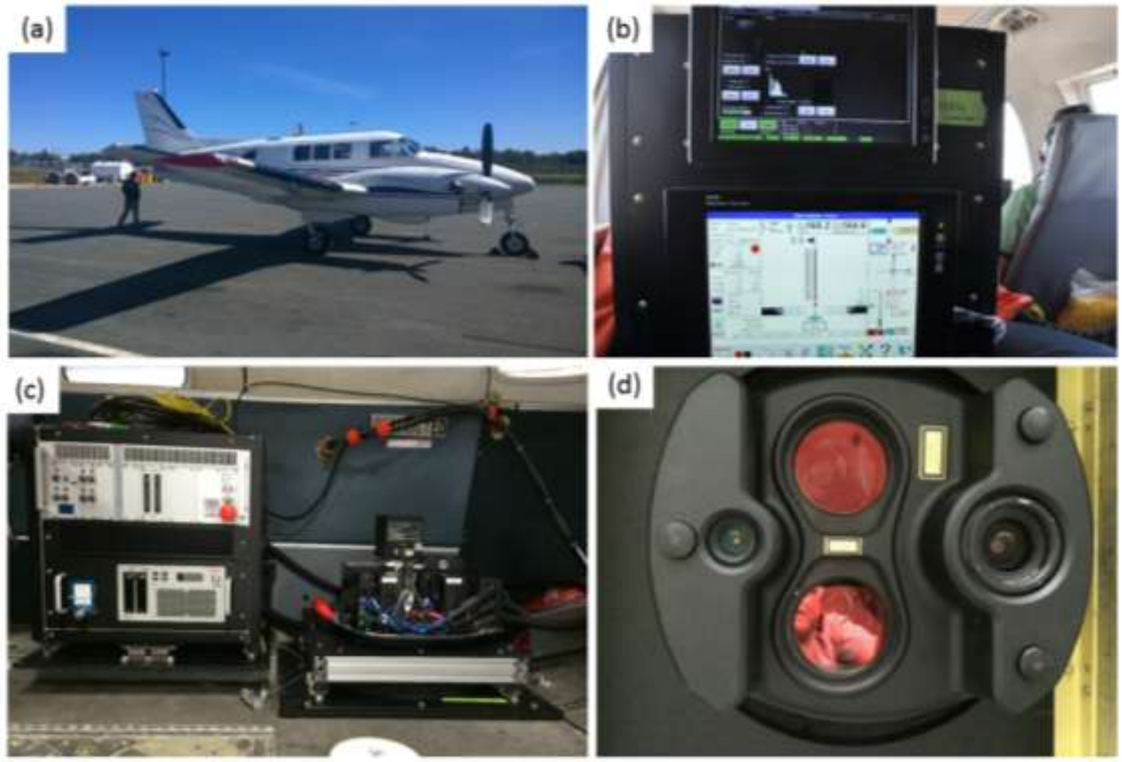

Figure 3: (a) Aircraft used for September 2014 lidar survey; (b) display monitors on a rack as seen by lidar operator in-flight; (c) main body of sensor control rack (left) and lasers and cameras located over the hole cut in the bottom of the plane (right); (d) large red circles are the lasers; the RCD30 lens (right) and low resolution camera (left) as seen from the bottom of the aircraft.

2.2 Meteorological Conditions

Meteorological conditions during topo-bathy lidar data collection are an important factor in successful data collection. As the lidar sensor is limited by water clarity, windy weather that stirs up sediment in the seawater can prevent good laser penetration. Rainy weather is not suitable for lidar collection, and the glare of the sun must also be factored in for aerial photography. A weather station was installed at Cape John (Figure 4a) as part of the previous studies at that location, and the data measured there was used to both check on the study area remotely, and also to use in post-processing. Figure 5 shows meteorological data at Cape John for the month of September. In the week before the survey, the data indicates several storm events during the planned survey times: a strong northerly wind event between Sept. 18 and 20, and shorter duration south-westerly wind events on Sept. 20 and 21. The drop in barometric pressure and rainfall associated with the Sept. 21-22 storm event is evident in the Cape John weather data (Figure 5). Figure 6a shows the wind data at Cape John in the week before the survey in more detail and shows the strong northerly wind event between Sept. 18 and 20. Figure 6b shows wind data at Cape John during the week of the lidar survey, Sept. 22- 29, showing strong southerly winds on Sept. 22, and strong north winds on Sept. 24.

At Little Harbour we do not have an AGRG weather station so relied on Environment Canada's permanent meteorological network for data. The nearest weather station was at Caribou, approximately 15 km away (Figure 4b). Wind data for

Caribou before and during the lidar survey are shown in Figure 7a and b and shows the same wind events as at Cape John, although of slightly different magnitudes and timing.

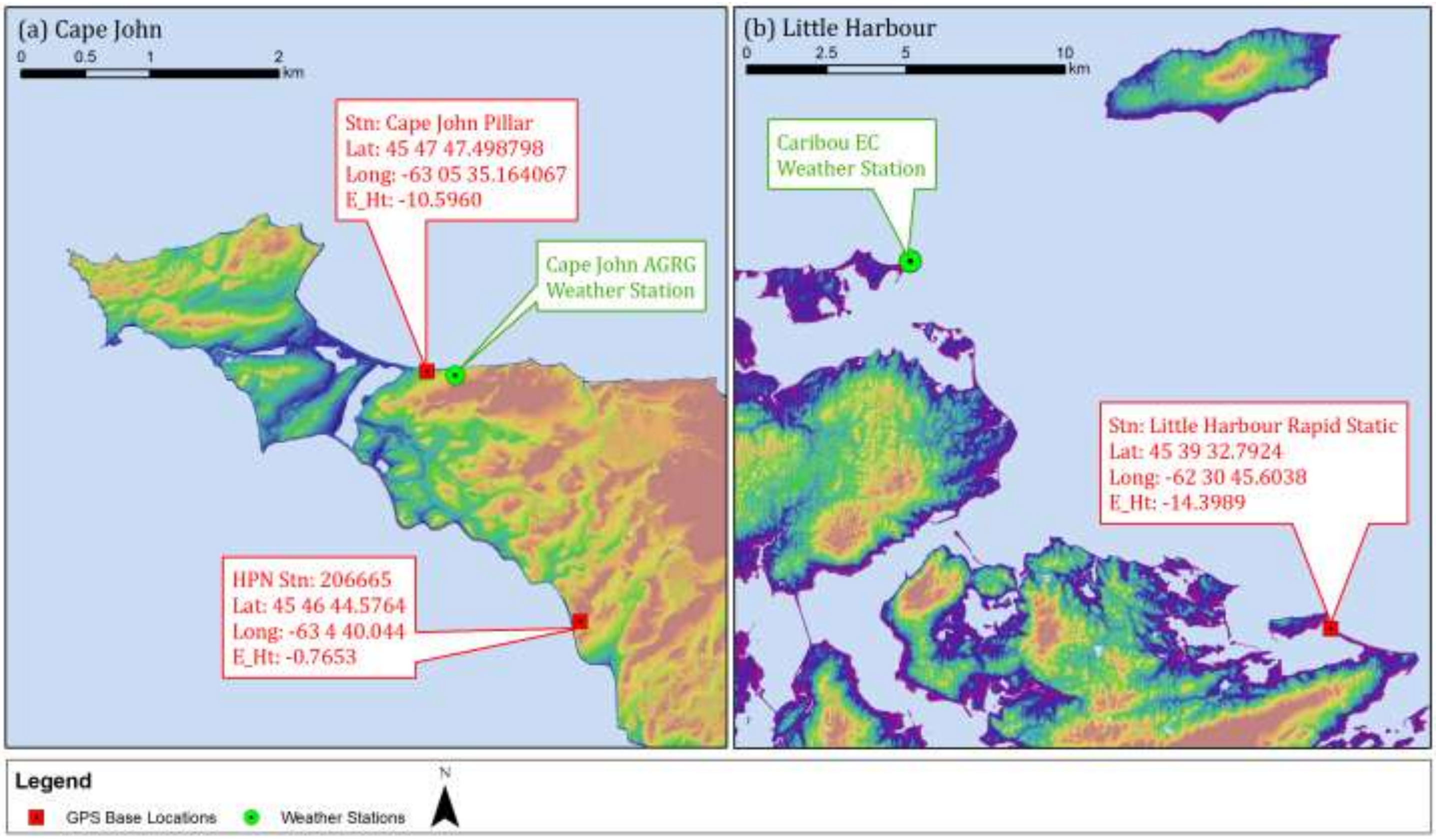

Figure 4: Cape John/John Bay and Little Harbour GPS base stations and weather station maps. Background map is a 20 m elevation model.

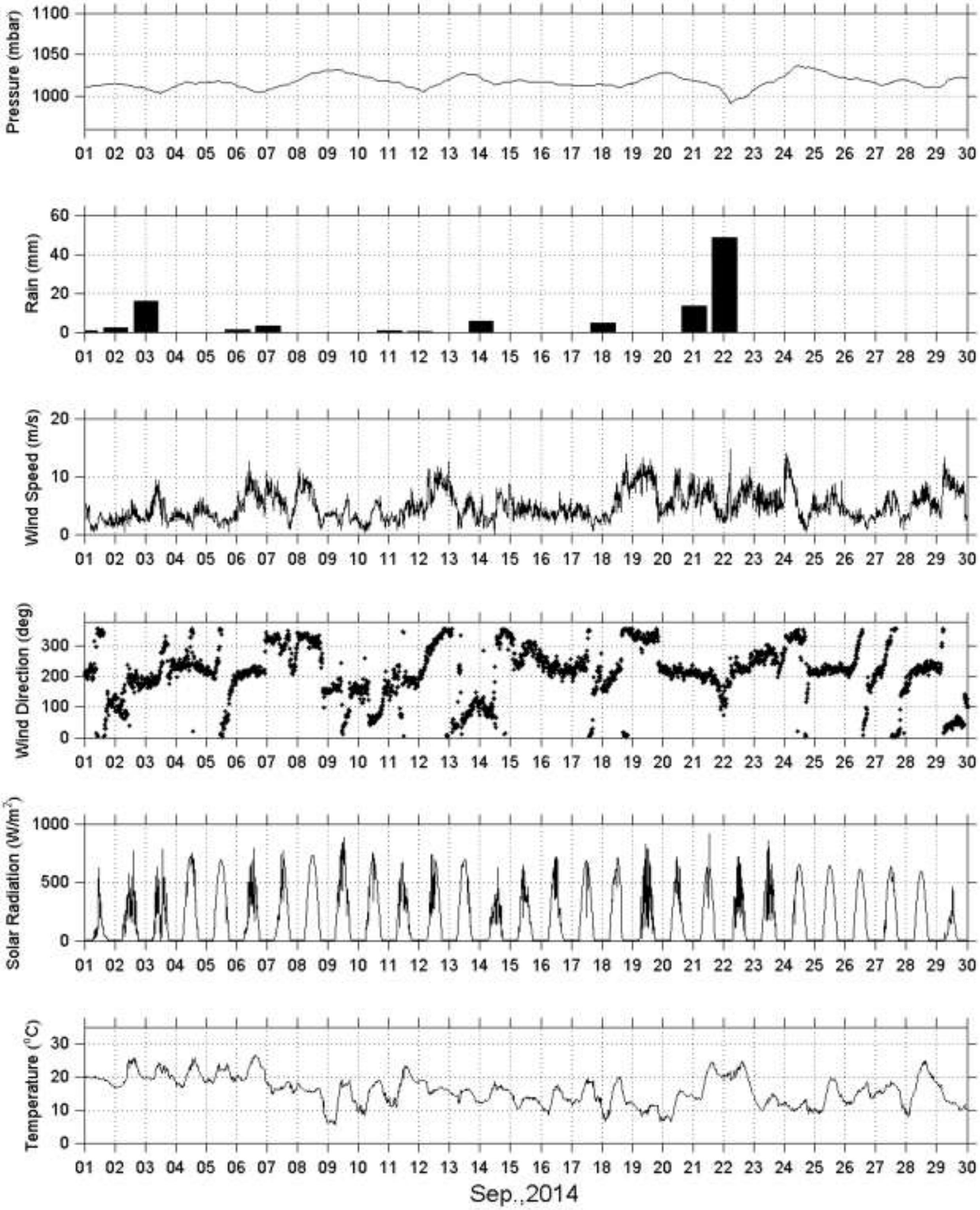

Figure 5: Meteorological data collected at the AGRG weather station at Cape John during September, 2014.

(a)

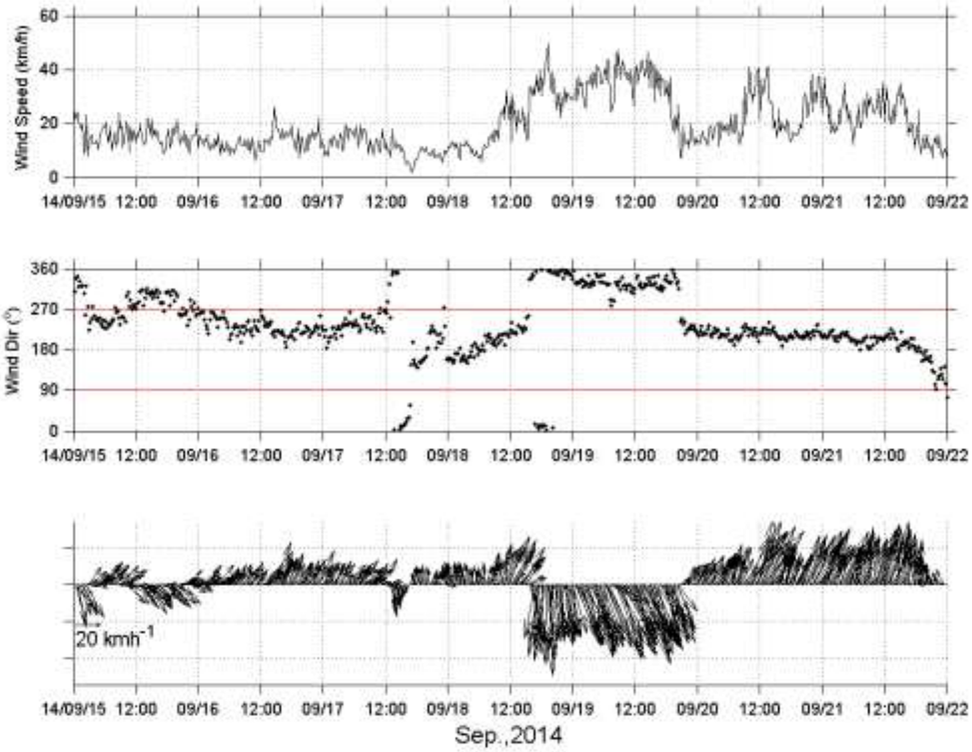

(b)

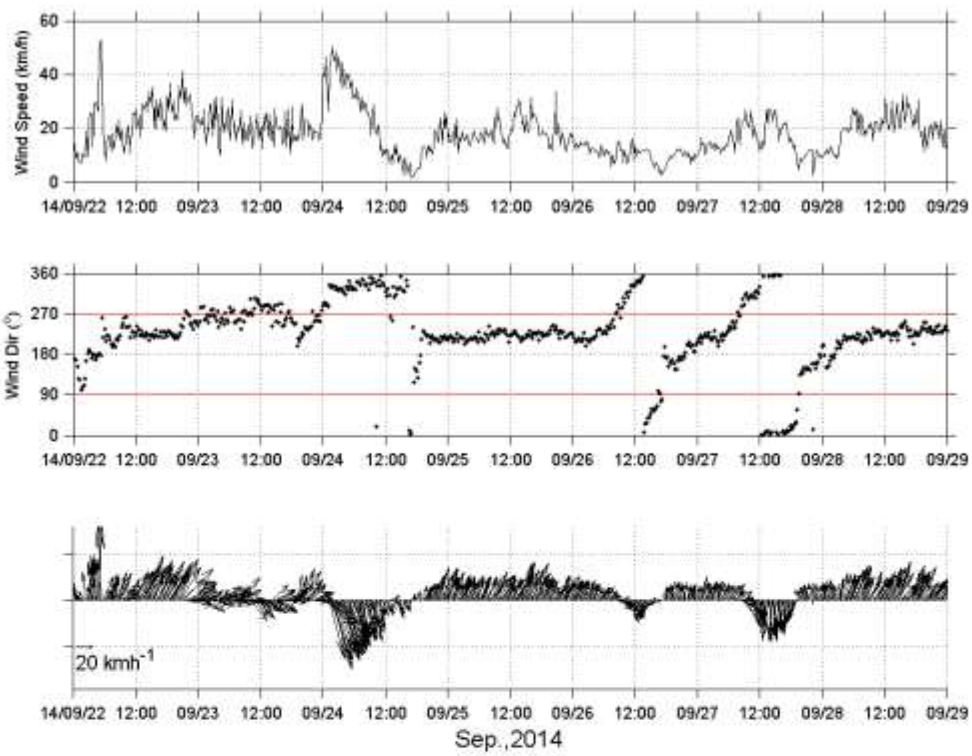

Figure 6: Wind speed (top panel) and direction (middle panel) collected at the AGRG weather station at Cape John between (a) September 15 and 22, and (b) September 22 and 29, 2014 at 15 minute intervals. The lower panels show a vector plot of the wind, where the arrows point in the direction the wind is blowing.

(a)

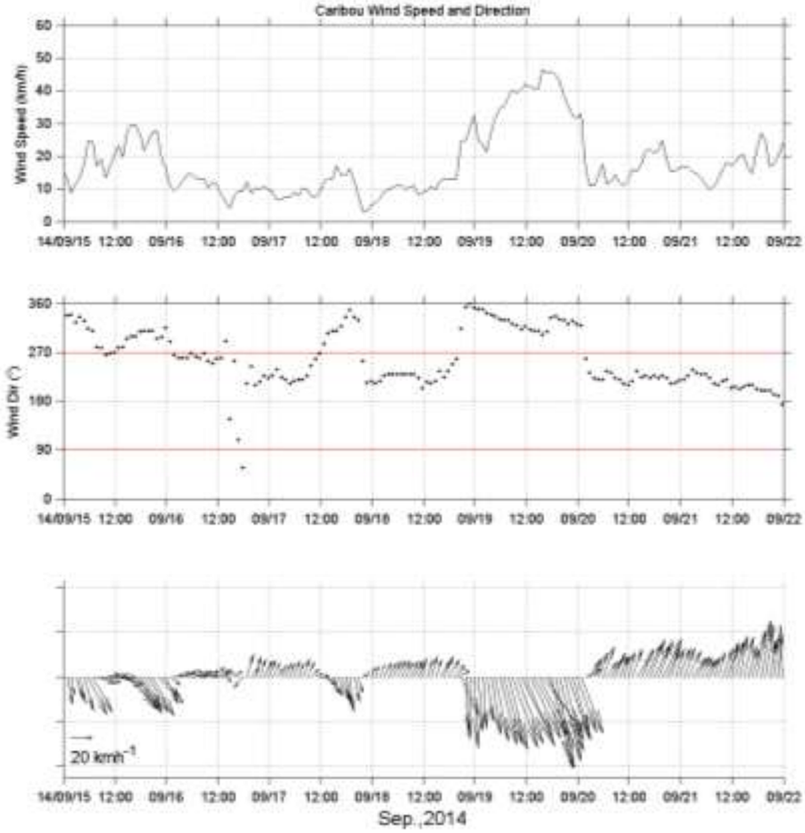

(b)

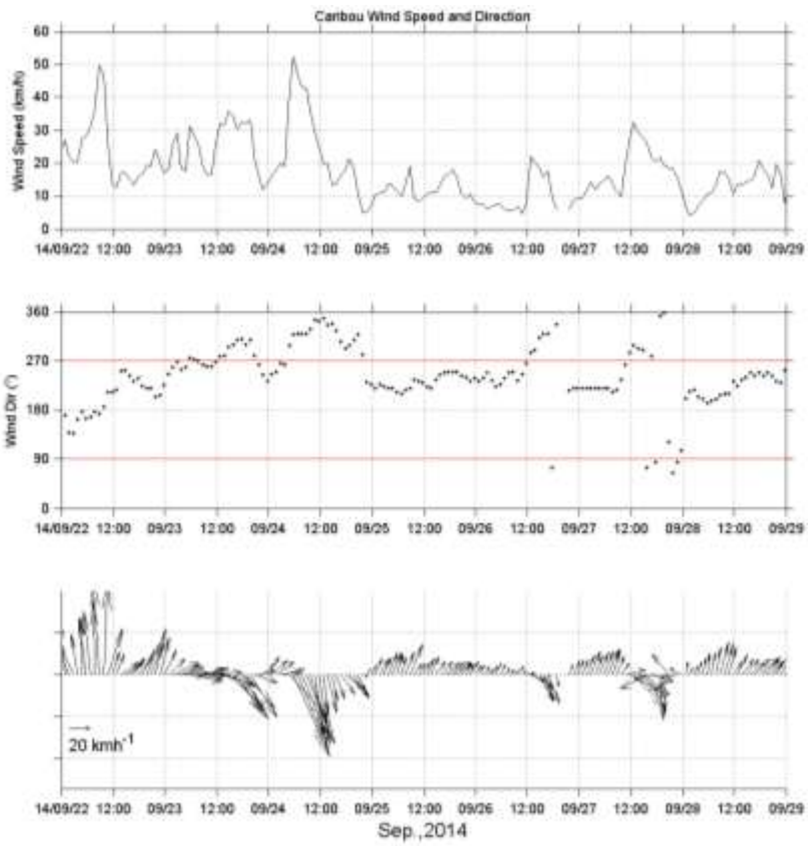

Figure 7: Wind speed (top panel) and direction (middle panel) collected at the EC weather station at Caribou between (a) September 15 and 22, and (b) September 22 and 29, 2014 at 1 hour intervals. The lower panels show a vector plot of the wind, where the arrows point in the direction the wind is blowing.

2.3 Lidar Survey Details

A lidar survey of Little Harbour was conducted on Sept. 25, 2014. Planned flight lines are shown in Figure 8. Planned survey lines for Cape John and John Bay are shown in Figure 9. Winds played a significant role in the lidar survey at Cape John and John Bay, as the fine sediment in the area is easily stirred up by even a moderate wind. The wind conditions at Cape John and John Bay were not ideal during the planned survey time. The winds speed at Cape John exceeded 40 km/hr on Sept. 18th and 19th (Figure 6a) and on the 20th and 21st the wind still persisted at just under 40 km/hr. On the 22nd the winds picked up again and exceeded 40 km/hr in the early morning then eventually died back to 20 km/hr through the 23rd but again picked up and exceeded 40 km/hr on the 24th when they moved around to come from the northwest before dying off late in the day on the 24th (Figure 6b). Though winds continued between 20-40 km/hr on the 25th from the southeast (Figure 6b) a survey was attempted at Cape John, but the survey was aborted due to poor water clarity. As the wind finally began to calm down on the 26th in the late afternoon a second survey was conducted. This provided the best opportunity for data collection during the time the aircraft was available, as the winds increased again on the 27th (Figure 6b).

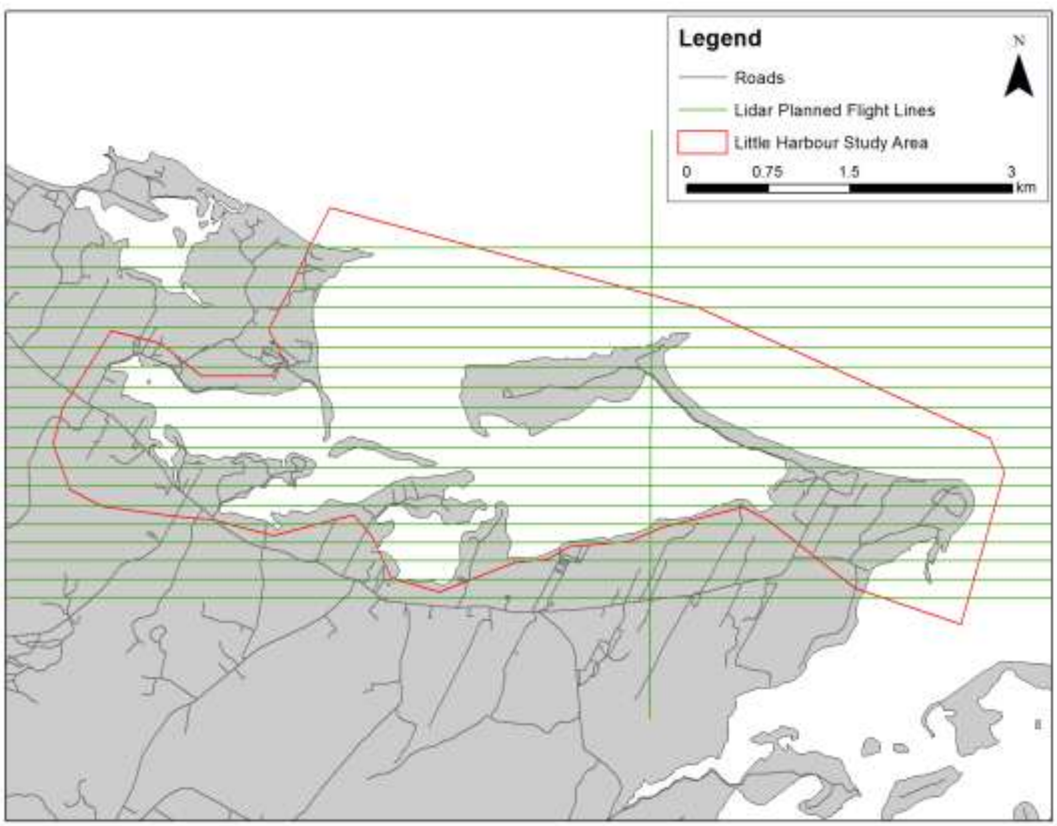

Figure 8: Little Harbour planned flight lines.

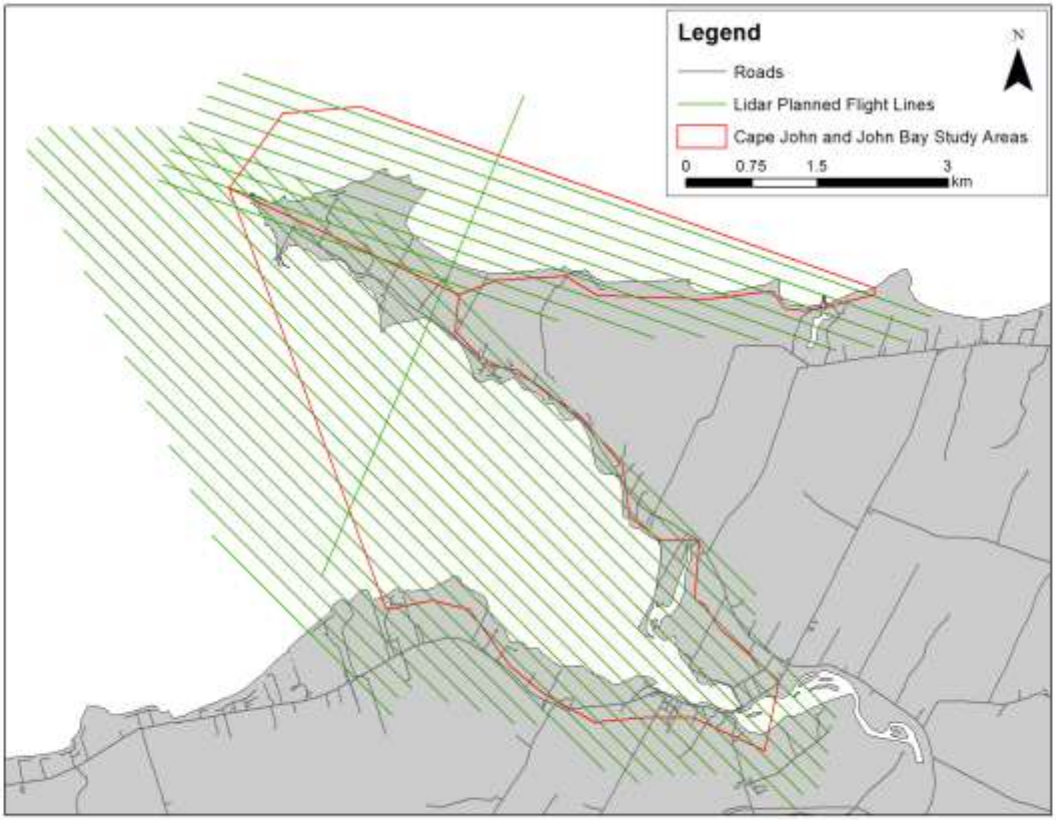

Figure 9: Cape John and John Bay planned lidar flight lines.

The difference of one day without significant wind and wave action can allow the suspended sediment to settle and reduce the turbidity (Figure 10 and Figure 11). Figure 10 and Figure 11 not only show the turbidity in the water at John Bay but also the waves on the 25th on the John Bay side of the peninsula as a result of the strong winds from the southeast. Figure 10 andFigure 11 show that no details of the seabed can be observed on the John Bay side on Sept. 25 but the sand bars are visible on the 26th.

Unfortunately, there was a trade-off situation to surveying in the late afternoon on the 26th, where winds were lower but light conditions were diminishing as the sun began to set. As will be shown in the results section, the fog and low sunlight ultimately did result in some loss of data, but nowhere near the amount that would have been lost had we surveyed during stronger winds. On September 27 another single line was flown across the Cape John study area to test the water clarity because the aircraft was in the vicinity, en route from another study area, but turbidity was again high due to wind.

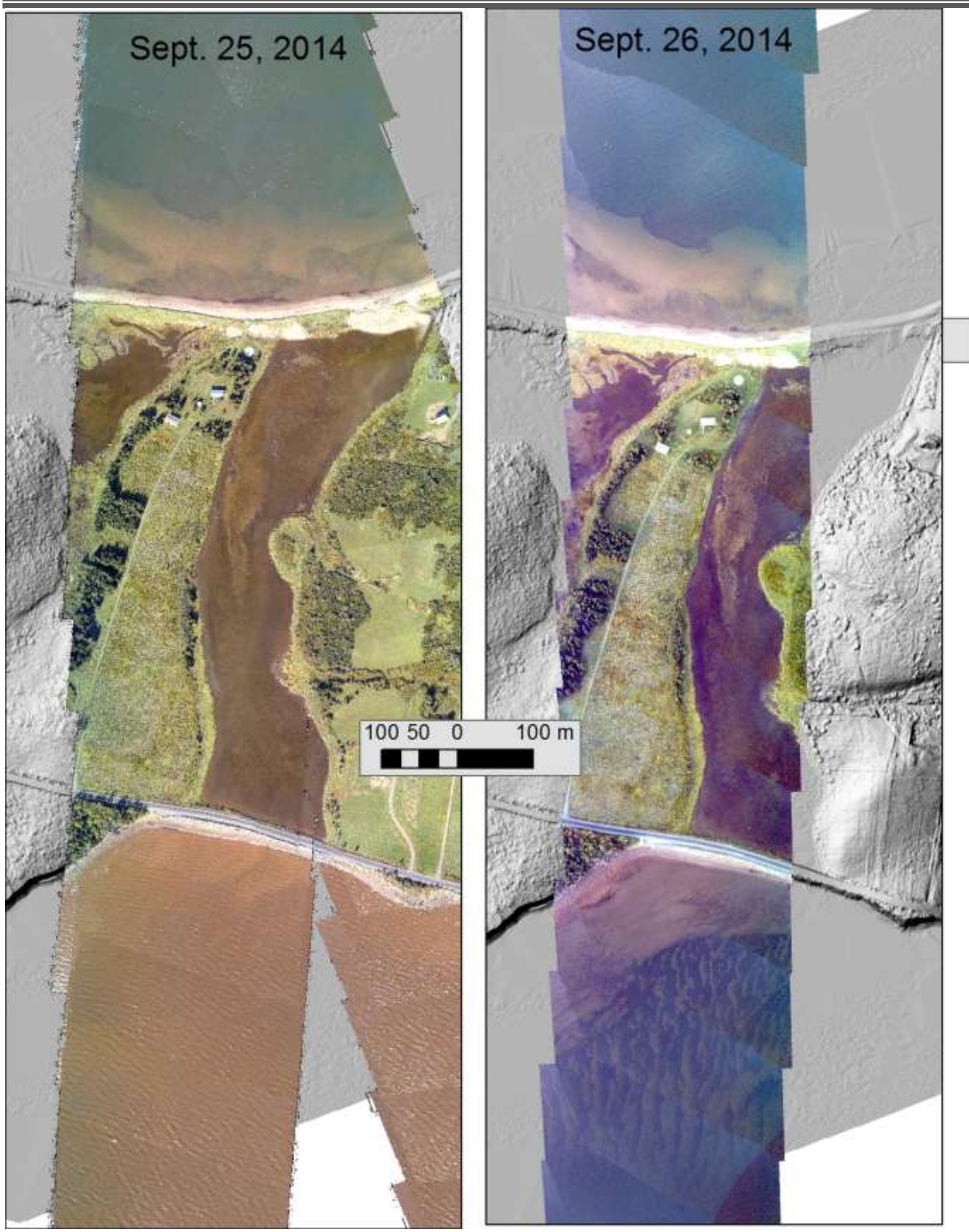

Figure 10: Comparison of water clarity at Cape John showing Sept. 25 on the left and Sept. 26 on the right.

Figure 11: Close up on John Bay side of the Cape John peninsula to show the difference in turbidity between Sept. 25 (left) and Sept. 26 (right). Note that the submerged sand bars are visible on the 26th but not on the 25th.

2.4 Ground Truth Data Collection

Ground truth data is another important aspect of topo-bathy lidar data collection. The ground truth data we collected for the Cape John, John Bay, and Little Harbour study areas are summarized in Table 2 and Figure 12, Figure 13, and Figure 14. Some sensors were able to collect continuous data, such as the echosounder, while other data were collected at waypoints randomly distributed throughout the study area. At Little Harbour, our partners from DFO Gulf Region from Moncton, NB were able to join us on the water and provide additional ground truth data. Poor weather leading up to the Cape John survey and the associated uncertainties about flying and the short notice to decide to acquire data on Sept. 26th meant that no ground truth data were collected during the lidar survey. Additional data were collected for Cape John and John Bay in late October, including underwater photographs.

At Little Harbour a 15 foot aluminum boat was used for boat-based ground truth data collection, and at Cape John and John Bay a 24 foot Bayliner was used. During the fieldwork Hydrolab turbidity sensors coupled with pressure sensors were used to measure turbidity at John Bay and Little Harbour. Figure 15 shows turbidity data in the top 0.5 m of water collected on Sept. 24, and shows that turbidity was generally higher near the mouth of River John. Figure 16 shows turbidity collected at Little Harbour on Sept. 25. The turbidity measurements at John Bay were 4-5 times higher than at Little Harbour. Secchi disks provide reliable indications of water clarity and were used to take measurements throughout the study areas.

Survey Area	Date of ground truth	Base station for aircraft	GPS on boat	Secchi	Turbidity	Depth	Photos
John Bay	Sept. 24	N/A	Garmin	Yes	Yes	Sonar	No
Cape John and John Bay	October	N/A	RTK	No	No	Sonar	GoPro
Little Harbour	Sept. 25	GS14 base rapid static from HPN	RTK	Yes	Yes	Single beam echo-sounder (2), lead ball	GoPro
Cape John and John Bay	Sept. 25	GS14 base AGRG Pillar					Landscape turbidity
Cape John and John Bay	Sept. 26	CANSEL Active GPS network					

Table 2: Ground truth data summary. The Little Harbour lidar survey was Sept 25; the Cape John and John Bay lidar survey was Sept. 26.

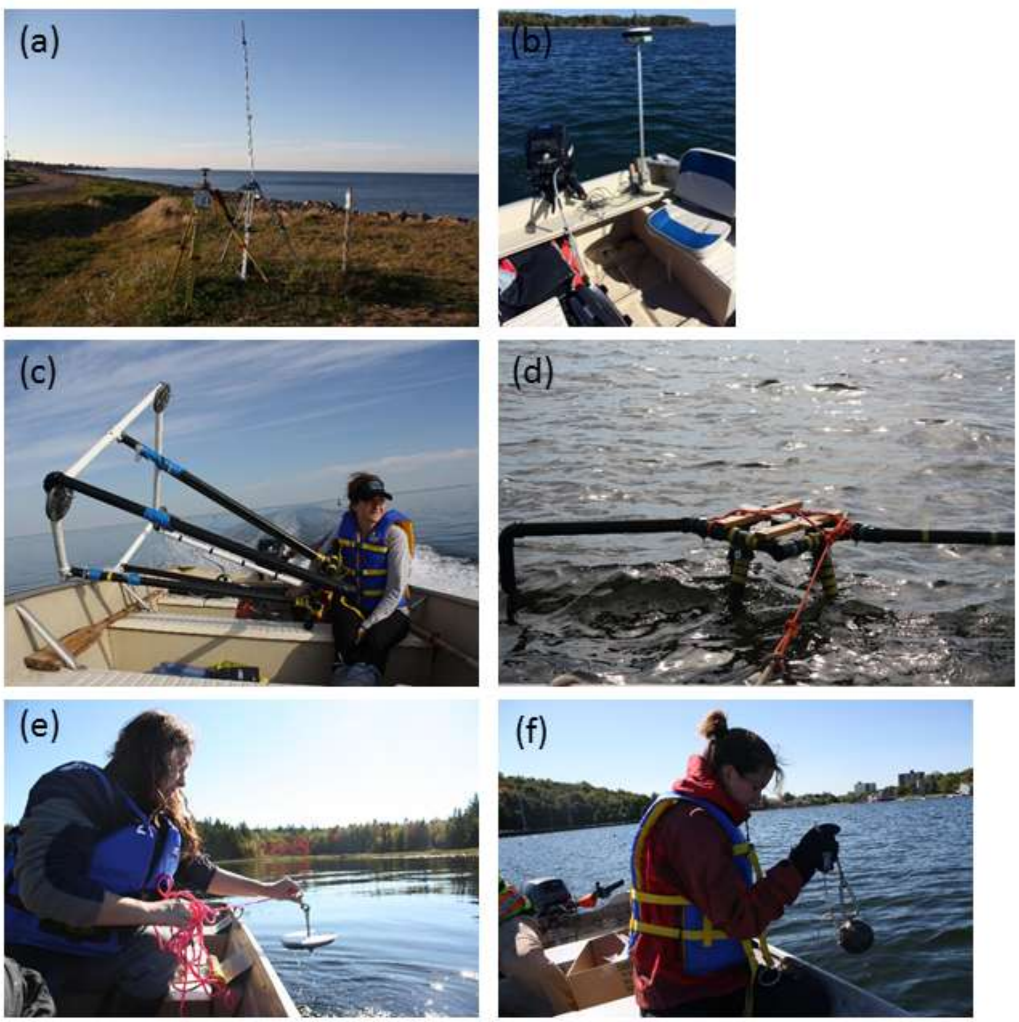

Figure 12: (a) RTK GPS base station; (b) RTK GPS on the 15' aluminum boat; (c, d) GoPro camera quadrat; (e) Secchi depth measurements; (f) depth validation with a lead ball.

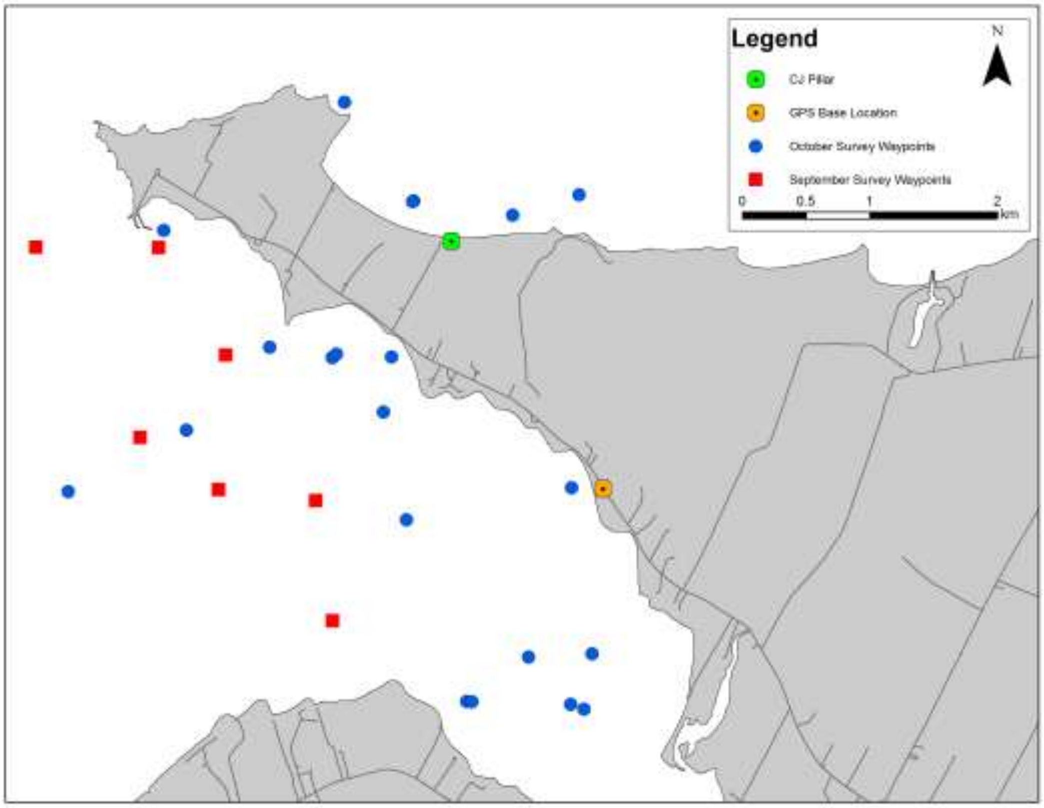

Figure 13: Ground truth data collected at Cape John and John Bay in September and October.

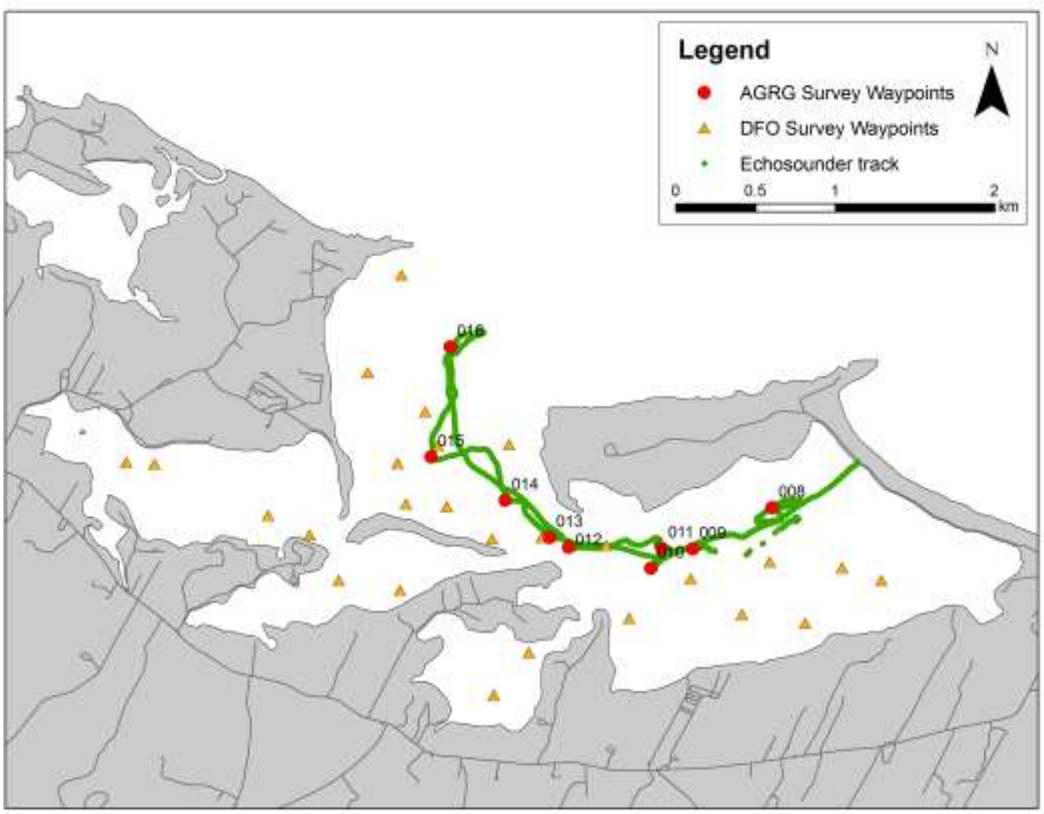

Figure 14: Ground truth data collection by AGRG and DFO at Little Harbour.

Figure 15: Turbidity data collected at John Bay on Sept. 24 in the top 0.5 m of water. Backdrop is a Worldview satellite image from 2010.

At Little Harbour our Leica GS14 RTK GPS system was used to set up a base station over a temporary marker established in the parking lot of the provincial park that was previously positioned relative to a NS High Precision Network (HPN) monument. At Cape John and John Bay the CANSEL virtual network was used. The local GPS data from the base and from the virtual network were required for the aircraft in order to obtain high accuracy positional data. Several methods of depth measurements were employed during ground truthing, including a lead ball on a graduated rope, and several different brands of sonar and echosounder. Having both depth and Secchi depth ground truth measurements throughout the lidar study areas will be valuable in post-processing when no returns were detected, as it will indicate whether the laser did not penetrate due to water depth or clarity or a combination.

Two GoPro cameras were mounted on a 1m by 1 m quadrat, one downward-facing and one facing parallel to the seabed. The quadrat was lowered over the side of the boat to take photographs of the seabed. Bottom type information is useful for research related to laser returns and the lidar reflectance, and also for submerged vegetation mapping validation. Sample images are shown in Figure 17 and Figure 18.

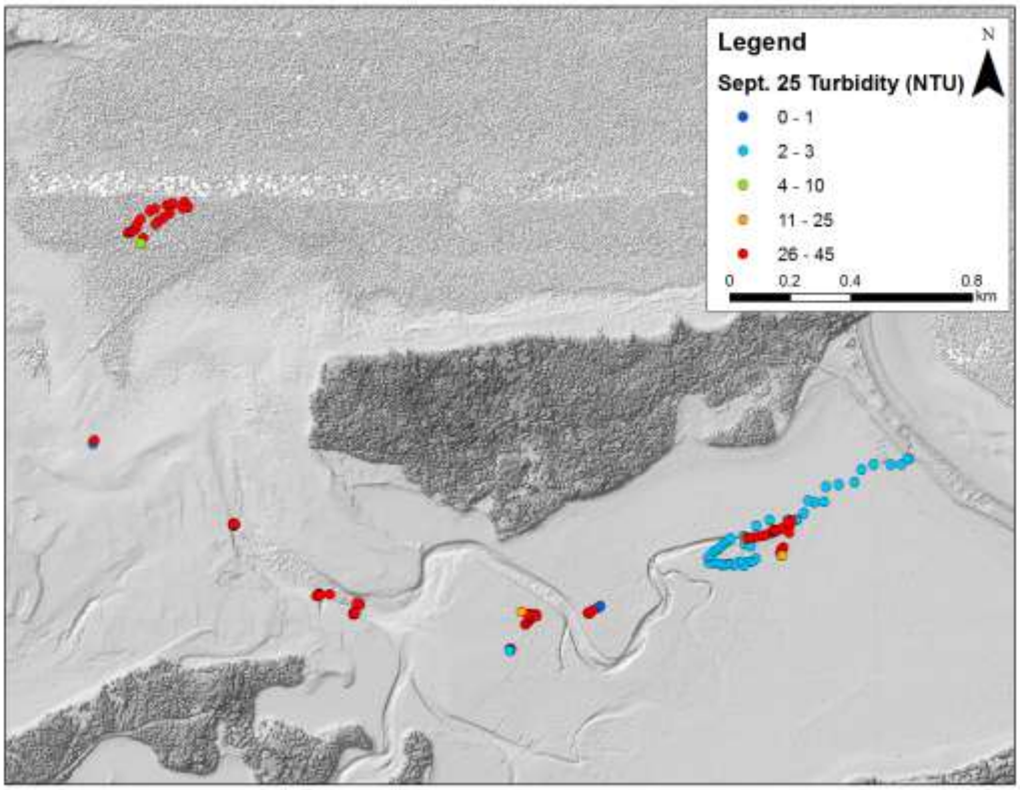

Figure 16: Turbidity data collected at Little Harbour on Sept. 25. Backdrop is DEM hillshade.

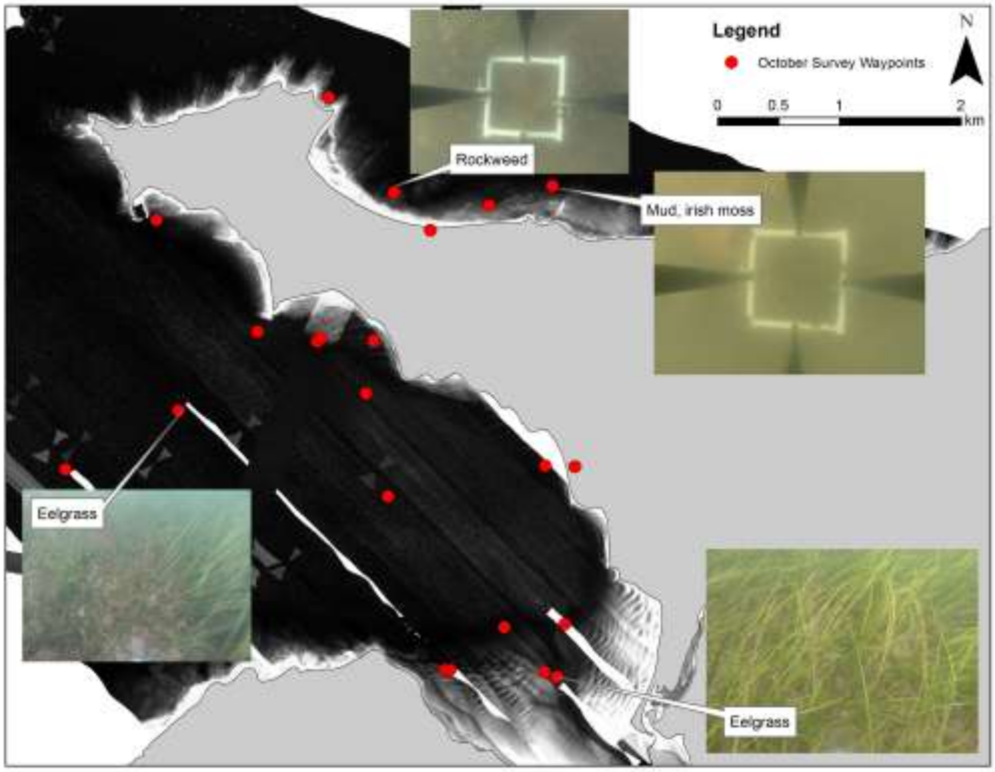

Figure 17: GoPro camera quadrat images at Cape John and John Bay showing all field sample locations (red dots) and with the lidar seabed reflectance as a backdrop.

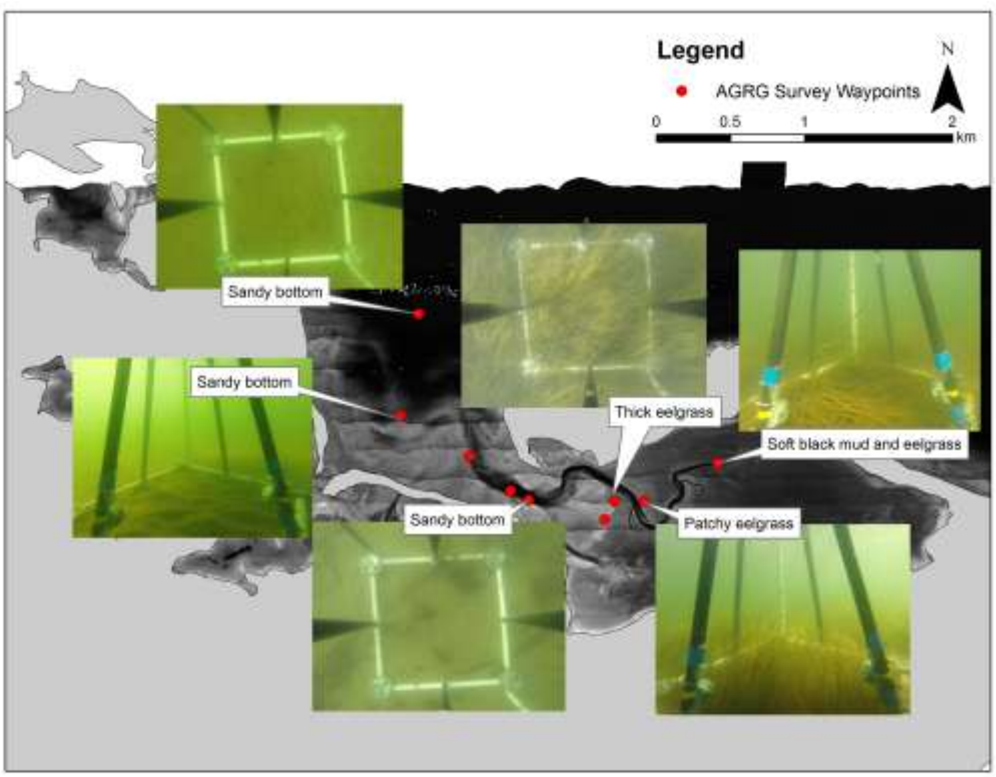

Figure 18: GoPro camera quadrat images at Little Harbour showing all field sample locations (red dots) and with the lidar seabed reflectance as a backdrop.

2.5 Lidar Data Processing

2.5.1 Point Cloud Processing

Once the GPS trajectory was processed for the aircraft utilizing the base station, aircraft GPS observations and combined with the inertial measurement unit, the navigation data was linked to the laser returns and georeferenced. Lidar Survey Studio (LSS) software accompanies the Chiroptera II sensor and is used to process the lidar waveforms into discrete points. The lidar points can be inspected to ensure that the entire study area was captured (Figure 19).

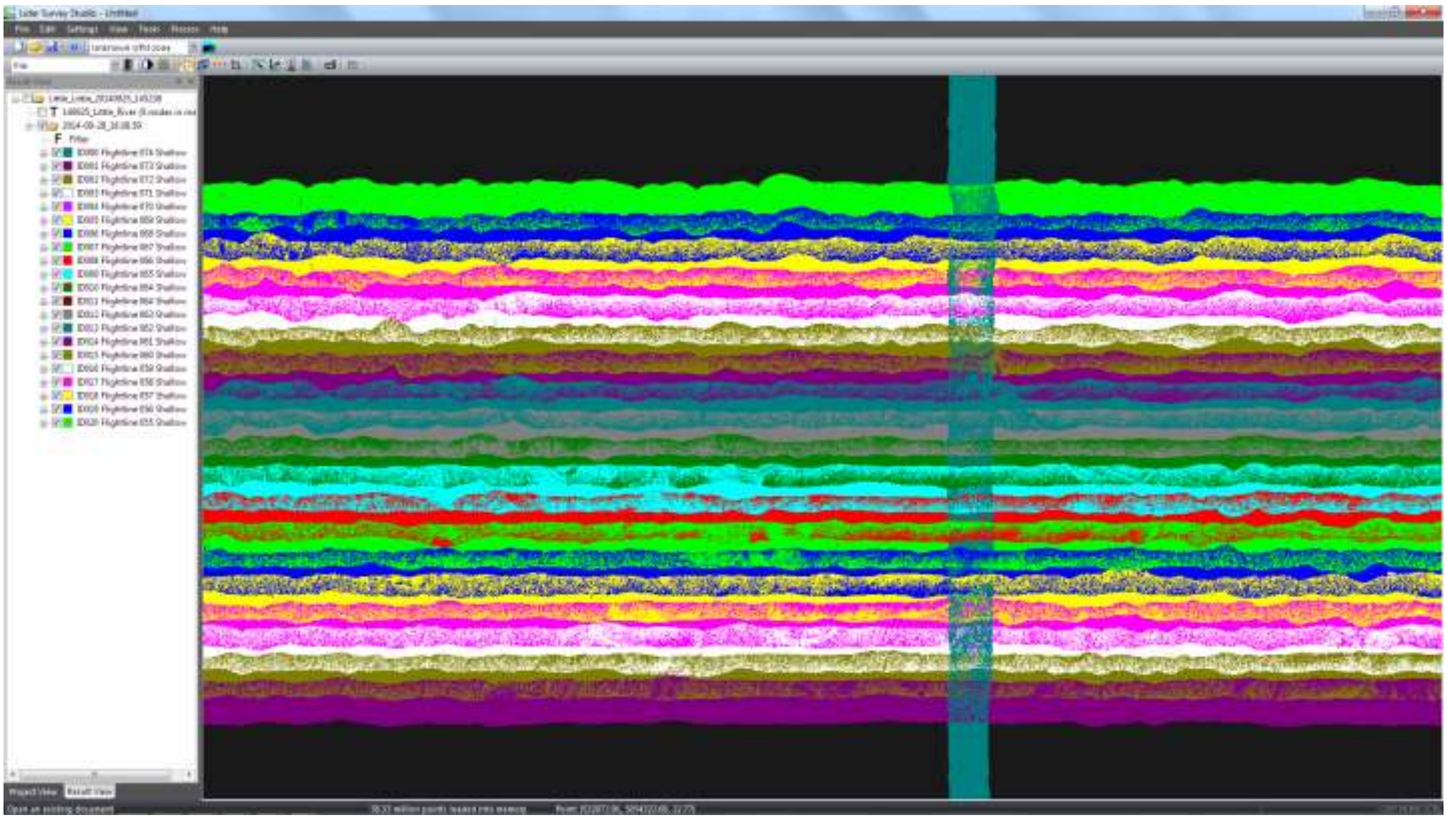

Figure 19: Screen shot from LSS examining the lidar points colour coded for each flight line for Little Harbour. The flight lines were planned with 30% overlap to ensure complete coverage.

One critical step in the processing of bathymetric lidar is the ability to map the water surface. This is critical for two components of georeferencing the final target or targets that the reflected laser pulse recorded: the refraction of the light when it passes from the medium of air to water and the change in the speed of light from air to water. The LSS software computes the water surface from the lidar returns of both the topo (TD) and hydro (HD) lasers. In addition to classifying points as land, water surface or bathymetry, the system also computes a water surface that ensures the entire area of water is covered regardless of the original lidar point density. As mentioned, part of the processing involves converting the raw waveform lidar return time series into discrete classified points using LSS signal processing; points include ground, water surface, seabed, etc. Waveform processing may include algorithms specifically for classifying the seabed through high turbidity water columns, where required. The points can be examined in LSS both in plan view and in cross-section view (Figure 20). The waveforms can be queried for each point so that the location of the waveform peak can be identified and the type of point defined, for example water surface and bathymetry; the 5MPIX image associated with the lidar points can be accessed as well to aid in processing (Figure 20).

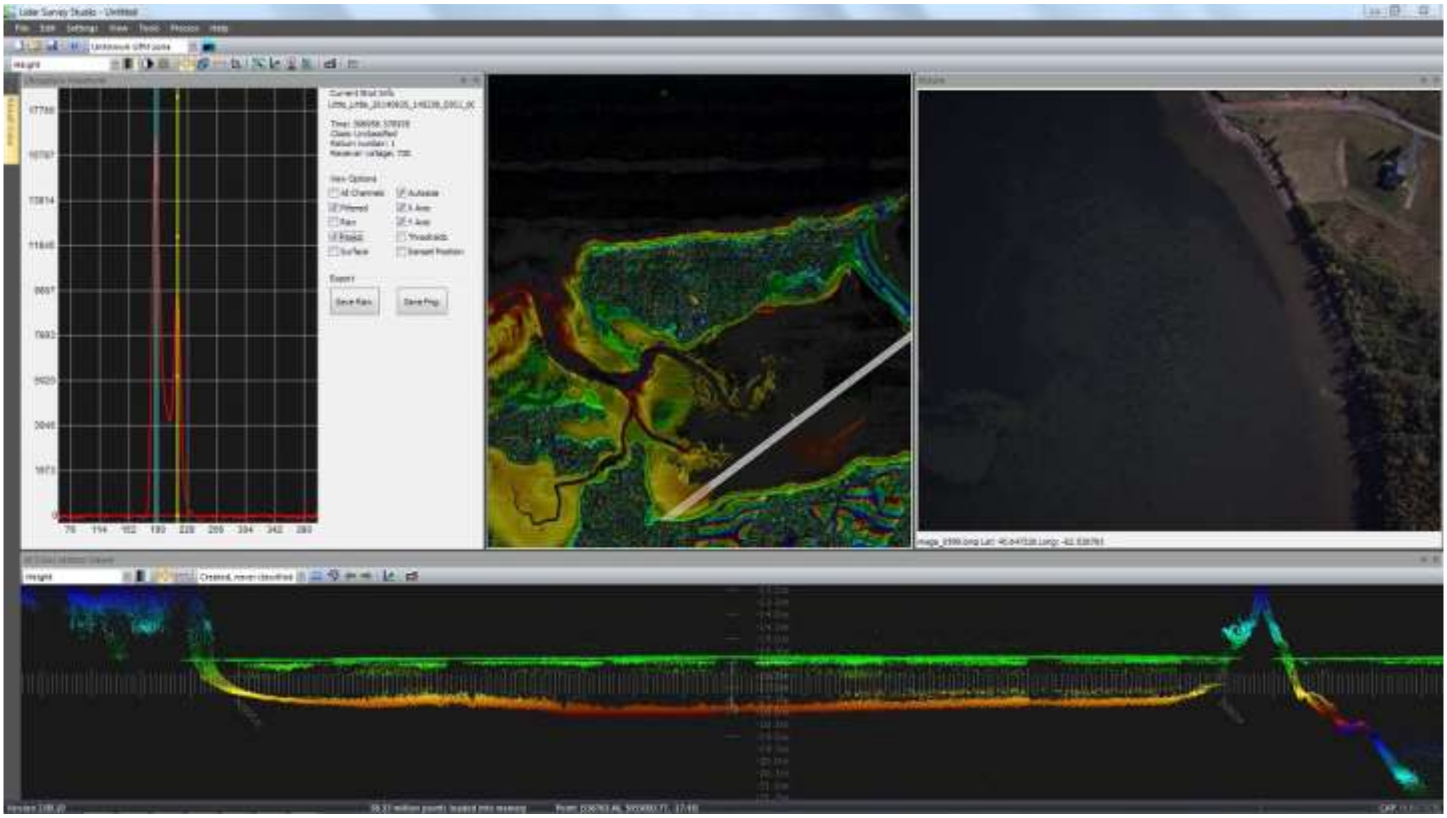

Figure 20: Example of LSS waveforms (top left panel). The top middle image represents the lidar points for Little Harbour colour coded by elevation with a cross-section location defined (heavy white line). The panel on the top right shows the 5MPIX photo associated with the lidar. The cross-section of the lidar point cloud colour coded by elevation are shown in the lower panel from left to right showing the inner bay and dune of Melmerby Beach.

Classified points are analyzed and further refined and filtered to reduce noise and eventually converted into a raster surface at a 2 m spatial sampling interval using ArcGIS. As can be observed in Figure 20 there is a band of lidar points associated with the seabed that must be filtered to obtain a clean surface. Various grids can then be constructed from the lidar classes and attributes including reflectance and elevation. Examples of the gridded surface models from the HD laser include the seabed reflectance (Figure 21) and the digital elevation model (DEM) (Figure 22).

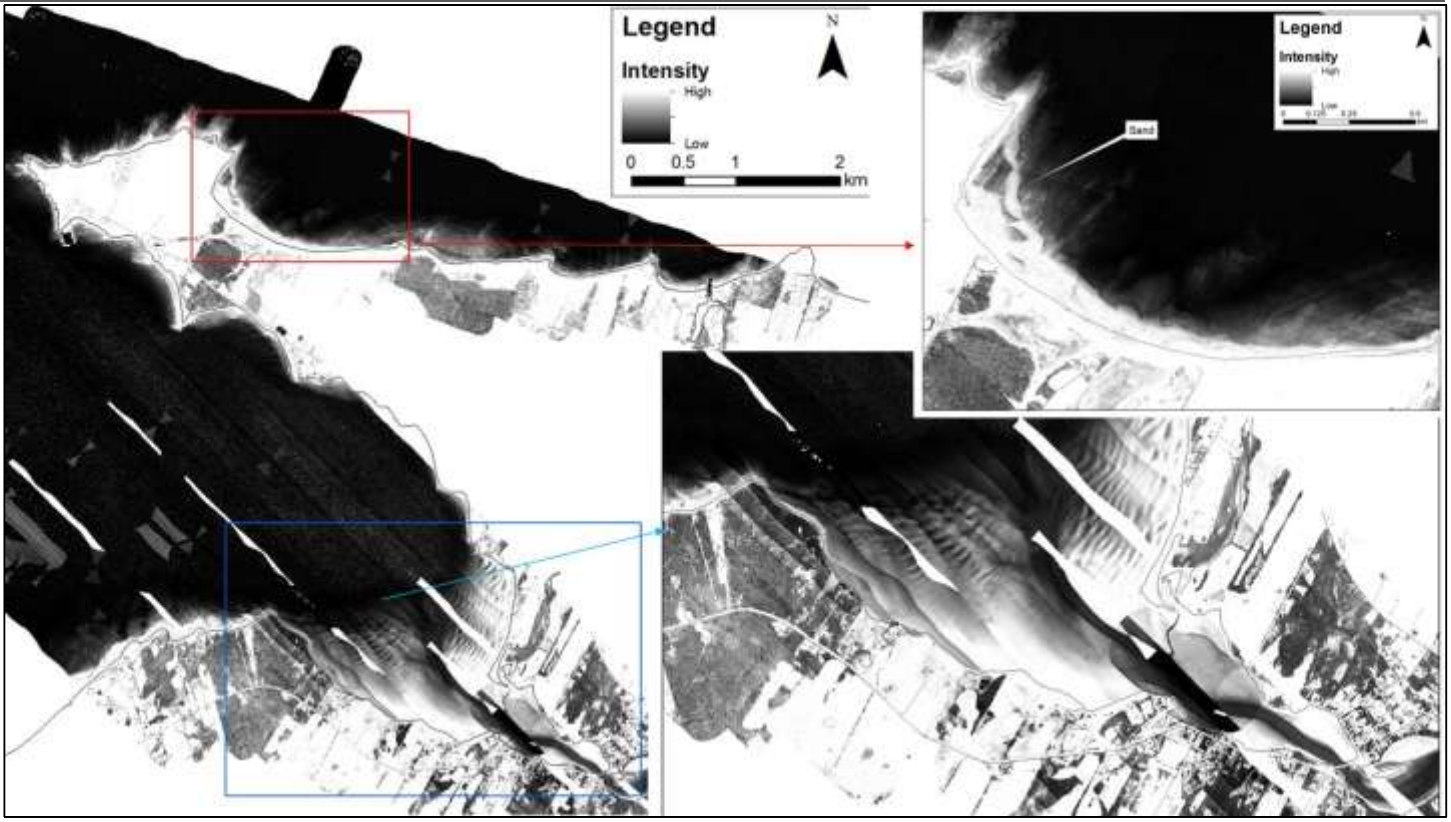

Figure 21: Lidar reflectance of Cape John and John Bay. Left image shows the entire study area with the location of the two inset maps red and blue boxes). Top right panel is of the ocean side of Cape John, the white areas indicate submerged sand bars. The lower right panel shows the mega sand ripples at the mouth of River John.

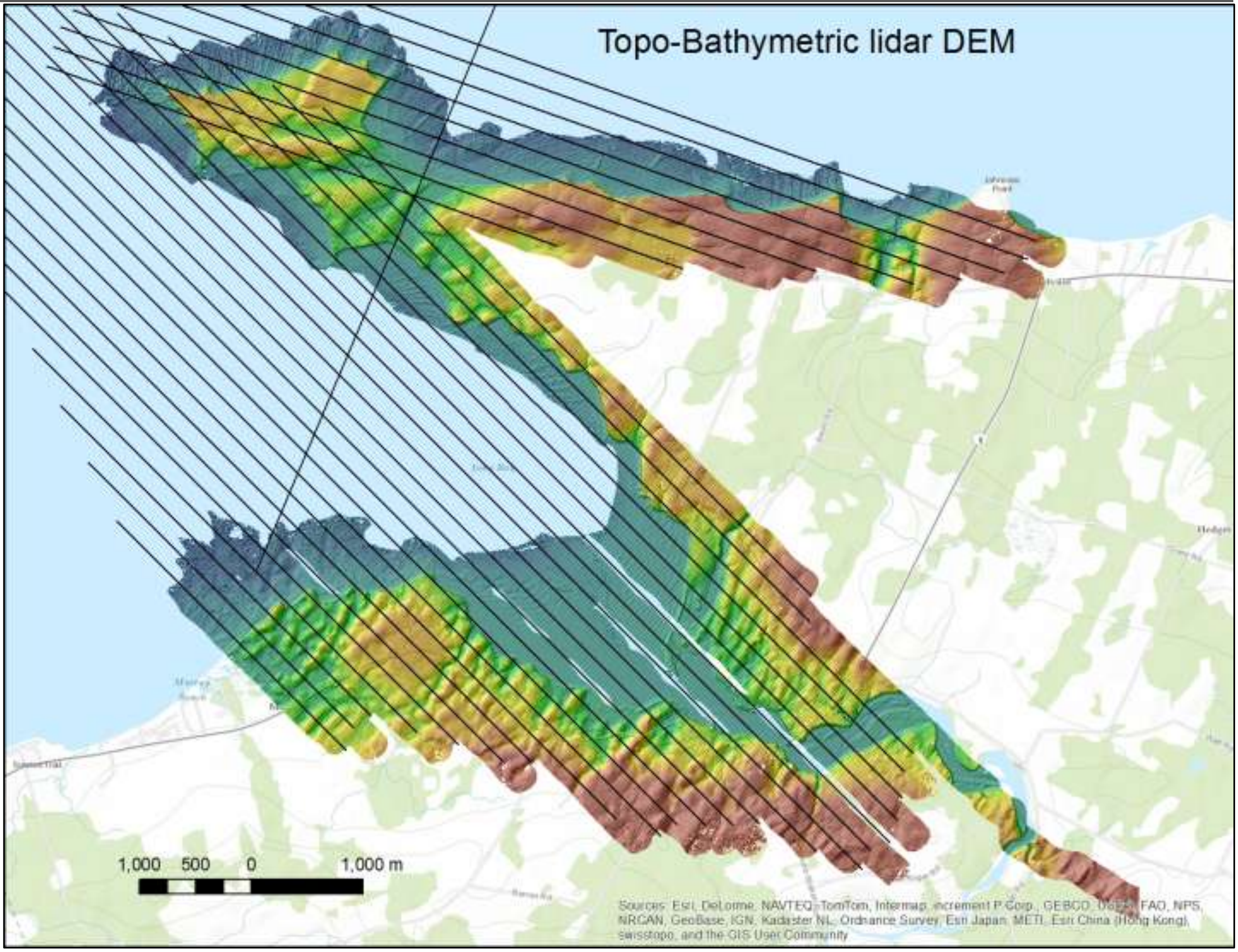

Figure 22: Example of gridded Digital Elevation Model of Cape John and John Bay with planned flight lines. Elevations below sea level in shades of blue, above sea level in shades of green, yellow and red-brown tones.

Terrascan was utilized to further classify and filter the lidar point cloud. Because of the differences in the lidar footprint between the TD and HD sensors it was decided that the HD lidar point returns would be used to represent the ocean surface and bathymetry points and the TD lidar points would be used to represent targets above ground. The total point cloud that utilized both sensors was processed in Terrascan where the ground was classified and erroneous points both above and below the ground were defined.

The standard classification numbers uses in the LAS format 1.2 do not adequately represent the bathymetric and water surface information, therefore a translation had to be used for the final point cloud. The overlap between flight lines also presented some challenges and it was decided to classify these points separately and code them such that the end user can decide if they want to utilize these points in the surface model construction by coding them uniquely. See Table 3 for the classification codes.

Class number	Description
0	Water model
1	Bathymetry (Bathy)
2	Bathy Vegetation
3	N/A
4	Topo laser (TD) Ground
5	TD non-ground (vegetation & buildings)
6	Hydro laser (HD) Ground
7	HD non-ground
8	Water
9	Noise
10	Overlap Water Model
11	Overlap Bathy
12	Overlap Bathy Veg
13	N/A
14	Overlap TD Ground
15	Overlap TD Veg
16	Overlap HD Ground
17	Overlap HD Veg
18	Overlap Water
19	Overlap Noise

Table 3 Table of delivered LAS classes combining the hydro (HD) and topo (TD) lidars.

2.5.2 Gridded Surface Models

There are three main data products derived from the lidar point cloud. The first two are based on the elevation and include the Digital Surface Model (DSM) which incorporates valid lidar returns from vegetation, buildings, ground and bathymetry returns, and the Digital Elevation Model (DEM) which incorporates ground returns above and below the water line. The third data product is the intensity of the lidar returns, or the reflectance of the HD lidar. The lidar reflectance, or the amplitude of the returning signal from the HD laser, is influenced by several factors including water depth, the local angle of incidence with the target, the natural reflectivity of the target material, and the voltage or gain of the transmitted lidar pulse. The original data is difficult to interpret because of variances as a result of water depth and loss of signal due to the attenuation of the laser pulse through the water column at different scan angles. The reflectance values were normalized by taking samples of the reflectance values of a common cover type, such as sand, over depth ranges and using these data to establish a relationship between depth and the logarithm of the reflectance value; the inverse of this relationship was used to normalized the data. Note how the flight lines are evident in the top panel of Figure 23 but the effect of flight lines has been minimized in the lower panel after the data has been normalized (Figure 23 lower panel).

The elevation of the lidar point cloud is relative to the WGS84 ellipsoid since the points are geolocated based on the GPS aircraft trajectory. However, once the surface models, DSM and DEM, have been constructed using different combinations of the point class elevations, these data were converted to orthometric heights and are now related to the Canadian Geodetic Vertical Datum of 1928 (CGVD28). The geoid-ellipsoid separation model, HT2, from Natural Resources Canada, was used to do this conversion to the surface models.

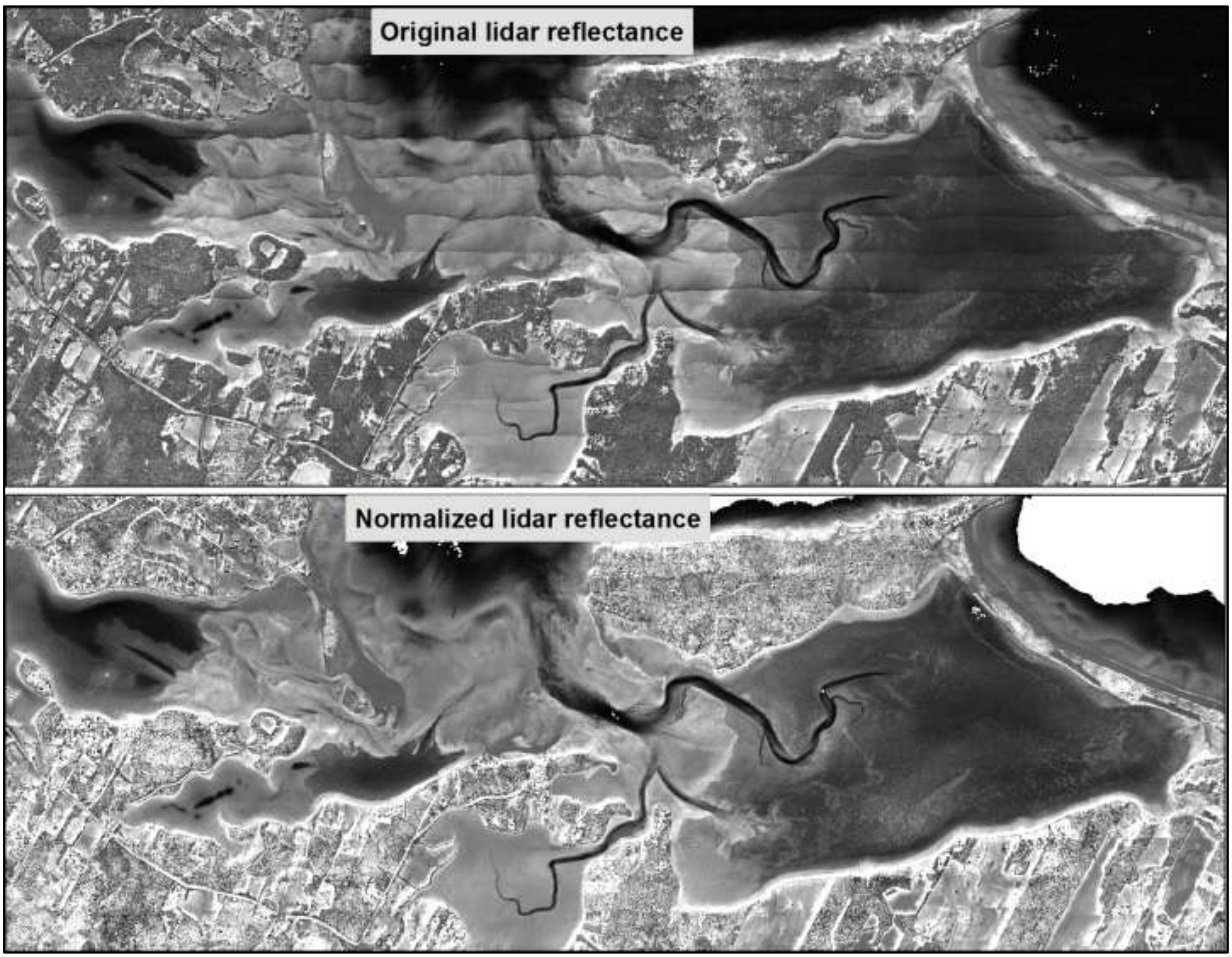

Figure 23: Top panel is the original lidar reflectance map from the HD laser. The bottom panel is the depth normalized reflectance based on water depth.

2.5.3 Aerial Photo Processing

The RCD30 60 MPIX imagery was processed using the aircraft trajectory and direct georeferencing. The low altitude and high resolution of the imagery required that the lidar data be processed first to produce bare-earth digital elevation models (DEMs) that were used in the orthorectification process. The aircraft trajectory, which blends the GPS position and the IMU attitude information into a best estimate of the overall position and orientation of the aircraft during the survey. This trajectory, which is linked to the laser shots and photo events by GPS based time tags, is used to define the Exterior Orientation (EO) for each of the RCD30 aerial photos that were acquired. The EO, which has traditionally been calculated by selecting ground control point (x,y, and z) locations relative to the air photo frame and calculating a bundle adjustment, was calculated using direct georeferencing and exploiting the high precision of the navigation system. The EO file defines the camera position (x,y,z) for every exposure as well as the various rotation angles about the x,y and z axis known as omega, phi and kappa. The EO file along with a DEM can be used with the aerial photo to produce a digital orthophoto. Initially processing was attempted to produce the orthophotos without the lidar DEM. This resulted in orthophotos from adjacent frames not lining up. After the lidar data was processed and classified into ground points, the lidar-derived DEM (above and below the water line) was used in the orthorectification process in Erdas Imagine software and satisfactory results were produced. An example of the relative alignment between the photos can be seen in Figure 24. In figure 24, the GPS tripod (yellow legs) is setup over our temporary benchmark. The location of the tripod yellow legs and GPS antenna (white dot) move because of the different perspectives of the photo frames and flight lines. A green triangle has been drawn on the figure to represent the base of the tripod and the green dot represents the GPS benchmark on the ground. These features do not change significantly in the photos from frame to frame demonstrating the accuracy of the resultant orthophotos (Figure 24).

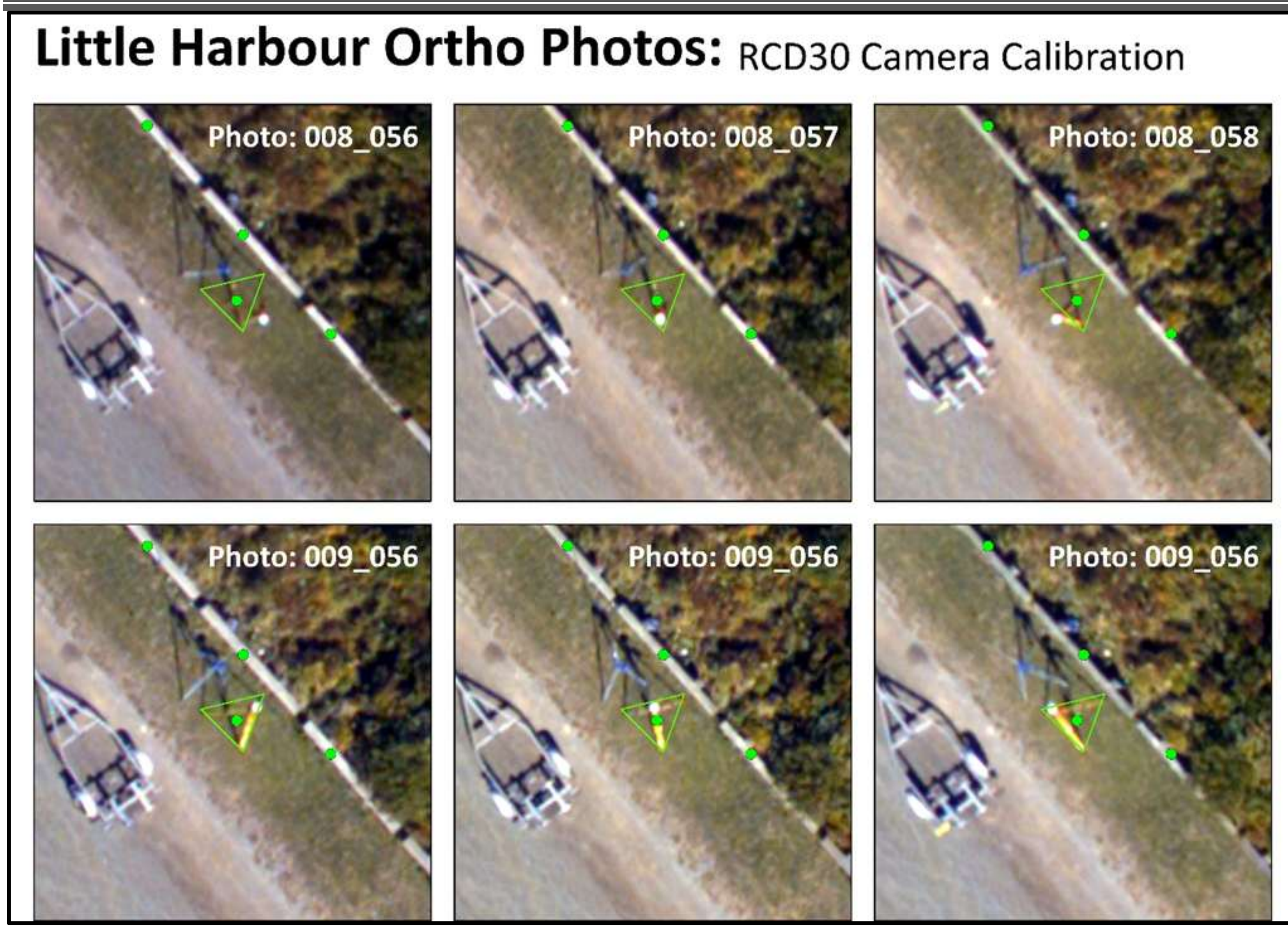

Figure 24: Example of multiple frames (56, 57, and 58) from multiple flight lines (008 on top and 009 below) of the GPS base station location at Little Harbour after orthorectification. The green dots are GPS locations along the parking lot rail and the aircraft control benchmark on the ground below the tripod where the bottom of the legs are represented by the green diamond.

2.5.4 Lidar Validation

Various GPS checkpoints were collected to compare to the lidar points and surface models to ensure the vertical accuracy of the data was sufficient. The GPS elevations were converted from ellipsoidal height to orthometric heights using HT2 within Leica GeoOffice. These GPS points that represent the bare ground were then overlaid with the lidar DEM and the raster cell value appended to the point file. The difference in elevation between the GPS point and the lidar derived DEM was then computed and summary statistics calculated. The delta Z values, or DZ, can then be displayed graphically on the map. In the case of Cape John, the road surface along the peninsula was resurfaced and no up to date GPS points were collected. Instead GPS points were collected along the wharf deck at Cape John and used for the validation. At Little Harbour the GPS antenna was mounted on a vehicle and GPS points were collected along the roads across the study area as well as from a pole at the parking lot and dune pathway at Melmerby Beach Provincial Park. The results of the validation will be shown in the results section.

3 Results

3.1 Lidar Point Cloud Features

The lidar point cloud was processed in LSS and then further refined in Terrascan. The LAS files from LSS were used to construct project blocks within Terrascan that facilitated the processing and filtering of the data. Various cross-sections of the data were examined in LSS and Terrascan to visualize the point density and classification. In addition to examining the HD laser returns for depth penetration and seabed morphology (Figure 25), land features such as the forest were examined in the topo laser (TD) point cloud (Figure 26 - Figure 28).

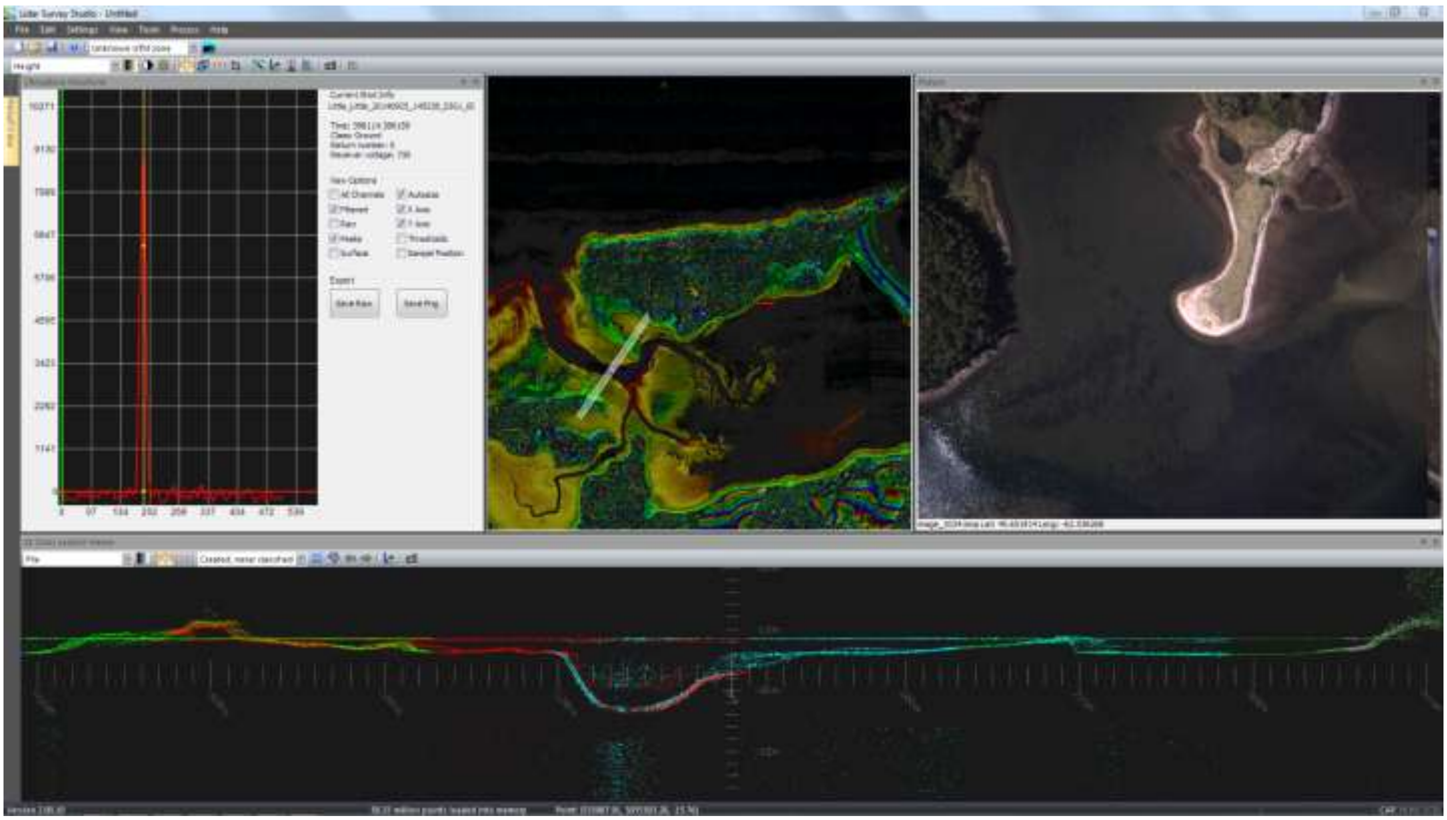

Figure 25: Cross-section of the main channel of the inner harbour at Little Harbour. The lower panel shows overlapping lidar points from multiple flight lines (different colours of points). Note there is no offset between the points from different flight lines.

The various cross-sections of the Cape John datasets were examined to demonstrate the level of detail for the topo laser for land target for forestry applications. The lidar point cloud can be visualized in 3D within LSS (Figure 26). Cross-sections of deciduous, coniferous and mixed forest were selected to be examined (Figure 26, Figure 27).

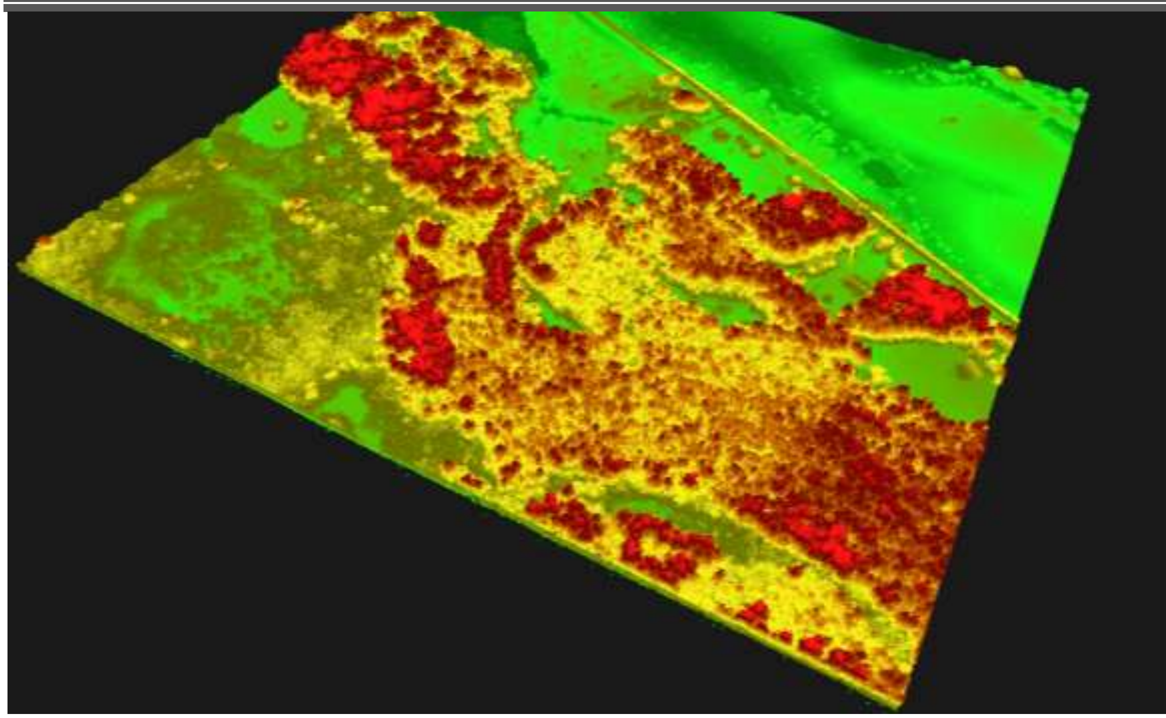

Figure 26: Example of a forested area along Cape John visualized within LSS. The lidar points are colour coded based on the height above the ground surface (red indicates the trees).

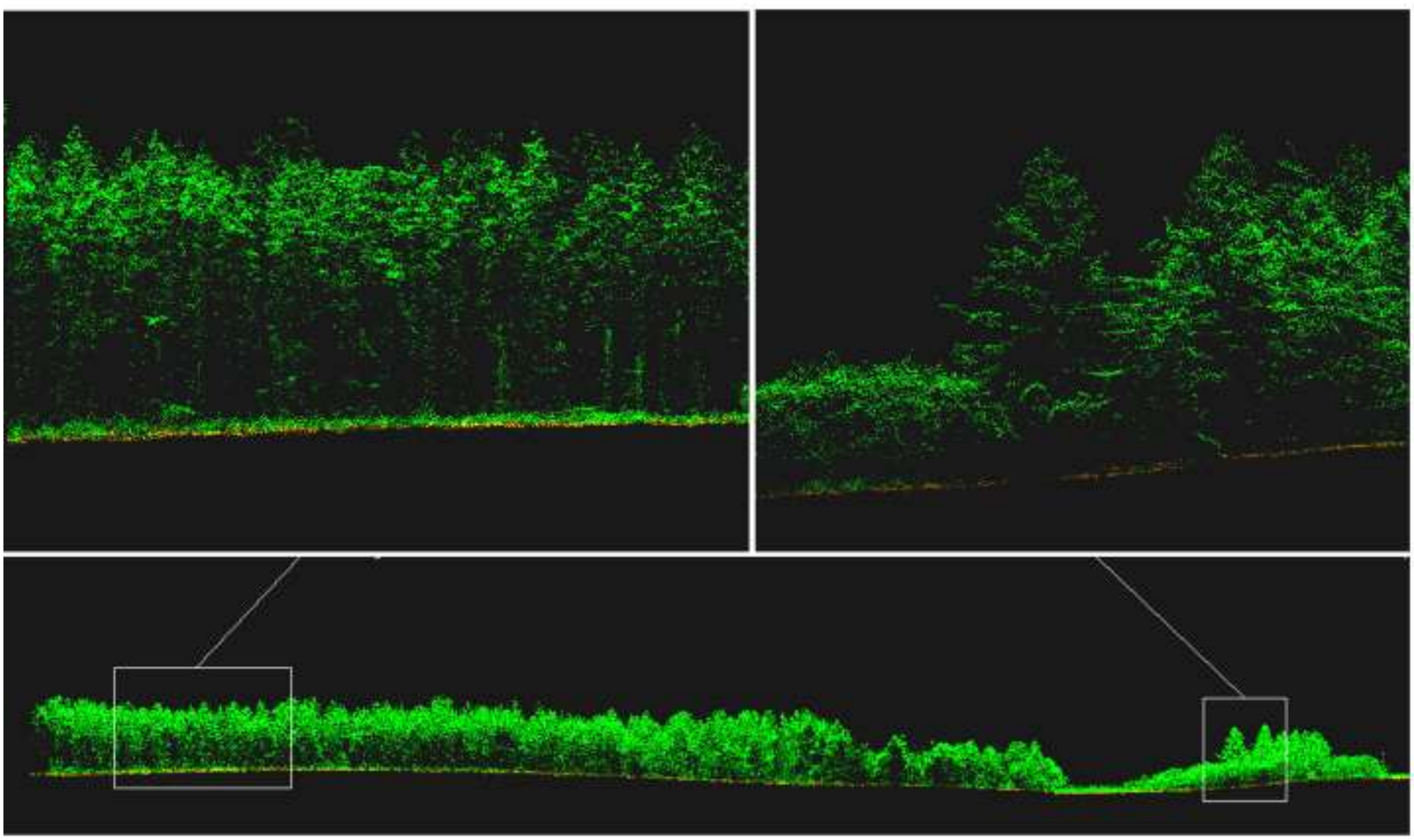

Figure 27: Example of cross-section of the topo lidar points in a forest area. Lower panel shows the cross-section of conifer forest with insets of sections in the upper panels.

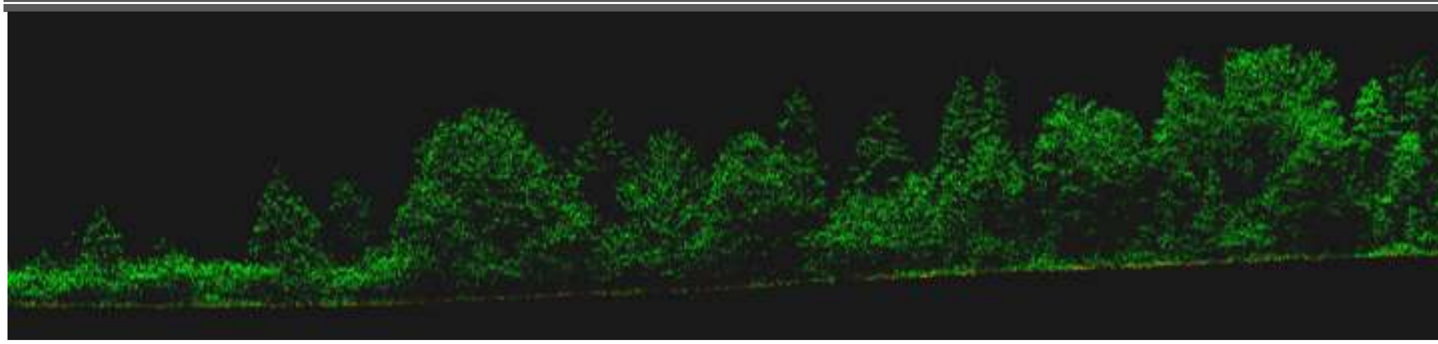

Figure 28: Example of cross-section of the topo lidar points in a mixed forest area.

As an experiment the orthophoto RGB values were appended to the LAS files for Little Harbour and various point cloud visualizations were constructed. The LAS points can be colourized by the RGB values and displayed in various orientations (Figure 29).

Figure 29: Experiments with RGB values from the orthophoto merged with the LAS files of Little Harbour. Top left image is a plan view; top right image shows the end of Melmerby beach dune. Lower image is a cross-section of a house and coastline.

3.2 Lidar Surface Models

3.2.1 John Bay and Cape John

The maximum depth of the HD lidar for John Bay and Cape John was 6 m. The lidar points were classified into bathymetric points, ground and non-ground as well as noise. Figure 30 shows the raw shaded relief Digital Elevation Model (DEM) for Cape John and John Bay in a greyscale. Gaps in the data are evident as white patches, or holes, and were caused by equipment issues related to the late time of day of the survey, when fog was forming. The Chiroptera II safety mechanism triggered on several lines during the John Bay survey. The safety mechanism terminated laser firing until the system could be re-initialized. We expect the system was receiving erroneous "low elevation" returns caused by fog formations under the operational survey elevation (400 m) at sundown. These low elevation returns triggered the eye-safety lock. The system was restored to a working state as soon as possible after each occurrence but the loss of laser returns resulted in survey gaps over the affected lines. These gaps could not be recollected given the fuel situation at the time.

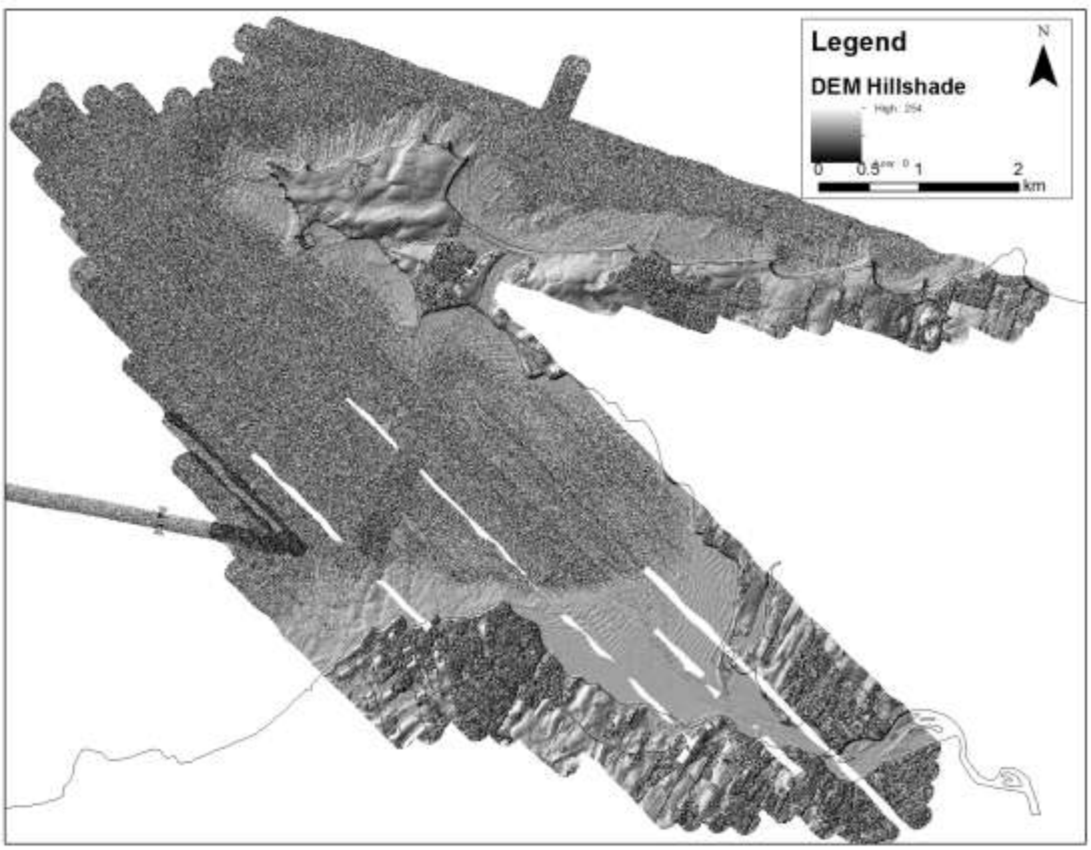

Figure 30: Preliminary shaded relief DSM for Cape John and John Bay. Note the white strips of missing data in John Bay.

In order to supplement the data that was not collected and to cover as much of the land area as possible, the lidar elevation data was merged with previous surface models from lidar surveys in the area in 2006 and 2007 and erroneous data clipped (Figure 31).

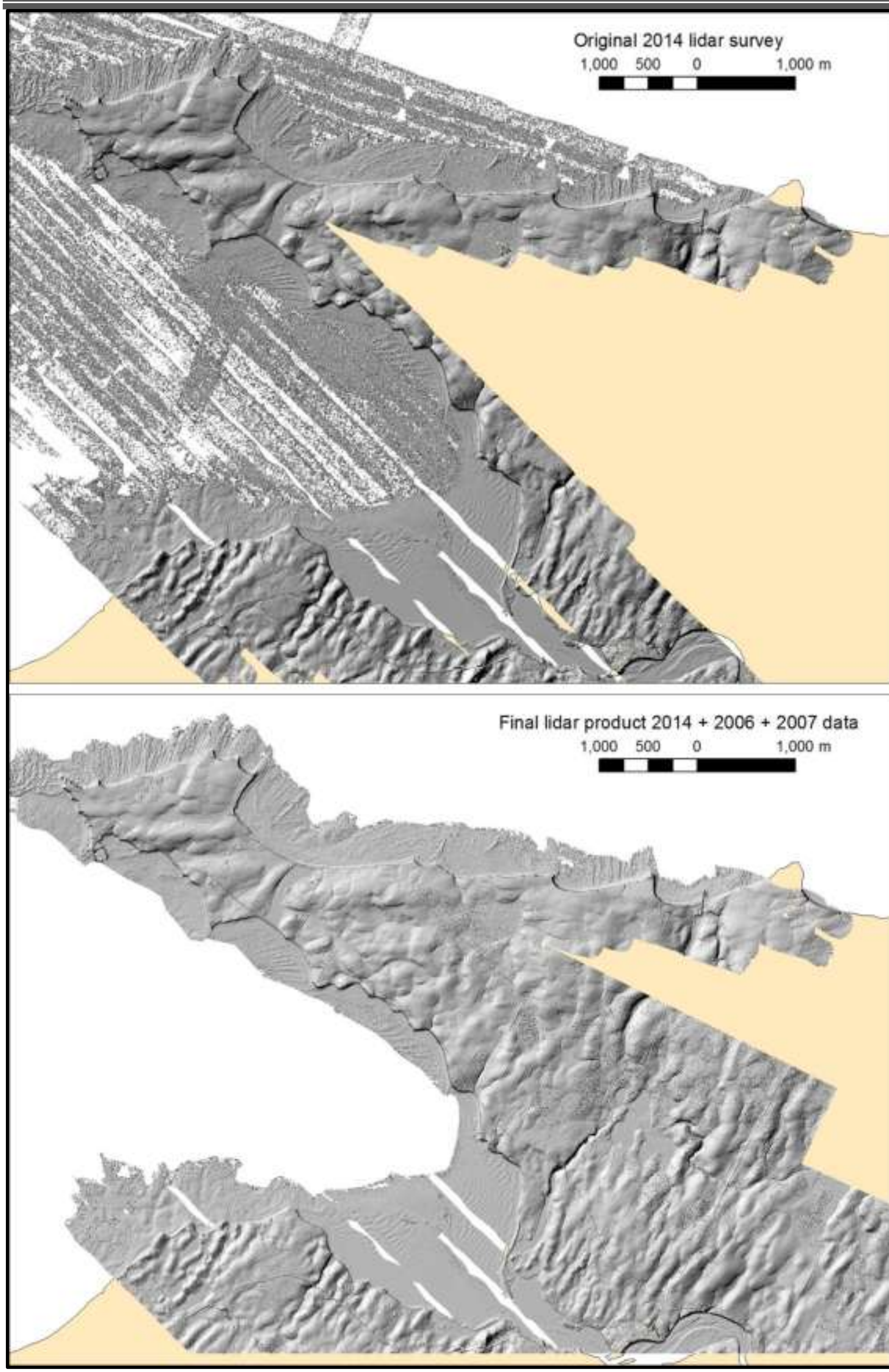

Figure 31: Topo panel shows the shaded relief DEM collected in the 2014 survey. The lower panel shows the shaded relief hybrid DEM from a composite of DEMs from surveys in 2006, 2007 and 2014.

In order to easily interpret the lidar surface models, colour shaded relief (CSR) models were constructed from the DSM and DEM for Cape John (Figure 32). These maps are meant to be for interpretation and are geocoded and compressed in Jpeg 2000 format. If the lidar elevation is required, the lidar DEM or DSM must be used. The CSR maps have been colourized to take advantage of Chroma-stereoscopy where the lower elevations are colour coded from the short wavelength blue to higher elevations at longer wavelength red. When the map is viewed with ChromaDepth glasses, it appears in 3-D. The map displays a strong contrast in the physiography and geomorphology of the area, especially in the DEM. The terrain above the influence of the tide is smooth and the influence of the last glaciation is apparent with smooth landforms giving a general hummocky appearance. In contrast the areas below the water show the scoured bedrock features, except where they are covered by sediment deposits in the form of sand bars and mega ripples. The exposed submarine bedrock shows significant folding in the vicinity of the Cape John wharf and several reefs are highlighted along the north shore. Large mega ripples of major sand deposits are evident at the mouth of River John.

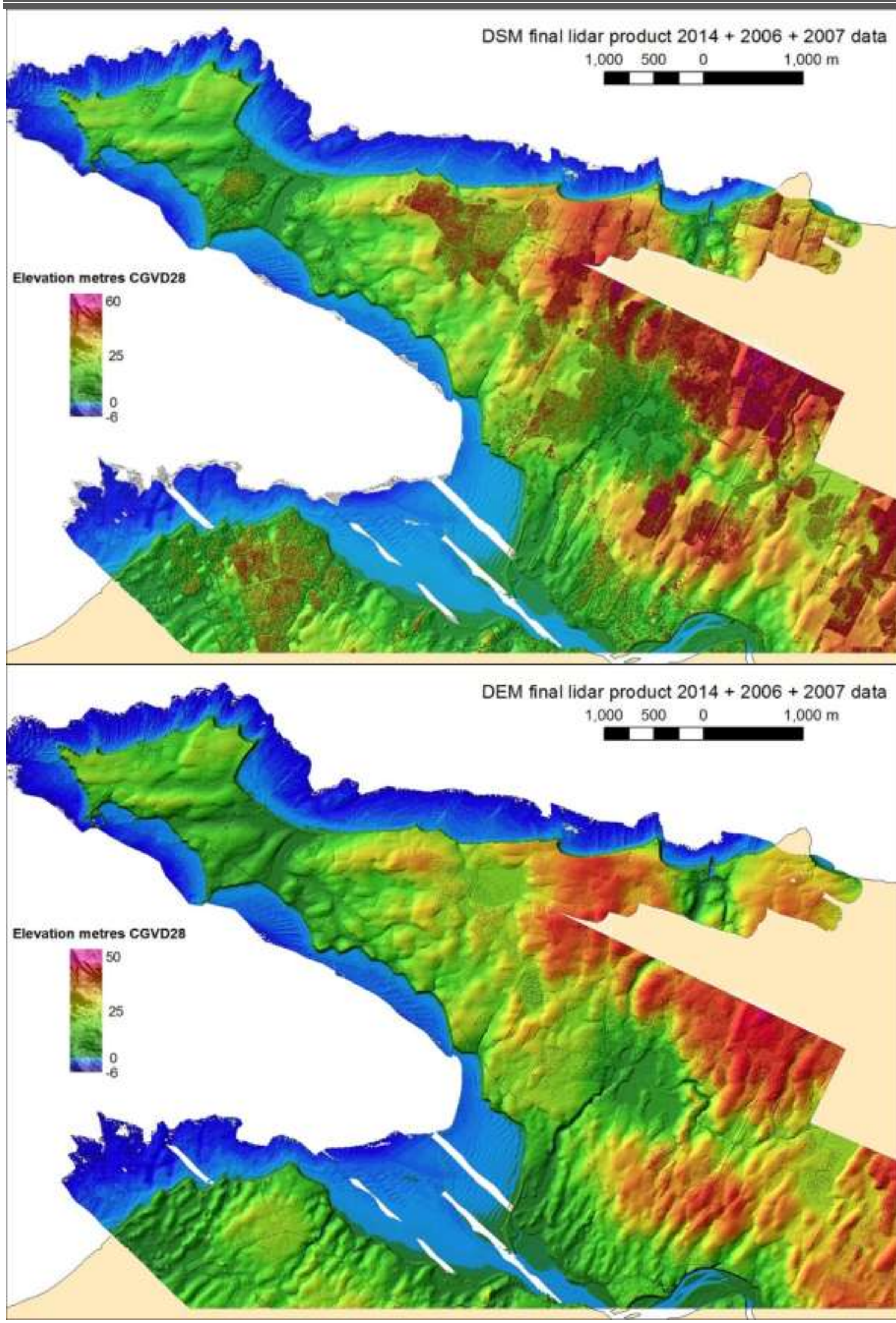

Figure 32: Top panel is the colour shaded relief of the hybrid DSM for Cape John. Lower panel is the colour shaded relief of the hybrid DEM for Cape John.

3.2.2 Little Harbour

Data collection was very successful at Little Harbour, and the DSM and DEM shows no data gaps and excellent laser penetration (Figure 33). The main channel can be seen in the harbour, surrounded by shallow, low-sloped plains.

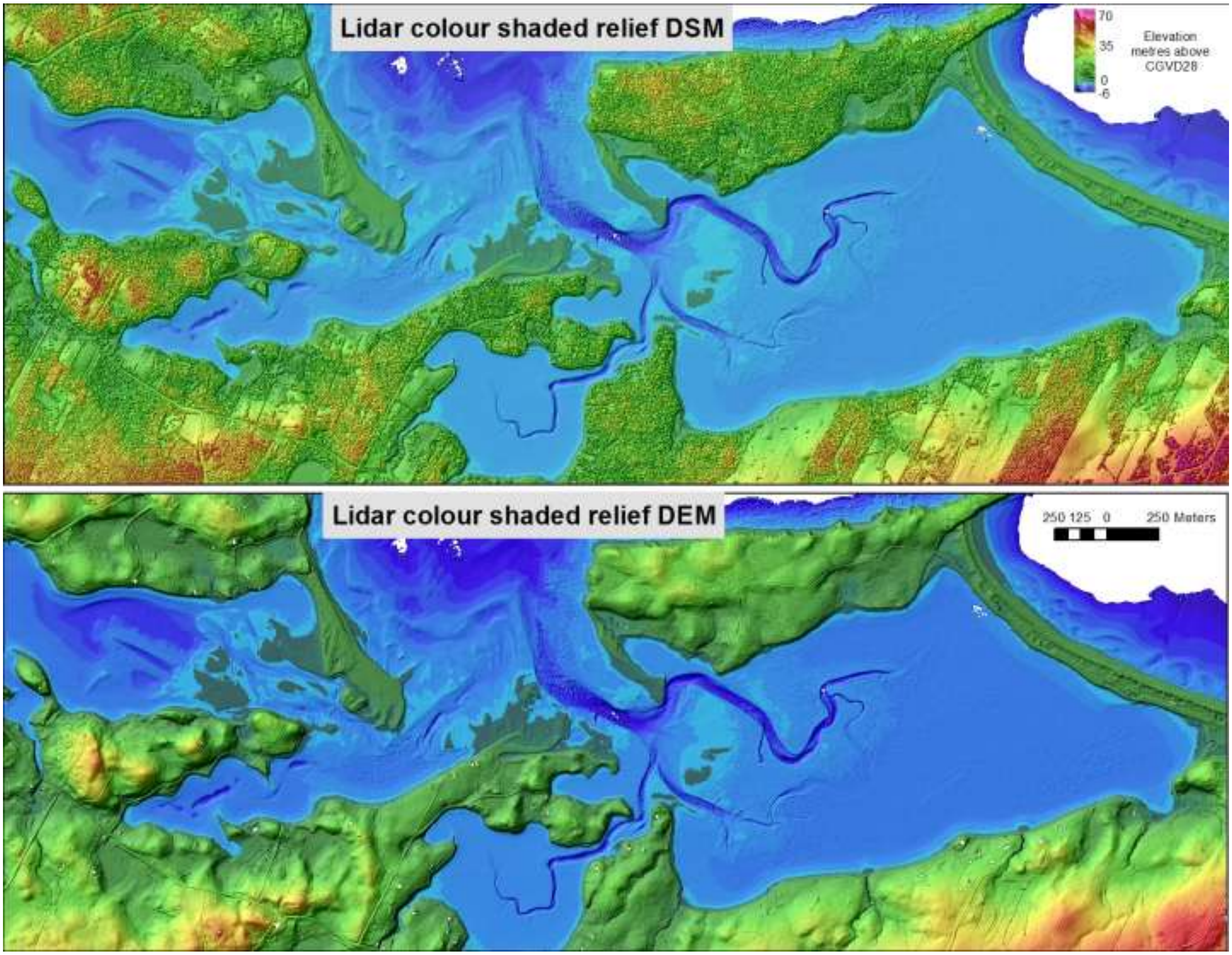

Figure 33: Top panel is the colour shaded relief of the hybrid DSM for Little Harbour. Lower panel is the colour shaded relief of the hybrid DEM for Little Harbour.

Major sand bars are evident offshore of Melmerby Beach to the northwest. Along with the main channel for Little Harbour that contains mega ripples, there are areas of the inner harbour that are shallow and relatively flat and featureless. In contrast the central area displays complex topography and the western bay appears to have had a large deposit of sand cover over a previous channel. The blockage of this channel undoubtedly affects the circulation and water exchange of this bay with the open ocean to the northeast.

Intensity or reflectance data is a measurement of the backscatter of the green HD laser returns, and varies according to bottom type. We expect that research into how reflectance is derived from intensity will lead to an algorithm which will allow us to classify bottom type as sand, eelgrass, rockweed, etc.

The intensity data for Cape John and John Bay are shown in Figure 34. The red rectangle represents a close-up of Cape John showing much greater detail (Figure 35) and the blue rectangle outlines a close-up of John Bay (Figure 36). In these cases the reflectance data, coupled with the DEMs, provide insight into geological formations, showing bedrock overlain by sediment at Cape John and sand waves in the seabed sediment at John Bay.

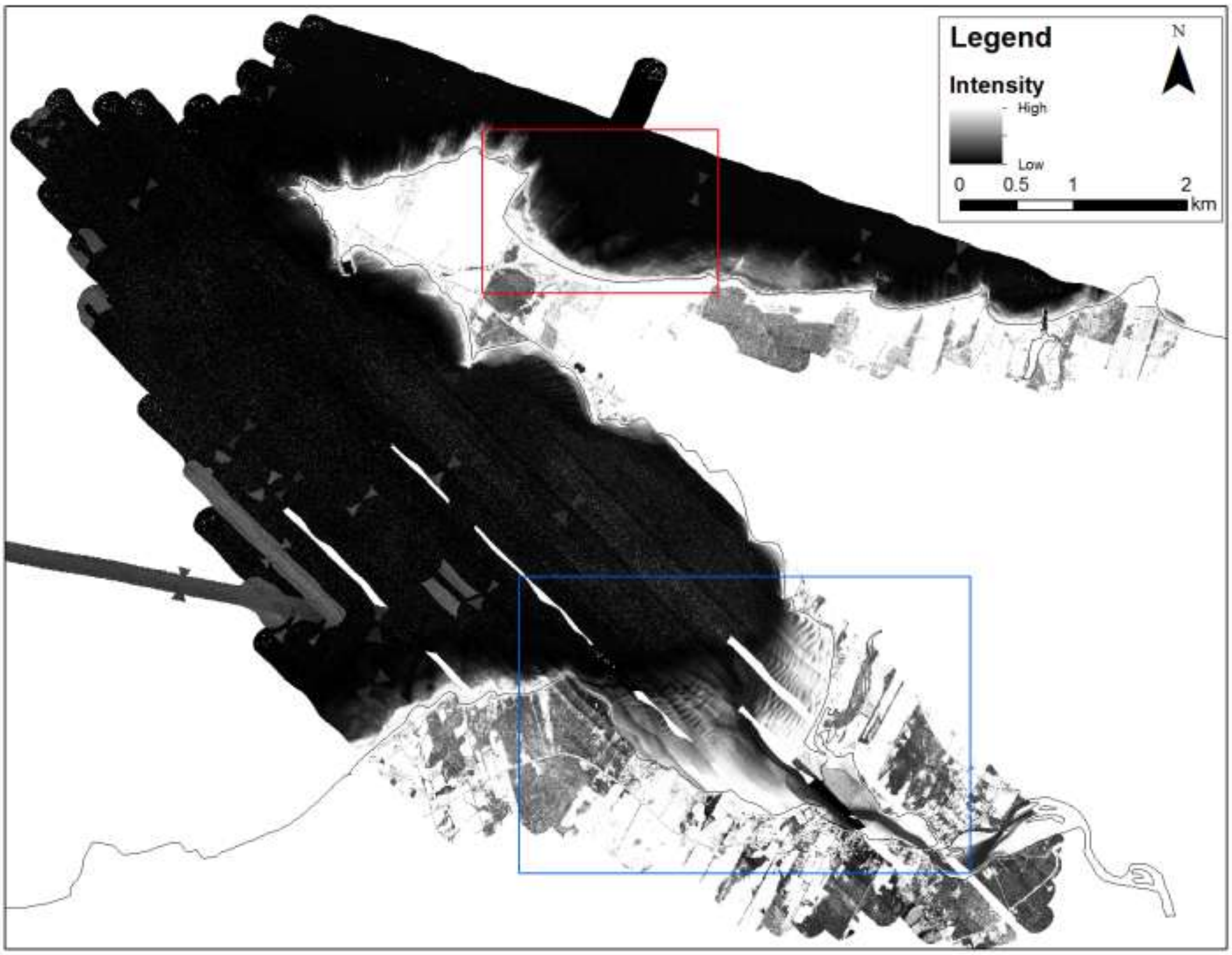

Figure 34: Intensity map of Cape John and John Bay. Areas of different intensity of backscattered light represent different bottom types. The red and blue rectangles represent the extents shown in Figure 35(a) and (b).

(a)

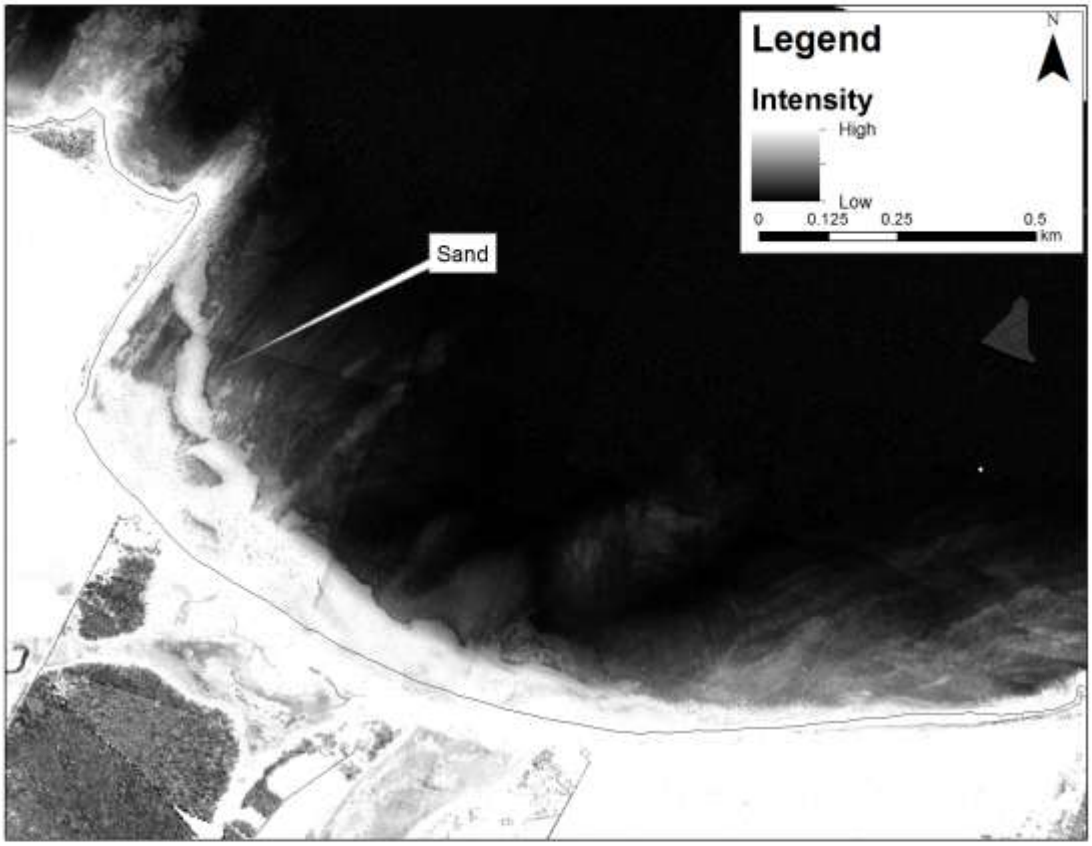

(b)

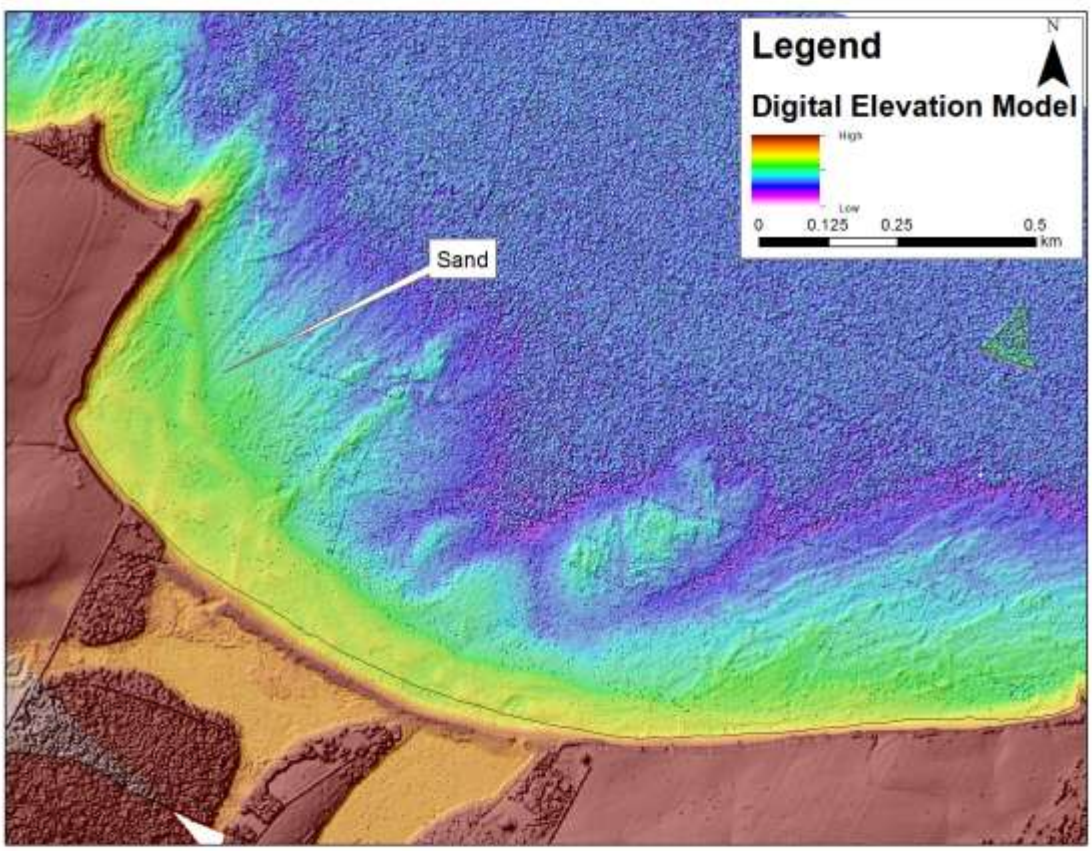

Figure 35: (a) Intensity and (b) DEM with hillshade at Cape John (red rectangle in Figure 34).

(a)

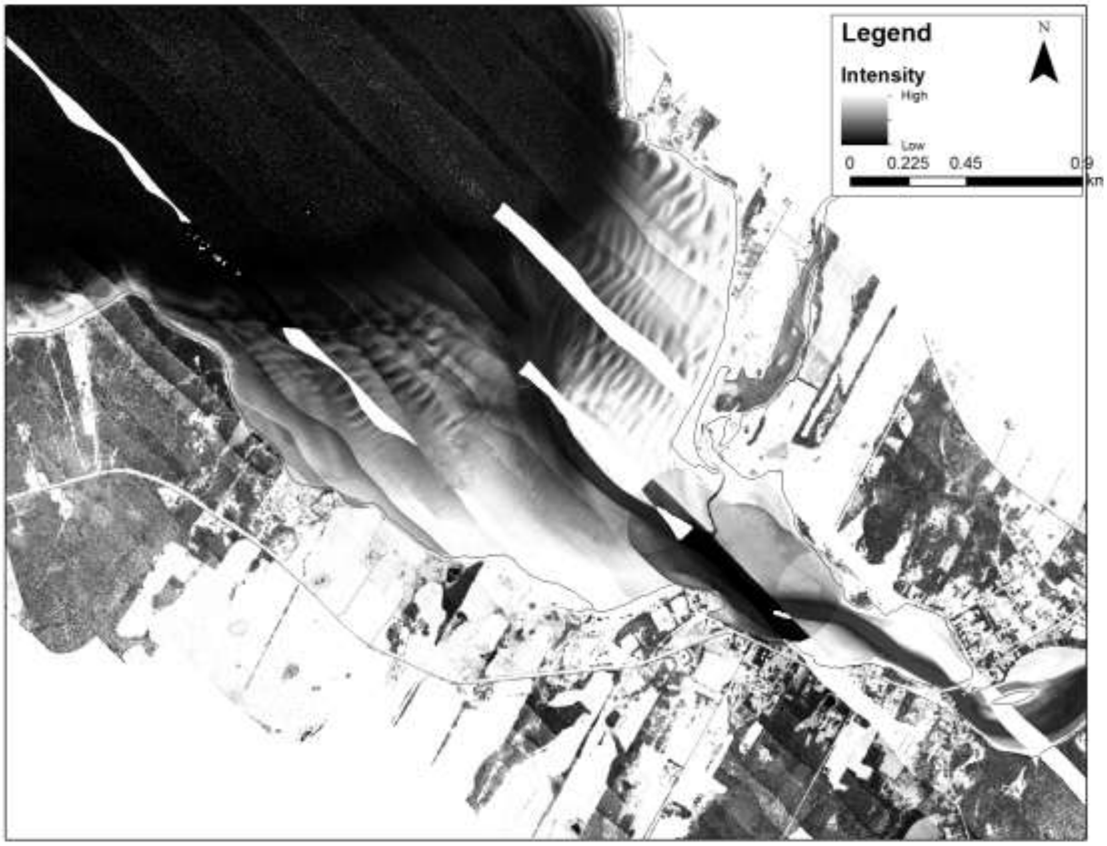

(b)

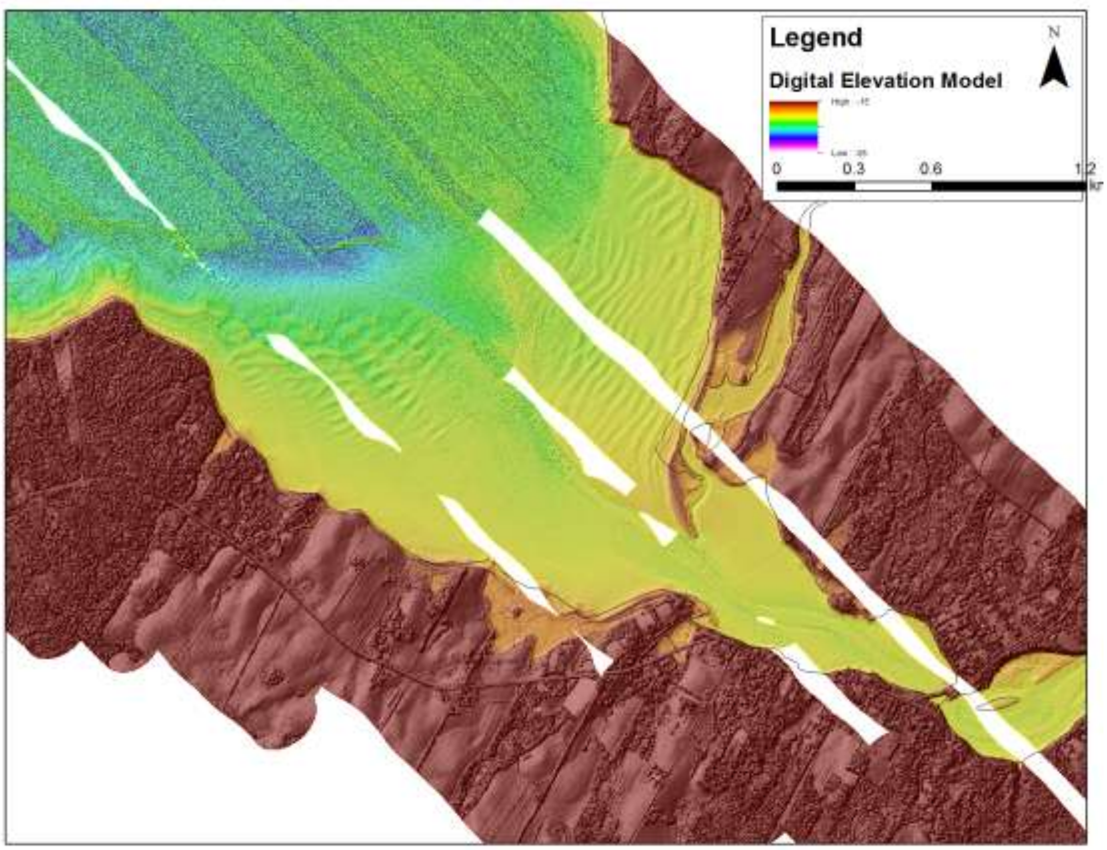

Figure 36: (a) Intensity and (b) DEM with hillshade at John Bay (blue rectangle in Figure 34).

Intensity/reflectance data for Little Harbour are shown in Figure 37. At Little Harbour, future research into how these data, possibly in combination with other lidar derivatives and/or aerial photos, can lead to maps of bottom type; specifically eelgrass. Our ground truth data of eelgrass presence or absence reveal patchy coverage that seem to correspond to differences in the intensity data (Figure 38a). The differences in seabed type that are seen in the intensity are highlighted in the DEM (Figure 38b). We anticipate great success in being able to map eelgrass with the lidar intensity data.

Figure 37: Original intensity-reflectance map of Little Harbour. Areas of different intensity of backscattered light represent different bottom types. The red rectangle represents the extent of the area shown in Figure 38.

(a)

(b)

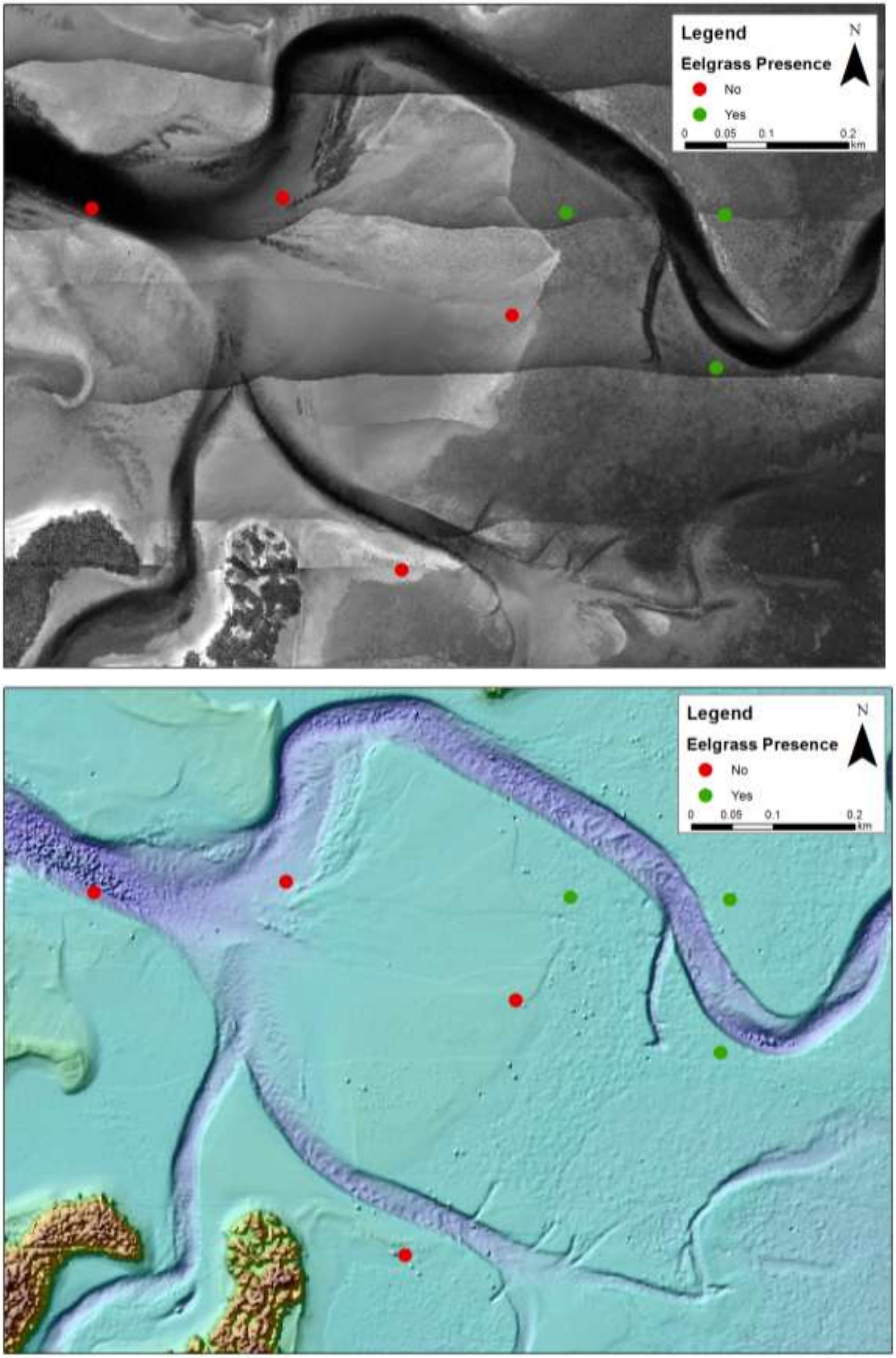

Figure 38: (a) Intensity-reflectance prior to being normalized by depth and (b) shaded relief DEM at Little Harbour showing eelgrass presence or absence ground truth data.

3.3 Aerial Photography

The aerial photography at Cape John and John Bay suffered from a low sun angle as a result of the lateness of the hour when the survey was conducted. As mentioned previously in the report this was a result of the prolonged winds and turbidity in the water which would adversely affect the bathymetric lidar survey, which was the prime focus of this mission. None the less, the aerial photos were processed into two orthophoto mosaics; one for the ocean side of Cape John and one for the northern shore of John Bay. It was too dark for any useful results to be obtained for the south shore of John Bay, however valid lidar returns were acquired as demonstrated in the previous section highlighting the active remote sensing nature of lidar and not requiring daylight to conduct surveys. The individual orthophotos were used to construct the two mosaics for the area at 20 cm cell size (Figure 39).

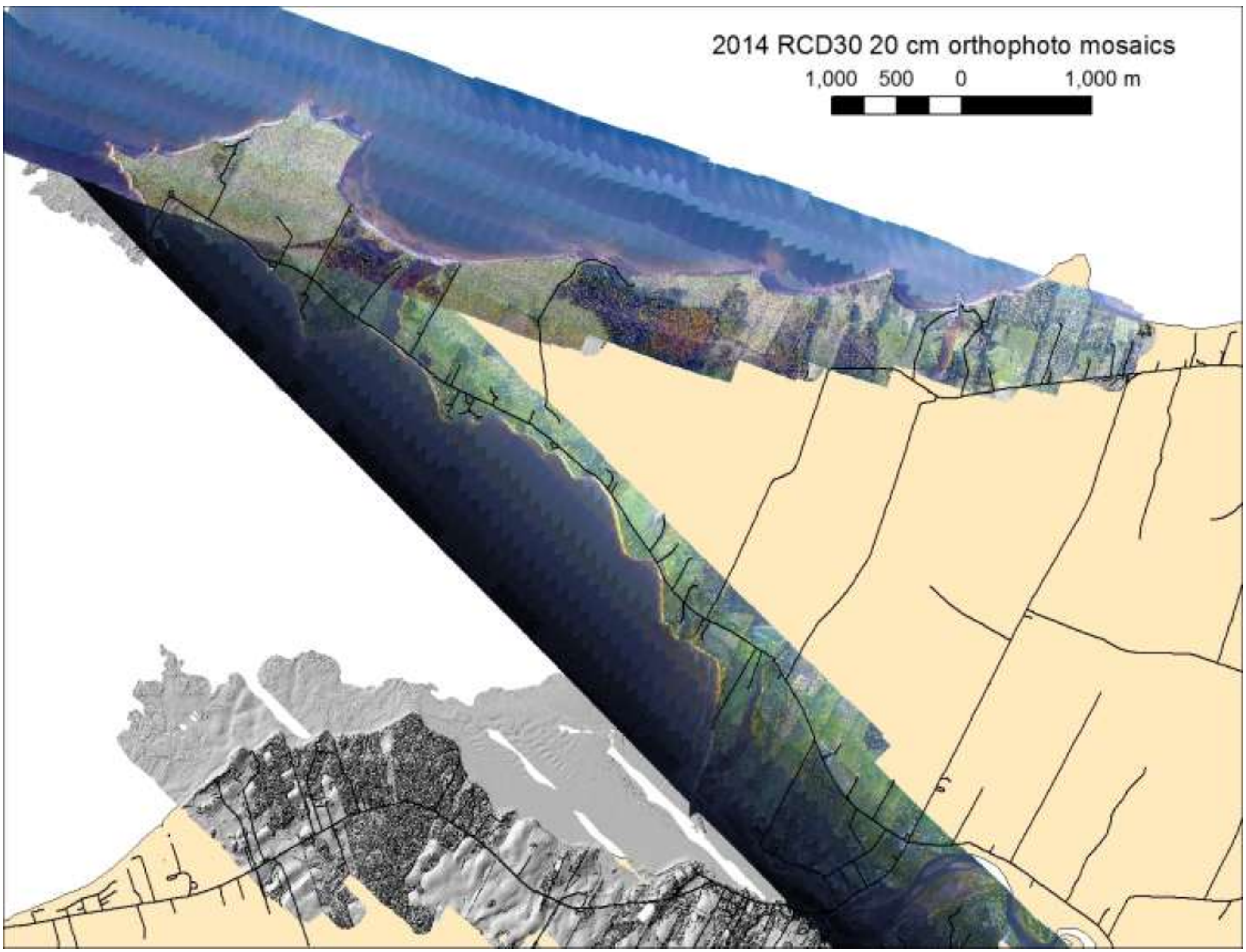

Figure 39: Cape John and John Bay mosaics of the orthophotos acquired on Sept. 26.

The aerial photos for Little Harbour were taken mid-day and the amount of sunlight was not an issue. Photos taken at this time of day, however, have the potential problem of sun glint over the water. The individual orthophotos were used to build a mosaic where the minimum pixel value was selected for the most nadir image to build the mosaic. This resulted in very few areas in the mosaic where sun glint was a problem and the imagery highlights the seabed very well (Figure 40).

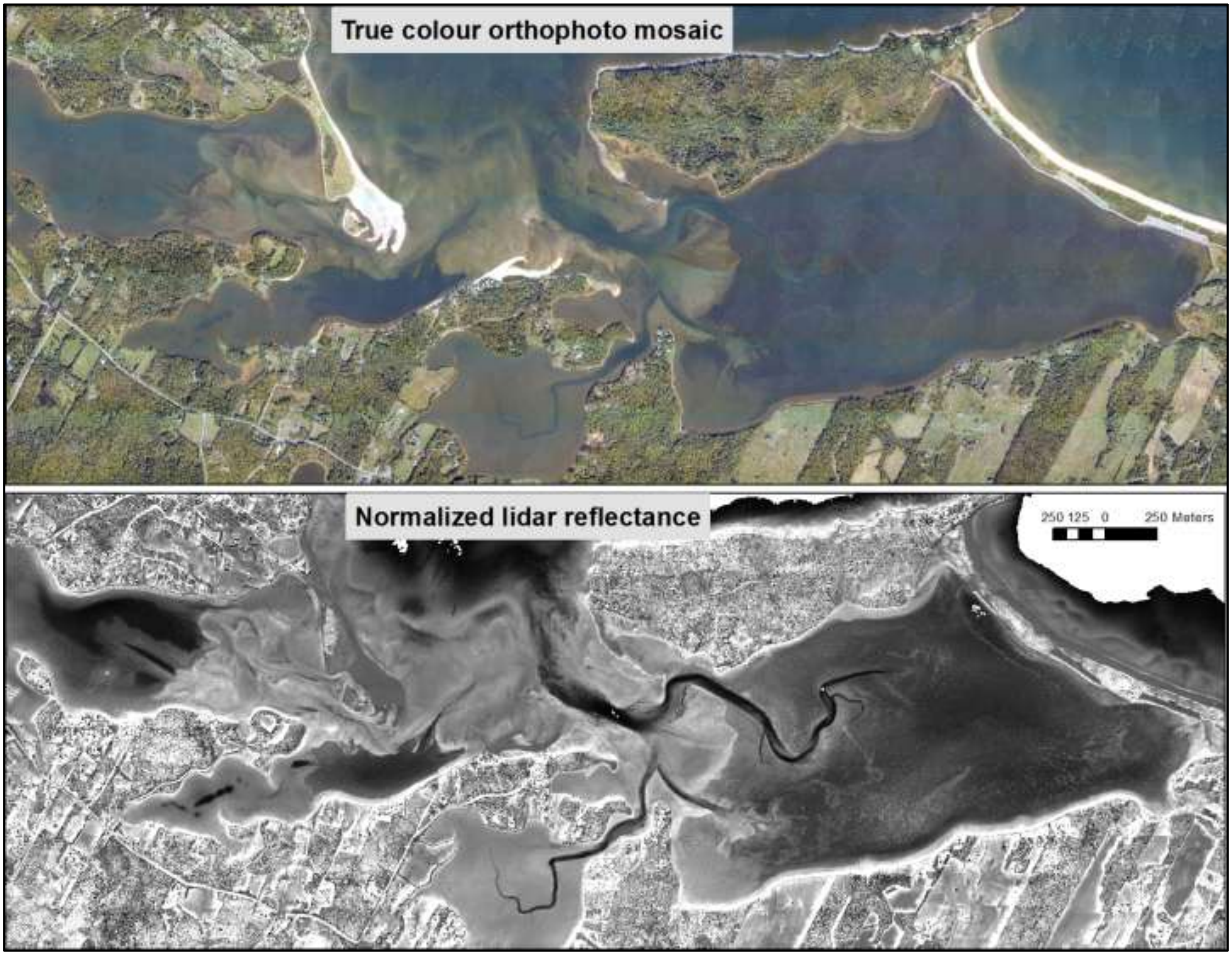

Figure 40: Top panel is an orthophoto mosaic of Little Harbour. The bottom panel shows the depth-normalized lidar reflectance for comparison of seabed features.

Figure 40 shows how the orthophoto mosaic complements the lidar reflectance image to map the seabed cover. Dark tones on both images represent the occurrence of submerged eelgrass while light tones represent submerged sand. The orthophoto mosaic aids in interpreting the lidar surfaces, especially in shallow areas, but does not provide the same level of detail in deeper areas.

The orthophoto mosaic, or other imagery such as high-resolution satellite imagery, can be used with the lidar surface models to visualize the terrain. In this case the orthophoto mosaic of Cape John has been draped over the lidar DSM to visualize the coastal terrain (Figure 41, Figure 42, Figure 43)

Figure 41: Orthophoto mosaic draped over lidar DSM at Cape John point.

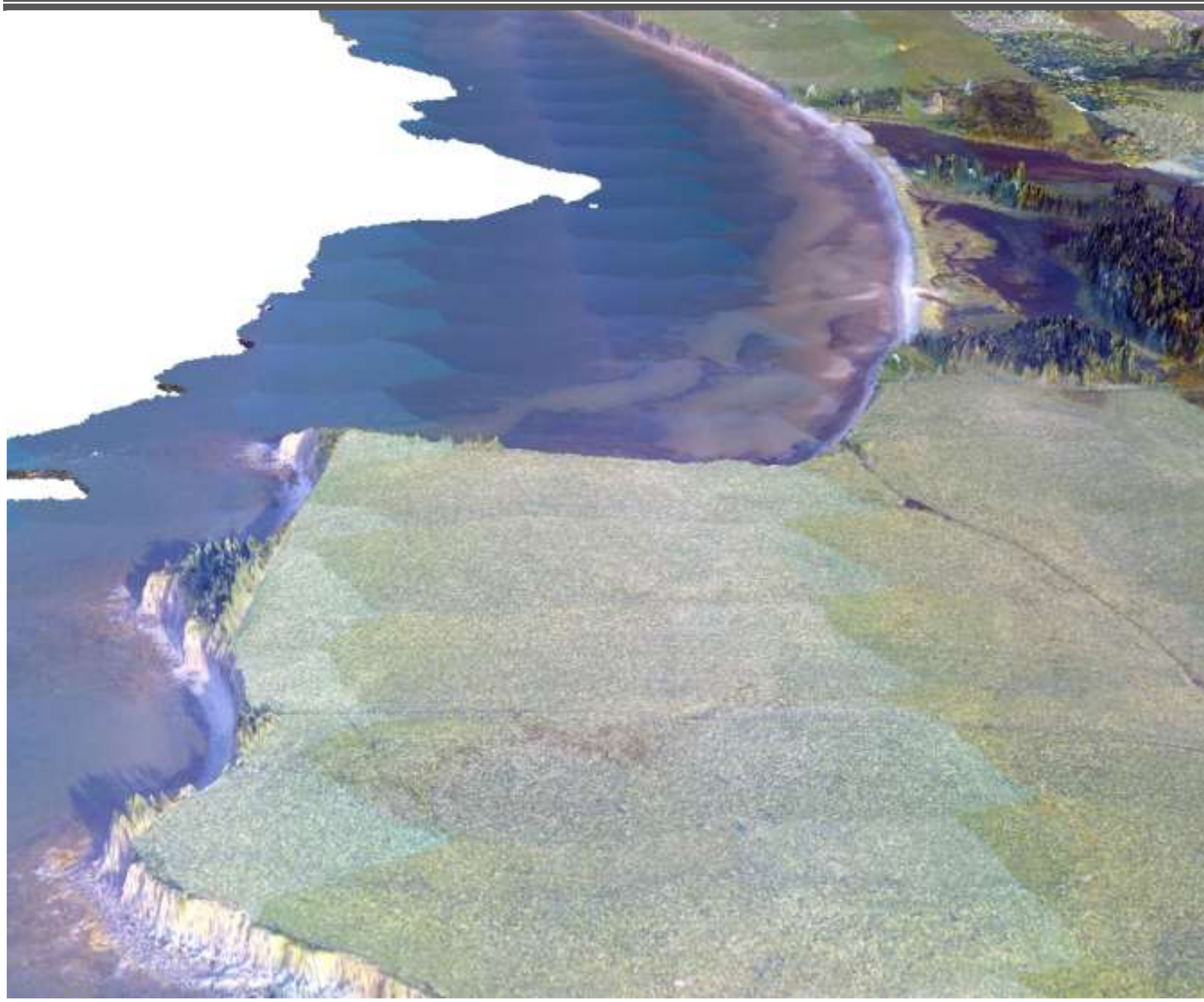

Figure 42: Drape of orthophoto showing the cliffed and low relief coastline on the north coast of Cape John. Note the submerged sand bars adjacent to the marsh separated by a small dune.

Figure 43: Drape of orthophoto mosaic over the DSM for Skinners Cover wharf, Cape John study area.

3.4 Lidar Validation

GPS points were acquired at the Cape John wharf and compared to the lidar DEM for this study area. The difference in elevation between the GPS and the lidar DEM was calculated and reported (Figure 44). The mean difference in elevation is -0.02 m with a standard deviation of the difference of 0.04 m for the 13 checkpoints.

GPS points were acquired by mounting the antenna on a truck and driving the road network for the Little Harbour study area. In addition to this transects were collected using a pole for the parking lot at Melmerby Beach and the path across the dune to the beach. The difference in elevation between the GPS and the lidar DEM was calculated and reported (Figure

45). The mean difference in elevation is -0.05 m with a standard deviation of the difference of 0.04 m for the 3606 checkpoints.

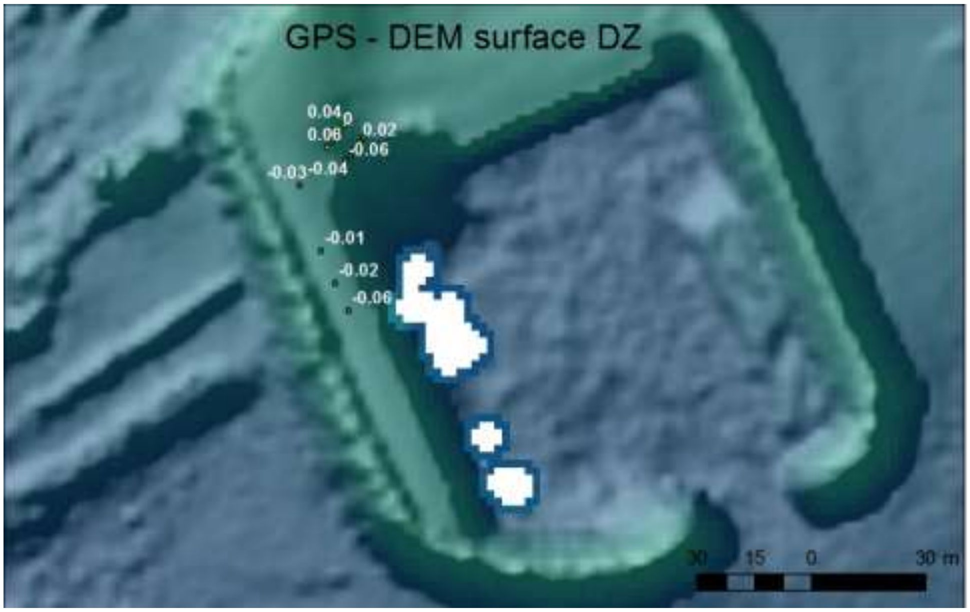

Figure 44: Comparison of GPS and lidar DEM elevations at Cape John wharf. The difference in elevation (m) are labelled.

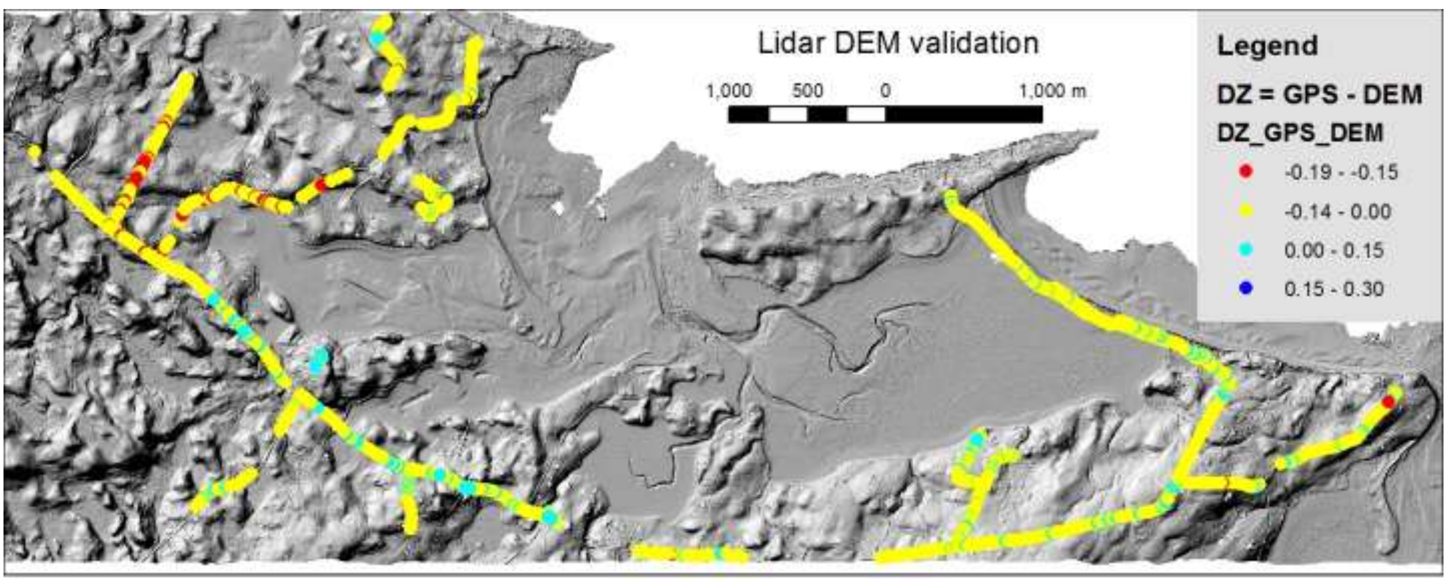

Figure 45: Map of the difference in elevation between the GPS points and the lidar DEM at Little Harbour. The image in the background is the shaded relief DEM. The difference in elevation is classified into groups of 0.15 m.

The histogram of the delta Z for the GPS validation of Little Harbour shows a near symmetric distribution centered on

-0.05 m (Figure 46).

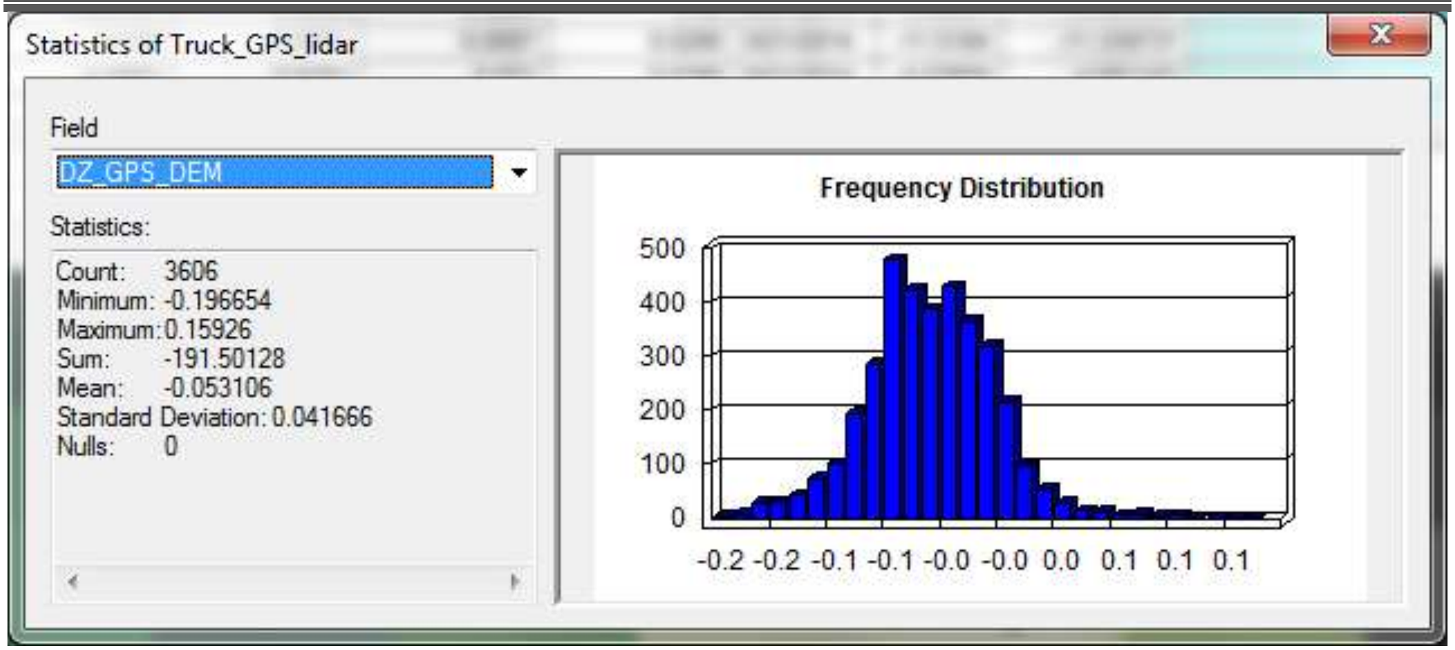

Figure 46: Histogram of the DZ between GPS and lidar DEM for Little Harbour.

The difference in elevation between the GPS points taken along the dune path show a higher value than those in the parking lot. This is a result of the interaction of the marsh grass and other materials on the earth. Ideally validation points should be taken on hard flat surfaces to examine the accuracy of the sensor (Figure 47).

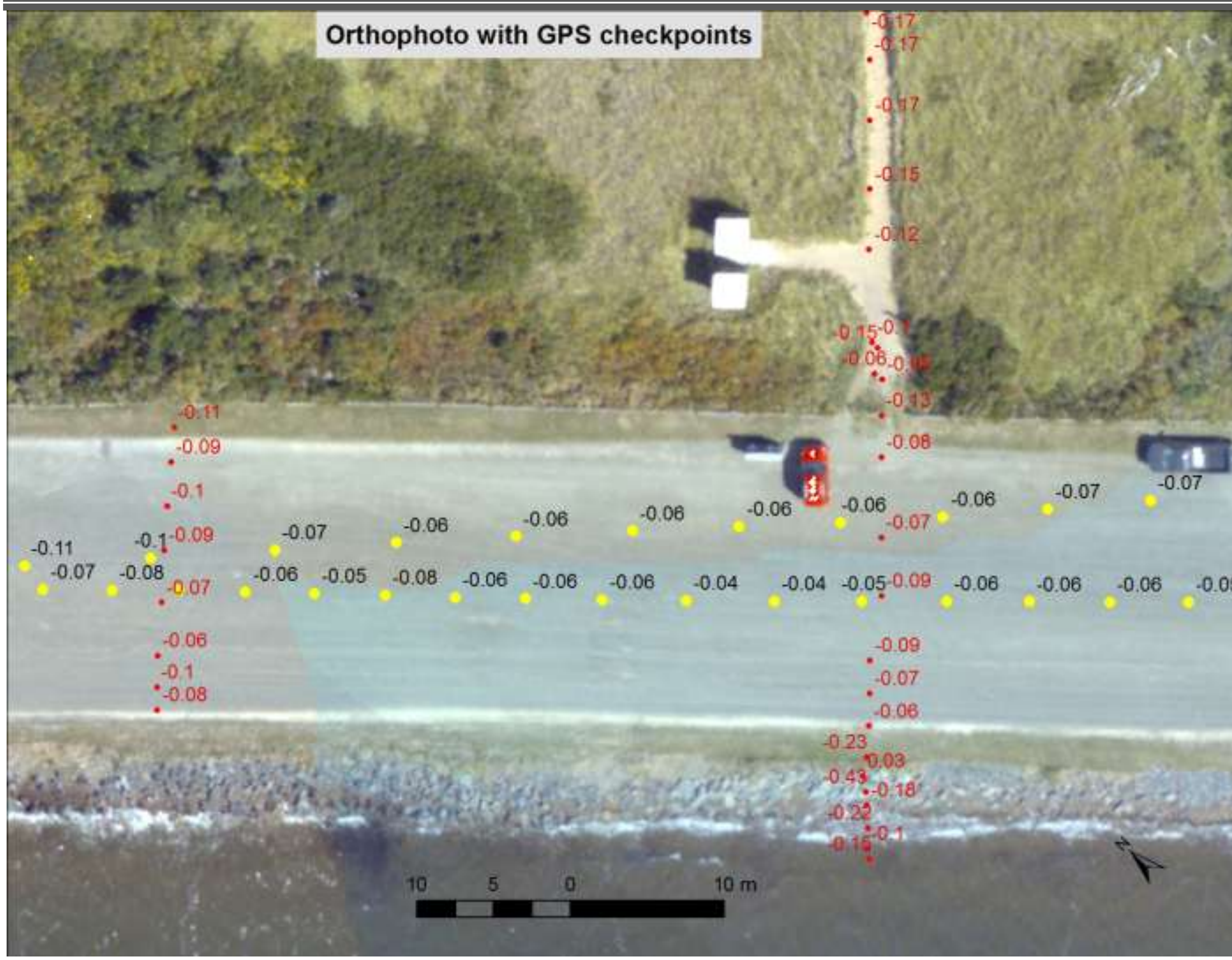

Figure 47: Comparison of GPS points collected with a vehicle (yellow) and those from a pole (red) with labels showing the delta Z difference with the lidar DEM for the parking lot area of Melmerby Beach.

4 Discussion

The researchers at AGRG consider this first mission of the Chiroptera II a huge success and are impressed with the quality of the data sets produced. The two study sites selected for this mission, Cape John/John Bay and Little Harbour, had contrasting coastal geomorphology. Cape John separates the open ocean of the Northumberland Strait from John Bay which contains the River John estuary. The ocean side of Cape John has a cliffed coastline with outer reefs and embayments where glacial till and dunes define the shore with intertidal sand bars. The bedrock geology is complex around the point of Cape John where folds in the bedrock are evident in the submerged topography highlighted by the new topo-bathy lidar data. John Bay has a similar mix of cliffed coastline with less sandy beach embayments until the entrance to River John where huge mega ripple sand bars have been deposited. Eelgrass occurs on both sides of Cape John, but is more prevalent in John Bay. The new detail provides improved information for near shore navigation compared to the previous charts, as well as details on the geology, coastal processes and ecology of the area through the terrain and lidar reflectance maps (Figure 48).

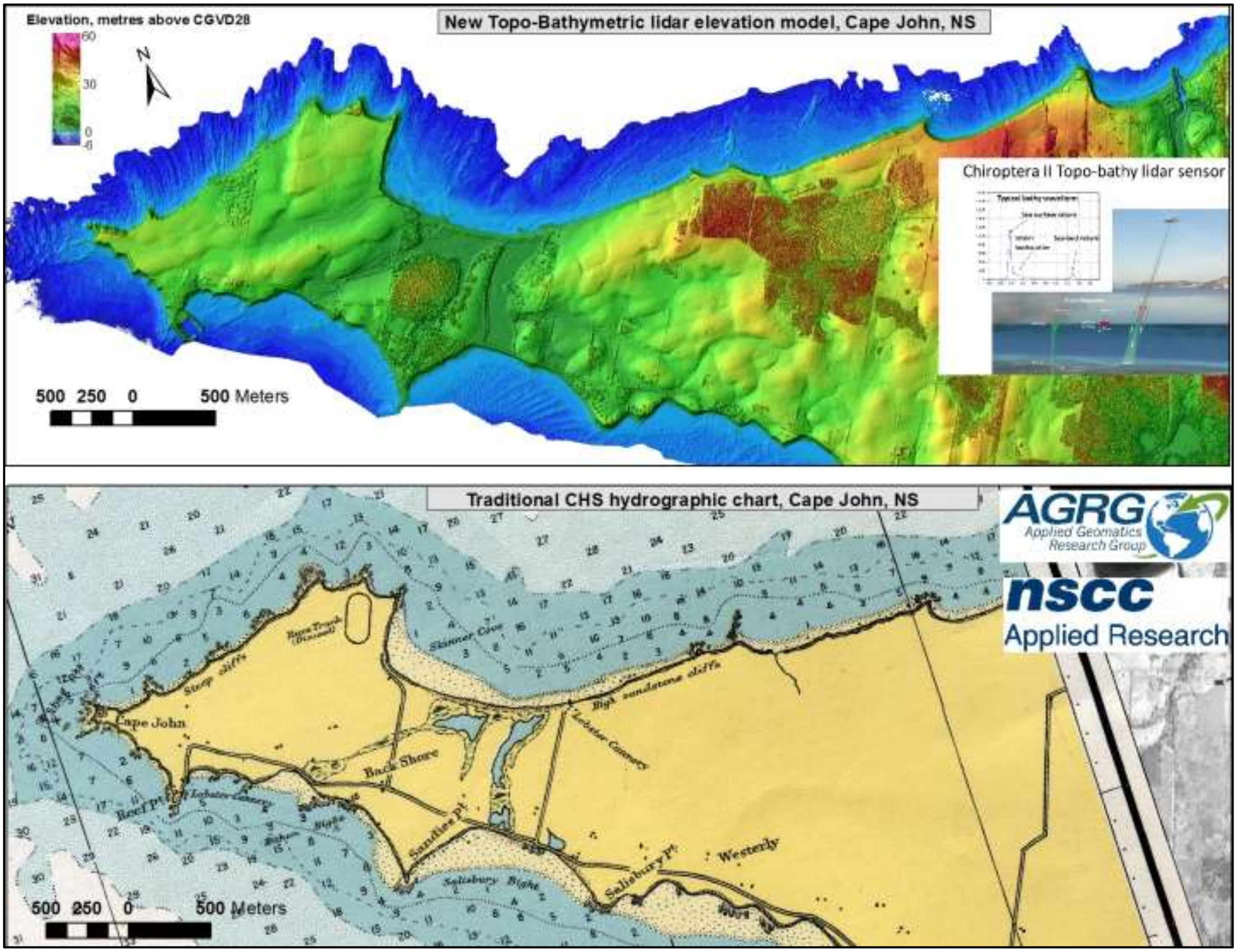

Figure 48: Comparison of the new level of bathymetry around Cape John from the topo-bathy lidar survey (top map) and the previous chart from the Canadian Hydrographic Service (lower map).

These new data can be used for a variety of scientific application to answer critical questions related to coastal development. For example the exposed coastline is vulnerable to erosion and coastal flooding from storm surge events. These data can support hydrodynamic models of storm surge and can also be used to advance wave runup modelling. These types of process-based models can improve our understanding of coastal processes and the sediment budget for coastal cells.

The Little Harbour study are contains Melmerby Beach Provincial Park, a major sand dune separating the open ocean of the Northumberland Strait with the sheltered inner harbor. The harbour itself has several channels connecting different bays within the harbor. The morphology of the sea floor is complex and dynamic within the harbour where these channels converge. The inner harbour is quite shallow in places and there are large sections of eelgrass which are considered to be an ecosystem health indicator. The new topo-bathy lidar data reveals details on the bathymetry that have never been surveyed and the lidar reflectance provides insights to the seabed cover including the distribution of sand and eelgrass. The new DEM provides an excellent data source to further evaluate the area for the potential for aquaculture operations through the development of hydrodynamic models to calculate currents and the exchange of water in the harbour. The richness of the new DEM compared to the previous hydrographic chart are evident in Figure 49. In addition to more detail on the bathymetry, a significant amount of change can be observed in the location of channels and the distribution of sand, which changes the hydrodynamics and flushing of the inner bays.

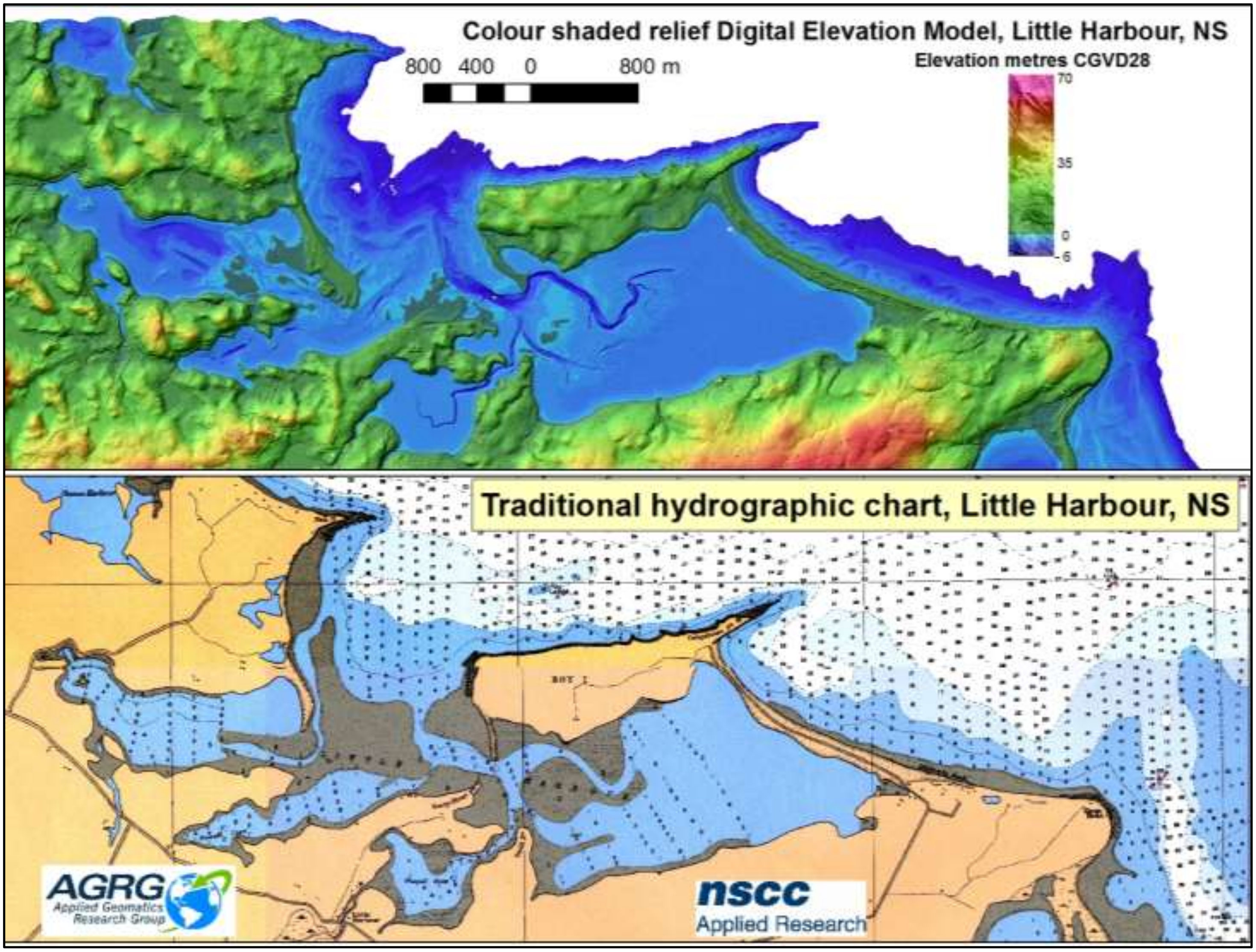

Figure 49: Comparison of the new topo-bathy lidar derived DEM for Little Harbour (top map) with the previous chart from the Canadian Hydrographic Service (lower map).

5 Conclusions

The inaugural mission of the new NSCC topo-bathy lidar sensor was a huge success with nearly 100% complete data collection in the two study sites. With the exception of a few missing lines in John bay as a result of night fog and sensor safety shut off features, all the sites were covered and excellent data were acquired. Researchers at AGRG and staff at Leading Edge Geomatics learned many valuable lessons about the operations of the sensor and the variability of local environmental conditions that affect water clarity, a major factor influencing the success of a near shore bathymetric lidar survey. The use of local weather stations and local contacts to inform the operations team of water clarity conditions is key in order to optimize flight time for successful data collection. An extensive ground truth campaign was mobilized for the surveys from scientists at AGRG and DFO Gulf Region. These data can be used in the future to further develop and refine information products that can be derived from the airborne data collected. The Little Harbour survey resulted in 100% complete coverage with excellent penetration in the harbor and near shore area. The production of a normalized lidar reflectance map allows the seabed cover to be interpreted and compared to information visible from the orthophoto mosaic. The detail of the topo and hydro lasers provide a rich dataset that many different users can access and derive information from including general mapping, coastal processes, coastal vulnerability assessment, forestry, agriculture, and fisheries and aquaculture development to name a few. Although the data at Cape John and John Bay were collected late in the day, orthophotos were constructed that can be interpreted and information derived for most of the study area. The detailed bathymetry reveals new insights into the near shore topography and geology and includes reefs that may pose navigation hazards, complex folds and faulting visible offshore, as well as the distribution of sand deposits and submerged vegetation. These data provide a rich environment for future studies of coastal processes and have the potential to advance our knowledge and improve coastal development in a responsible and sustainable way.

6 Acknowledgements

We would like to thank ACOA, GeoNOVA, NS Natural Resources, NS Fisheries and Aquaculture, DFO- Gulf Fisheries Centre, NS Agriculture, and NS Inland Fisheries Division for funding support. We would especially like to thank Marc Ouellette and Monique Niles of DFO Gulf Region for the collection of additional ground truth data for Little Harbour. Thanks to staff from Airborne Hydrography and Leica Geosystems, LEG staff for operations and AGRG staff for administrative support, the pilots from Dynamic Aviation.

7 Appendix: Data Dictionary

7.1 Overview

A total of 55.3 GB of raw and derivative data collected from the pilot bathymetric lidar campaign has been provided along with this document for submission in accordance with the ACOA initiative. Data included in the submission is in accordance with the deliverables as proposed.

Data provided was collected September 26, 2014 using a Leica-AHAB Chiroptera II Topo-Bathymetric airborne lidar system. The system incorporates a Leica RCD30 camera system for high resolution visible-near infrared photography.

Study areas collected include the Cape John Peninsula/John Bay Area, Nova Scotia, and the Little Harbour Area, Nova Scotia. Both Surveys were conducted at approximately 400 m above ground level.

The data delivered in the top level directory (201412_ACOA) falls into one of four categories: Grids, LAS, Orthomosaics, and Report, as shown below. Details on each of these data types follows.

- 201412_ACOA
  - Grids
  - LAS
  - Orthomosaics
  - Report

7.2 Grids

Topographic bathymetric grid data is presented as two variants; Digital Surface Models (DSM), and Digital Elevation models (DEM). Both data variants are constructed using bathymetric sea bed laser returns; combined with infrared topo-laser returns over land features. Land features include all ground (fields, forest bottom, roads etc.) as well as valid non-ground land features (trees, vegetation, buildings, power lines, etc…). DEMs are built from bathymetric and all ground returns only (i.e., no trees, power lines etc… included) whereas DSMs additionally include all valid non-ground laser returns.

All lidar derived grid datasets are delivered in a geographic .TIF raster format; each with a spatial resolution of 2 meters as 32-bit depth floating point, and suitable to be viewed in ArcGIS. Grid data is stored in the Universal Transverse Mercator projection (UTM, Zone 20N) and referenced to the North American Datum 1983 (NAD83). Grid data which contains elevation data (DEMs, DSMs, and water surface models) are referenced to the Canadian Geodetic Vertical datum (CGVD28, HT2) whereas lidar reflectance grids contain relative values representative of lidar pulse return intensity. The lidar reflectance information delivered is derived from the green bathymetric channel laser of the Chiroptera II for seabed and on ground laser pulse returns.

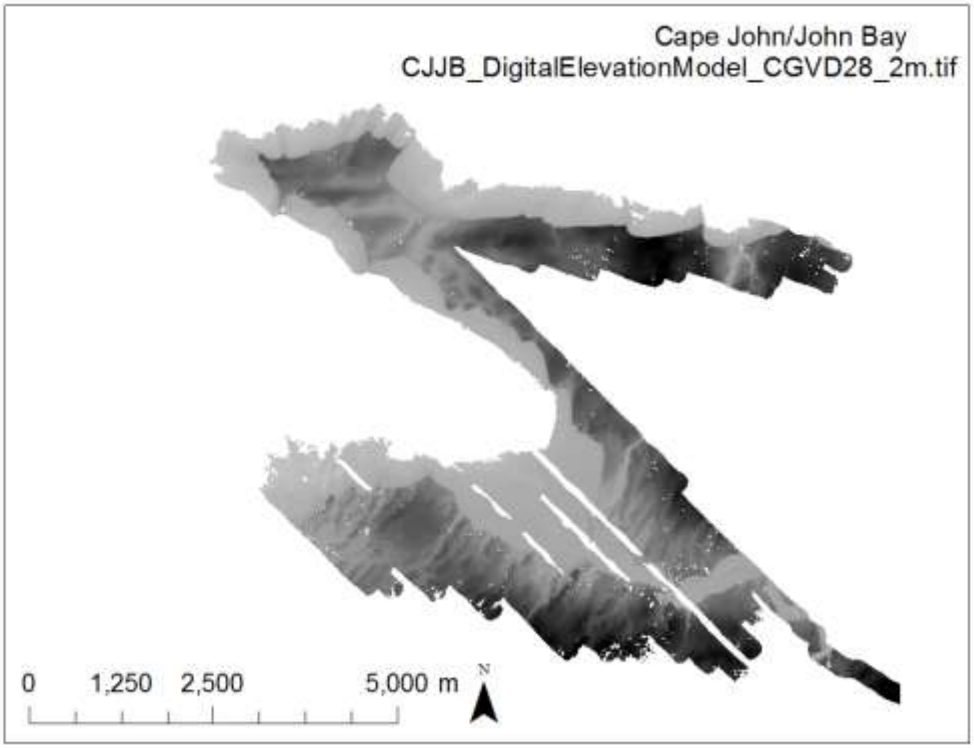

Figure 50: Cape John/John Bay 2 m Digital Elevation Model.

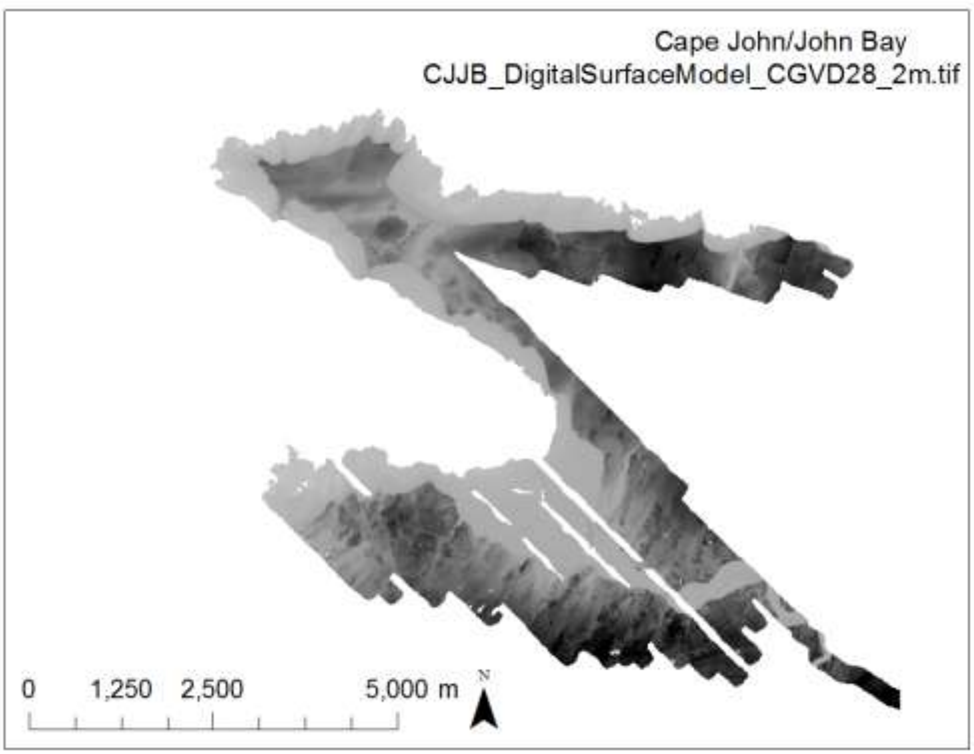

Figure 51: Cape John/John Bay 2 m Digital Surface Model.

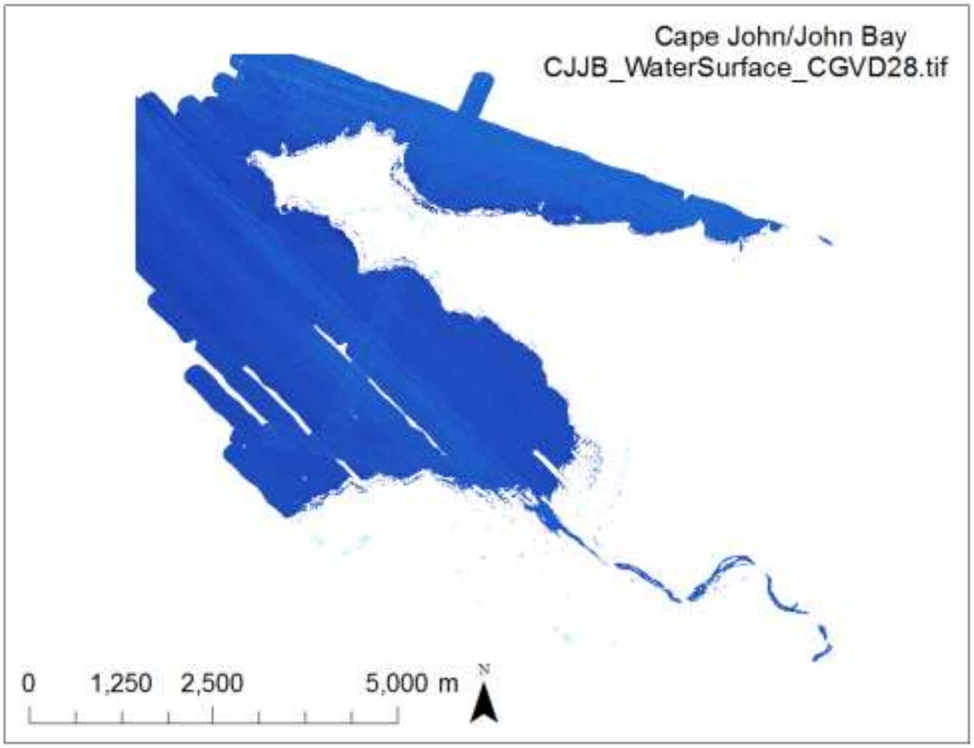

Figure 52: Cape John/John Bay Water Surface.

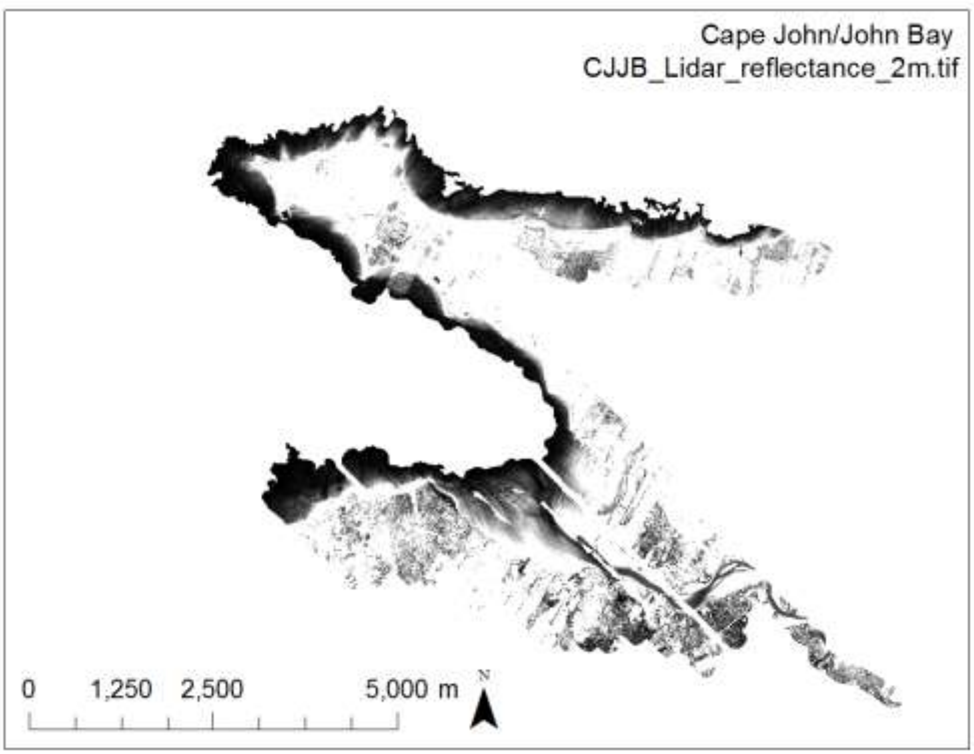

Figure 53: Cape John/John Bay 2 m Lidar Reflectance. Note that lidar reflectance for the Cape John/John Bay dataset has not been compensated for the increase of laser attenuation with depth.

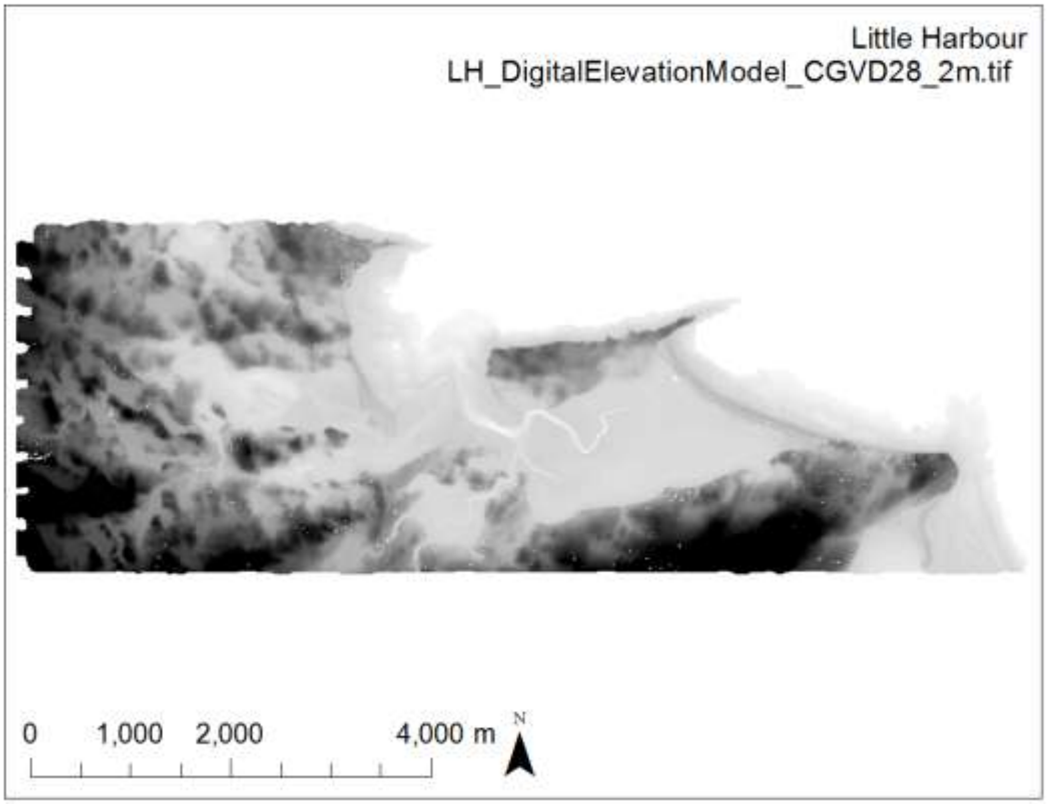

Figure 54: Little Harbour 2 m Digital Elevation Model.

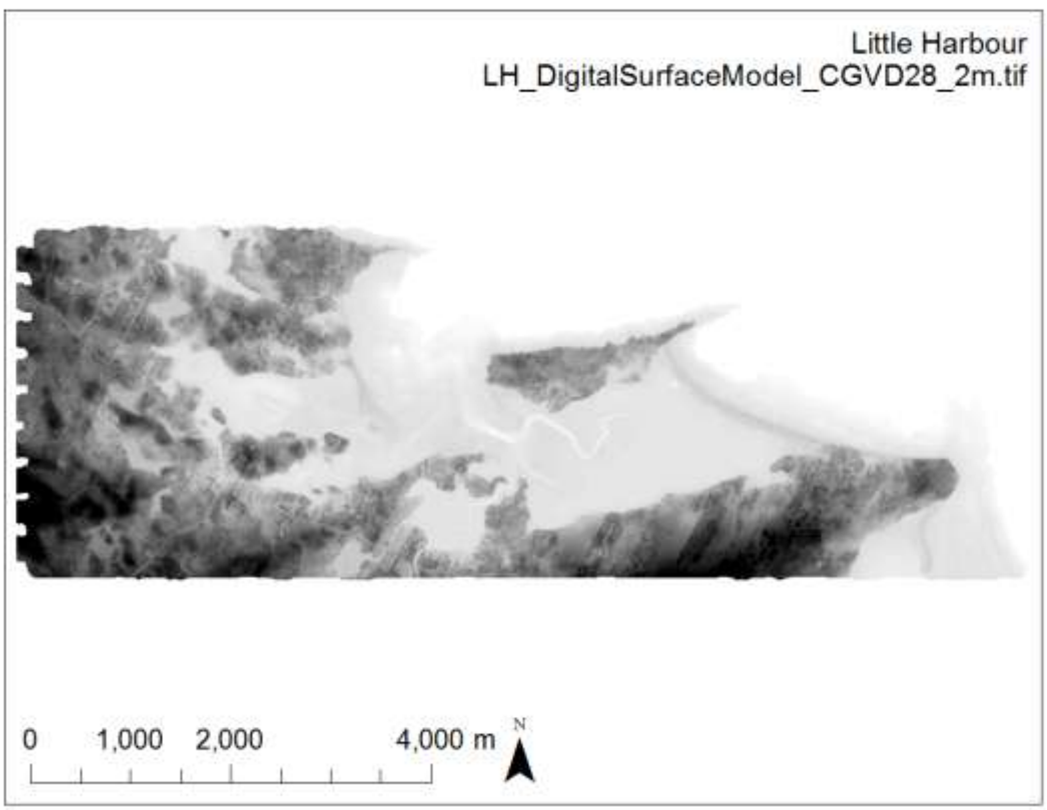

Figure 55: Little Harbour 2 m Digital Surface Model.

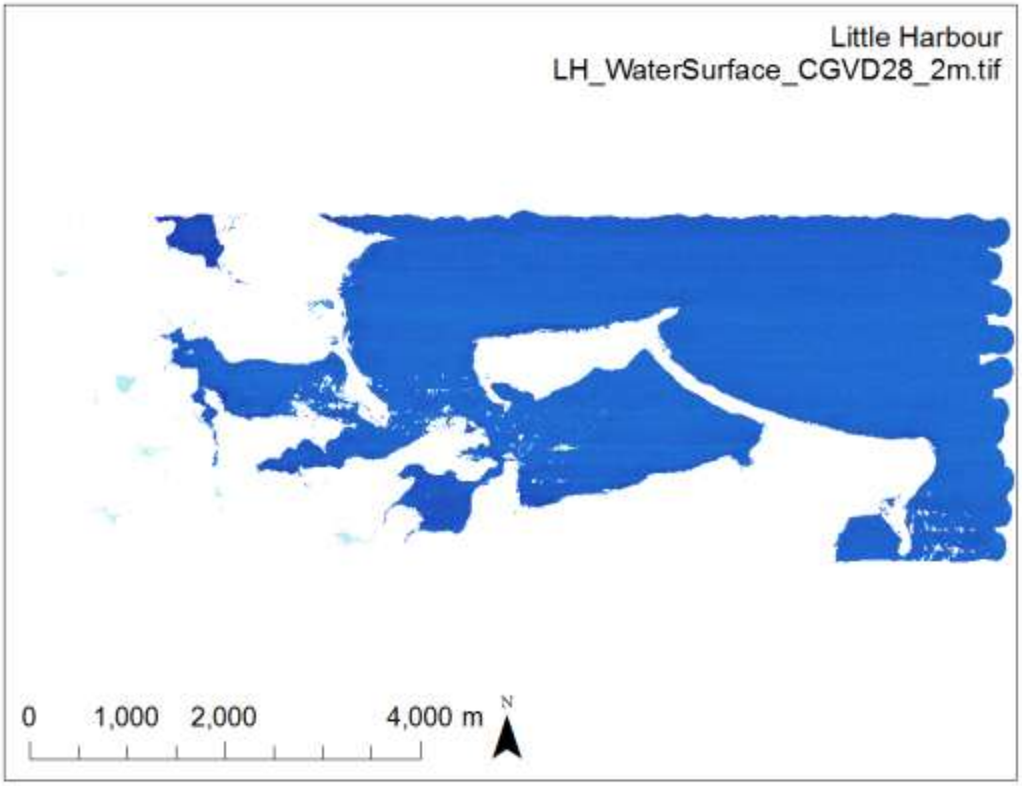

Figure 56: Little Harbour Water Surface.

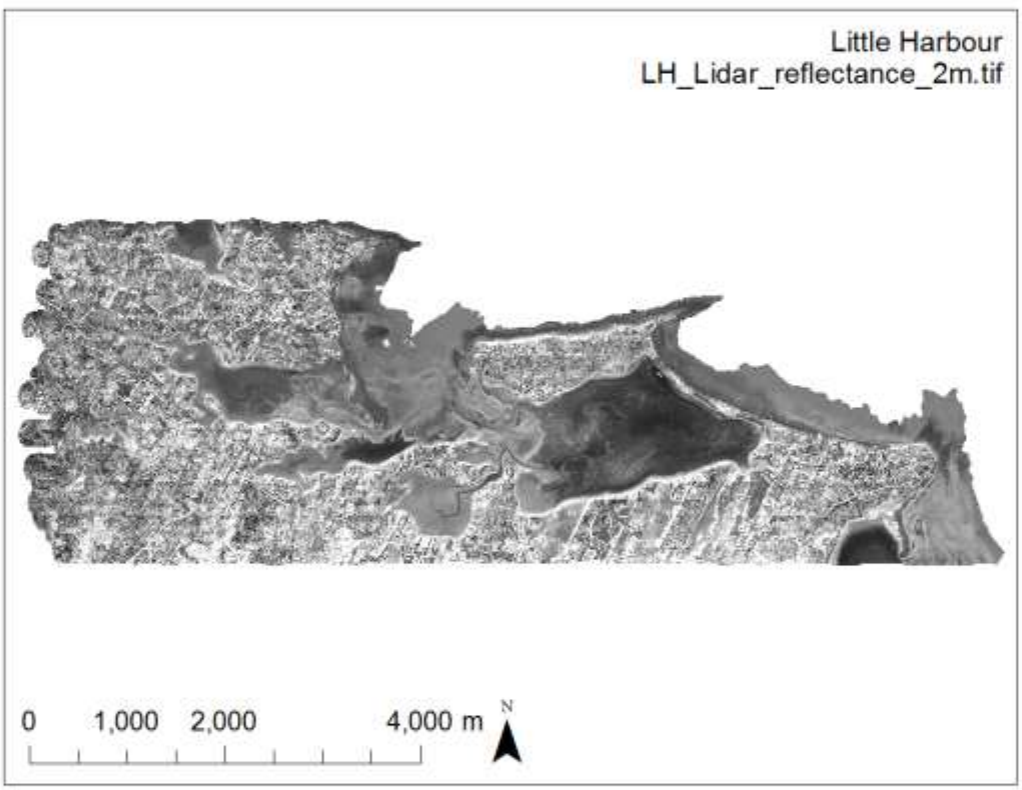

Figure 57: Little Harbour 2 m Lidar Reflectance. Note that lidar reflectance values for the Little Harbour dataset have been compensated with regard to light attenuation with an increase water depth.

7.3 LAS

3-D point cloud of all lidar returns (i.e. ground features, vegetation, sea surface, and seabed). This data is presented in the form of classified .LAS files. Point data is stored in the *Universal Transverse Mercator* projection (UTM, Zone 20N) and referenced to the *North American Datum 1983* (NAD83) including the *Geodetic Reference System 1980* (GRS80). Elevation information for the point datasets is referenced to the ellipsoid.

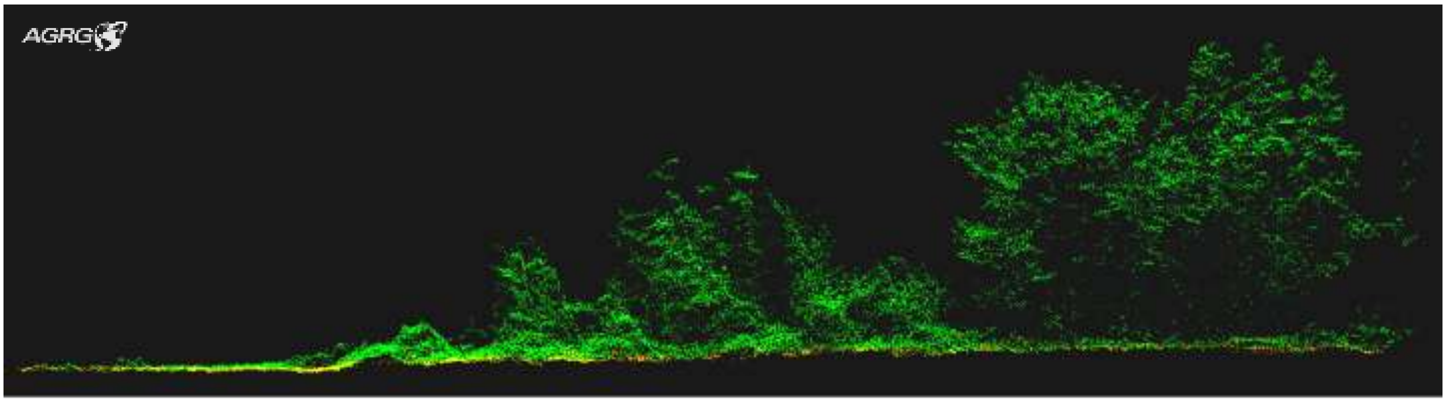

Figure 58: An example of the dense topographic lidar point cloud as captured around the Cape John Peninsula.

This data is provided in 500m square blocks, each containing all overlapping flight lines and classified as presented in Table 4.

Classification Code	Lidar Point Classification Description
0	Modelled water surface
1	Bathymetric seabed
2	Underwater Vegetation
3	N/A
4	NIR Topo-laser Ground
5	NIR Topo-laser Non-Ground
6	Green bathymetric-laser Ground
7	Green bathymetric-laser Non-Ground
8	Measured water surface
9	Noise
10	*Overlapping Modelled water surface*
11	*Overlapping Bathymetric seabed*
12	*Overlapping Underwater Non-Ground*
13	*N/A*
14	*Overlapping NIR Topo-laser Ground*
15	*Overlapping NIR Topo-laser Non-Ground*
16	*Overlapping Green bathymetric-laser Ground*
17	*Overlapping Green bathymetric-laser Non-Ground*
18	*Overlapping Measured water surface*
19	*Overlapping Noise*

Table 4: Lidar point classification Codes and descriptions. Note that 'overlap' is determined for points which are within a desired footprint of points from a separate flight line; the latter of which having less absolute range to the laser sensor.

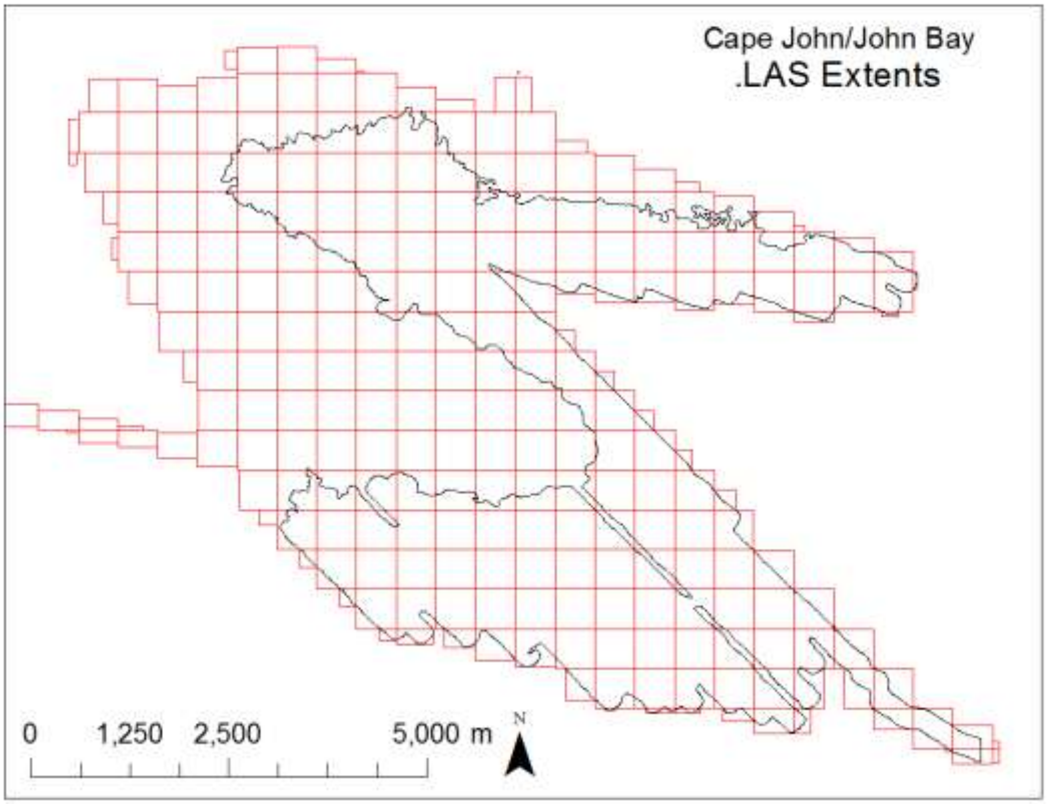

Figure 59: Cape John/John Bay LAS extents with Point counts: 832,032,532

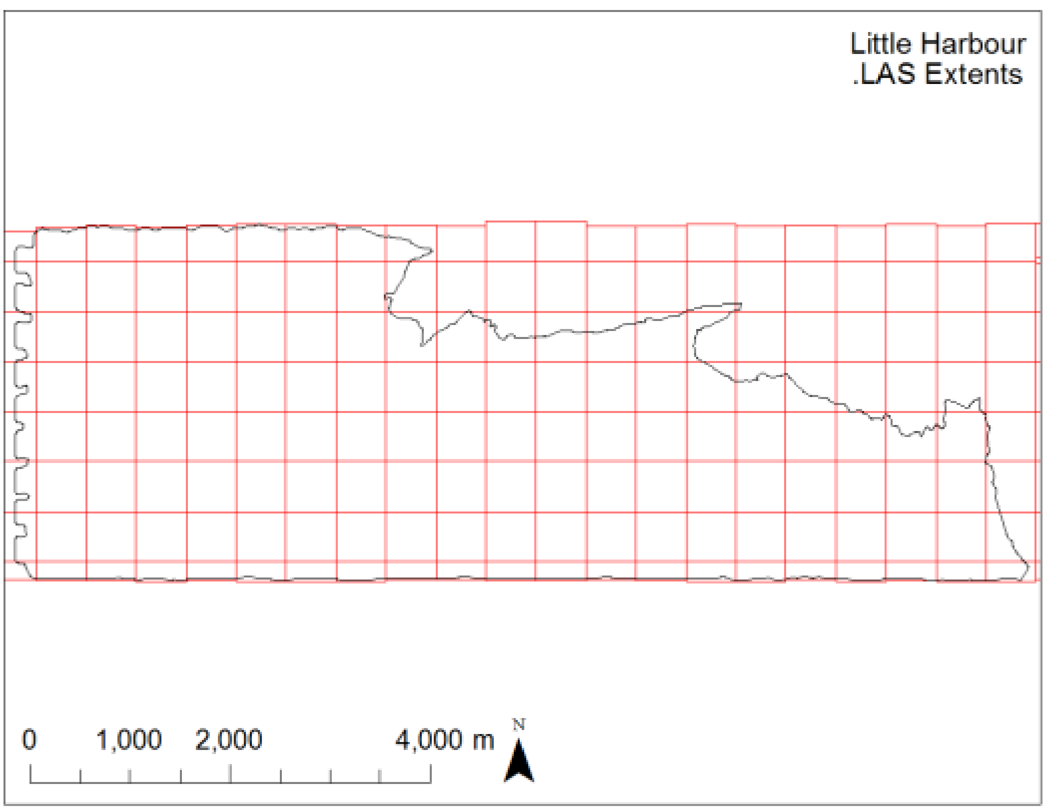

Figure 60: Little Harbour LAS extents with point counts 889,554,626.

7.4 Orthomosaics

Orthomosaics are delivered in georeferenced .TIFF format, and similarly projected in NAD 83 UTM zone 20N. Photos were acquired using a LEICA RCD30 CH62 NAG-D in tandum with the Chiroptera 2 lidar system.

Spectral range and filters	(λ nm)
Blue:	435-495 (at = λ 50%)
Green:	530 – 580 (at = λ 50%)
Red:	610-660 (at = λ 50%)
Near-infrared:	840-900 (at = λ 50%)

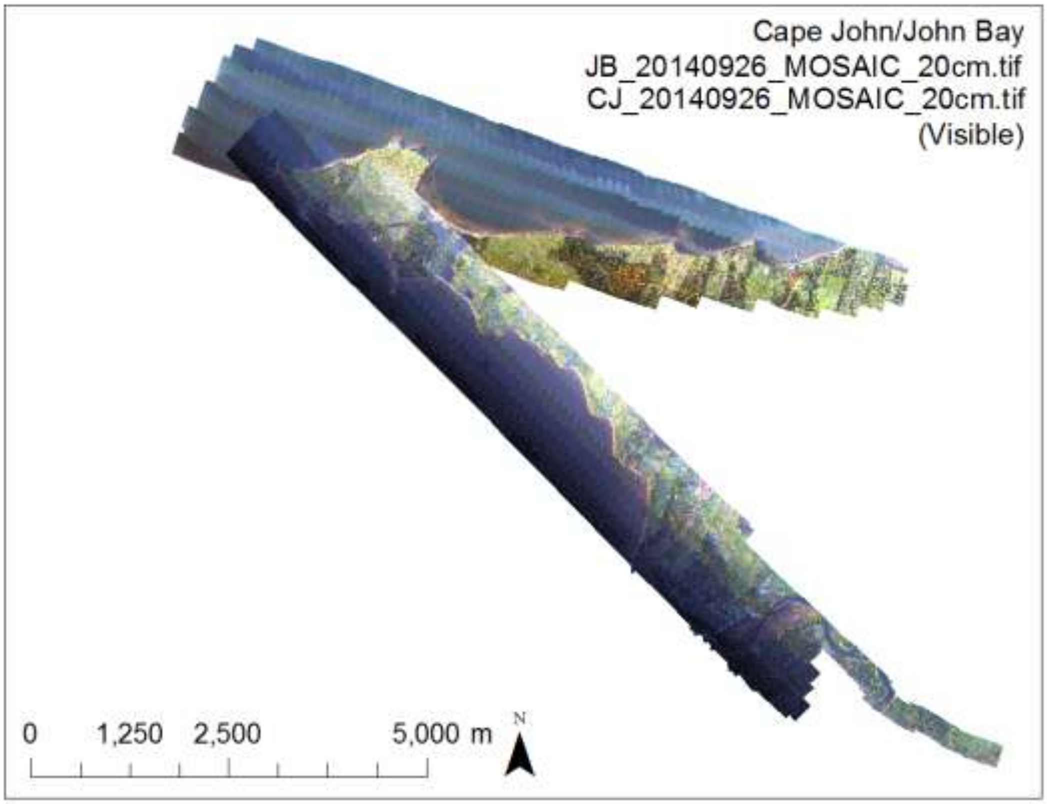

Figure 61: Cape John/John Bay orthophoto mosaic at 20 cm resolution.

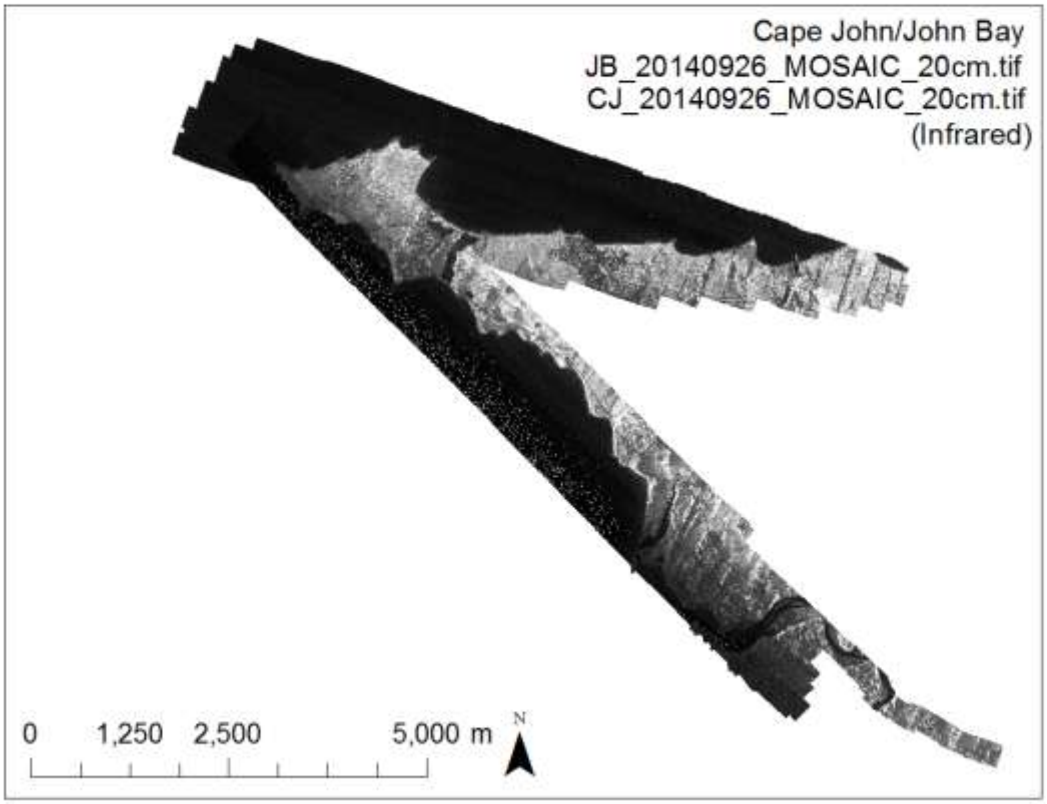

Figure 62: Cape John/John Bay infrared orthophoto mosaic at 20 cm resolution.

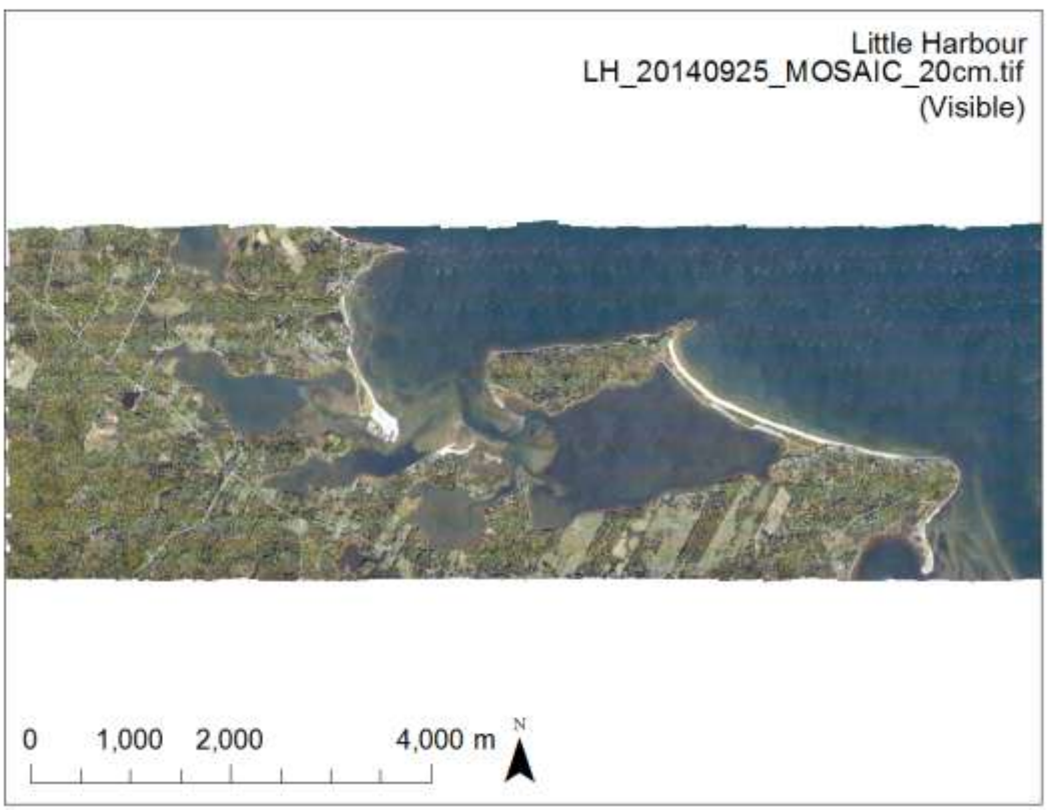

Figure 63: Little Harbour orthophoto mosaic at 20 cm resolution.

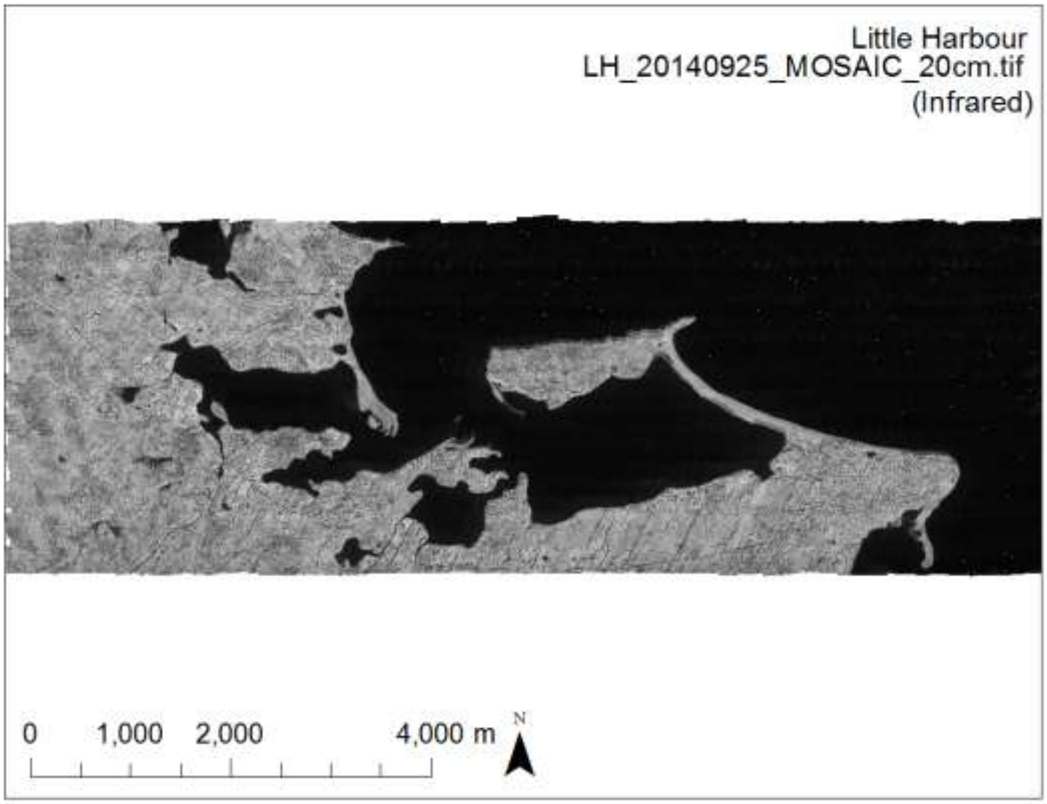

Figure 64: Little Harbour infrared orthophoto mosaic at 20 cm resolution.